



UNIL | Université de Lausanne

Unicentre

CH-1015 Lausanne

<http://serval.unil.ch>

---

Year : 2022

## Evaluation of the lactate receptor-mediated effects on neuronal activity in rodent and human brain tissue

Briquet Marc

Briquet Marc, 2022, Evaluation of the lactate receptor-mediated effects on neuronal activity in rodent and human brain tissue

Originally published at : Thesis, University of Lausanne

Posted at the University of Lausanne Open Archive <http://serval.unil.ch>

Document URN : urn:nbn:ch:serval-BIB\_F1268E07C48B6

### **Droits d'auteur**

L'Université de Lausanne attire expressément l'attention des utilisateurs sur le fait que tous les documents publiés dans l'Archive SERVAL sont protégés par le droit d'auteur, conformément à la loi fédérale sur le droit d'auteur et les droits voisins (LDA). A ce titre, il est indispensable d'obtenir le consentement préalable de l'auteur et/ou de l'éditeur avant toute utilisation d'une oeuvre ou d'une partie d'une oeuvre ne relevant pas d'une utilisation à des fins personnelles au sens de la LDA (art. 19, al. 1 lettre a). A défaut, tout contrevenant s'expose aux sanctions prévues par cette loi. Nous déclinons toute responsabilité en la matière.

### **Copyright**

The University of Lausanne expressly draws the attention of users to the fact that all documents published in the SERVAL Archive are protected by copyright in accordance with federal law on copyright and similar rights (LDA). Accordingly it is indispensable to obtain prior consent from the author and/or publisher before any use of a work or part of a work for purposes other than personal use within the meaning of LDA (art. 19, para. 1 letter a). Failure to do so will expose offenders to the sanctions laid down by this law. We accept no liability in this respect.



UNIL | Université de Lausanne

Faculté de biologie  
et de médecine

Département des neurosciences fondamentales

## **Evaluation of the lactate receptor-mediated effects on neuronal activity in rodent and human brain tissue**

### **Thèse de doctorat en Neurosciences**

présentée à la

Faculté de biologie et de médecine  
de l'Université de Lausanne

Par

**Marc BRIQUET**

diplômé du Master en Biologie médicale de l'Université de Lausanne

#### **Jury**

Prof. Olivier Braissant, Président

Prof. Jean-Yves Chatton, Directeur de thèse

Prof. Manuel Mamei, Expert

Prof. Nicolas Toni, Expert

Dr. Alexandre Bouron, Expert

Thèse n° 330

Lausanne 2022

***Programme doctoral interuniversitaire en Neurosciences  
des Universités de Lausanne et Genève***



UNIL | Université de Lausanne



**UNIVERSITÉ  
DE GENÈVE**

# Imprimatur

Vu le rapport présenté par le jury d'examen, composé de

<b>Président·e</b>	Monsieur	Prof.	Olivier	<b>Braissant</b>
<b>Directeur·trice de thèse</b>	Monsieur	Prof.	Jean-Yves	<b>Chatton</b>
<b>Expert·e·s</b>	Monsieur	Prof.	Manuel	<b>Mameli</b>
	Monsieur	Prof.	Nicolas	<b>Toni</b>
	Monsieur	Dr	Alexandre	<b>Bouron</b>

le Conseil de Faculté autorise l'impression de la thèse de  
**Monsieur Marc Briquet**

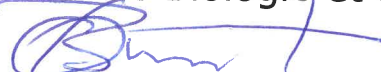
Master ès Sciences en biologie médicale,  
Université de Lausanne, Suisse

intitulée

**Evaluation of the lactate receptor-mediated effects  
on neuronal activity in rodent and human brain tissue**

Lausanne, le 29 avril 2022

pour Le Doyen  
de la Faculté de Biologie et de Médecine

  
Prof. Olivier Braissant

## Table of contents

Acknowledgments.....	5
List of abbreviations.....	6
Abstract.....	7
Résumé .....	8
Introduction .....	10
History of lactate.....	10
Lactate in the brain .....	11
Brain metabolism.....	11
Astrocyte-neuron lactate shuttle.....	14
Lactate function in the brain.....	16
Lactate, learning, and memory .....	17
Lactate and neuropathology.....	18
Lactate and neuronal excitability.....	19
Hydroxycarboxylic Acid Receptors.....	21
Signaling pathways of HCAR1 .....	24
Localization of HCAR1 .....	24
HCAR1 functions in the body .....	25
HCAR1 functions in the brain.....	27
Results.....	30
Preamble.....	30
Study 1 .....	30
Summary of the results.....	30
Personal contribution .....	31
Study 2 .....	51

Summary of the results.....	51
Personal contribution .....	51
Discussion and Perspectives .....	63
HCAR1 localization in the brain.....	63
HCAR1 activation in rodent hippocampus.....	65
Epilepsy .....	66
Memory.....	66
Neurogenesis .....	68
HCAR1 – dual mode of action ? .....	70
Human tissue .....	73
References .....	75
Appendix 1 .....	82
Appendix 2 .....	83
Summary of the results.....	83
Personal contribution .....	83

## Acknowledgments

First of all, I would like to truly thank Jean-Yves Chatton for giving me the opportunity to work in his lab, initially as a Master student and finally for my PhD. It's been an exciting journey and I couldn't appreciate more his availability, the trust that he gave me and all the knowledge he shared helping me to grow as a scientist.

Second, I would like to thank the members of the lab.

Thanks Nadia for teaching me electrophysiology, helping me to shape my critical thinking and discussing science. Thank you for being present and generous in any situation. You can always call me if you forget your cards, keys, phone, etc.

Then, I thank Maxime, "le Bouliste", for these endless conversations and listening to all my stories. We worked together for his Master project and keep collaborating all along our respective projects. Thanks for your motivation and science enthusiasm.

I also thank my former colleagues with whom I shared hours of lab life. Haissa, my "BSE", for being my supervisor during my master, Joel for always relates the best stories, Yann for his contagious entrepreneurial spirit, and Anne for the work we accomplished in the paper we published.

A massive big up to my DNF colleagues, especially the "bandidos crew", Andrea, Arnau, Laura, and Alvaro. Thanks Andrea for these coffee breaks and your unconditional support , I probably couldn't have made it without you !

I thank Carole for always being present and listening to my complicated scientific explanation. Having you by my side is a real source of inspiration.

I thank my family, my sister, my brother, and especially my parents to whom I dedicate this thesis. You gave me the chance to study in the best conditions and I will always be grateful.

Finally, I warmly thank my thesis committee, Prof. Olivier Braissant, Prof. Manuel Mameli, Prof. Nicolas Toni, and Dr. Alexandre Bouron for taking the time to follow my project, giving input during the midterm, and for the time spend on my thesis evaluation.

## List of abbreviations

3.5-DHBA	3.5-dihydroxybenzoic acid	La <sup>-</sup>	Lactate
3Cl-HBA	3-chloro-5-hydroxybenzoic acid	LC	Locus coeruleus
AC	Adenylyl cyclase	LDH	Lactate dehydrogenase
acetyl-CoA	Acetyl coenzyme A	MCAO	Middle cerebral artery occlusion
ANLS	Astrocyte-neuron lactate shuttle	MCs	Mossy cells
ATP	Adenosine triphosphate	MCT1	Monocarboxylate transporters 1
cAMP	Cyclic adenosine monophosphate	mEPSC	Miniature excitatory post-synaptic currents
cpGFP	Circularly permuted green fluorescent protein	mRFP	Monomeric red fluorescent protein
DCA	Dichloroacetate	MWM	Morris water maze
DG	Dentate gyrus	NADH	Nicotinamide adenine dinucleotide
ETC	Electron transport chain	NPCs	Neural precursor cells
FADH <sub>2</sub>	Flavin adenine dinucleotide	OSS	Oscillary shear stress
FFA	Free fatty acid	PKA	Protein kinase A
GABA	γ-aminobutyric acid	PLC	Phospholipase C
GCs	Granule cells	qRT-PCR	Quantitative Real-Time Polymerase Chain Reaction
GFAP	Glial fibrillary acidic protein	rtPA	Recombinant tissue plasminogen activator
GPCRs	G-protein coupled receptors	sEPSC	Spontaneous excitatory post-synaptic currents
GTP	Guanine triphosphate	SVZ	Subventricular zone
HCAR	Hydroxycarboxylic acid receptors	TBI	Traumatic brain injury
HCAR1	Hydroxycarboxylic acid receptor 1	TCA	Tricarboxylic acid
HK	Hexokinase	TLE	Temporal lobe epilepsy
HLa	Acid lactic	TLR	Toll-like receptors
IA	Inhibitory avoidance	VMN	Ventromedial hypothalamic neurons
KO	Knock-out	WT	Wild-type

## Abstract

Lactate has been shown to be used as an energy substrate in the brain to maintain neuronal activity. Evidence suggests that lactate also acts on a metabotropic receptor called HCAR1, first described in the adipose tissue. Whether HCAR1 also modulates neuronal circuits is still unclear. In this study, using qRT-PCR, we show that HCAR1 mRNA transcripts are present in the human brain of epileptic patients who underwent resective surgery. In acute brain slices from these patients, pharmacological HCAR1 activation using the non-metabolized agonist 3CI-HBA decreased the frequency of both spontaneous neuronal  $\text{Ca}^{2+}$  spiking and spontaneous excitatory post-synaptic currents (EPSCs). In mouse brains, we found HCAR1 expression in different regions using a fluorescent reporter mouse line and *in situ* hybridization techniques. In the hippocampus, HCAR1 was mainly present in mossy cells of the dentate gyrus. Mossy cells are key players in the hippocampal excitatory circuitry. Their partial loss is a major hallmark of temporal lobe epilepsy. By using whole-cell patch clamp recordings in both mouse and rat acute slices, we found that HCAR1 activation causes a decrease in excitability, spontaneous EPSCs, and miniature EPSCs frequency of granule cells, the main output of mossy cells. These effects were absent in HCAR1 KO mouse slices, confirming the inhibitory role of the receptor. Overall, we propose that lactate acting on HCAR1 can be considered a neuromodulator decreasing synaptic activity in both human and rodent brains, which makes HCAR1 an attractive target for the treatment of epilepsy.



## Résumé

Le cerveau est l'organe le plus énergivore et consomme jusqu'à 20% du glucose total alors qu'il ne fait que 2% de la masse totale de notre corps. En plus du glucose, il a été démontré que le lactate est également utilisé comme substrat énergétique dans le cerveau afin de maintenir l'activité neuronale. Alors que le lactate est surtout étudié pour ses propriétés métaboliques, de récentes preuves suggèrent que le lactate agit également sur un récepteur métabotrope appelé HCAR1. Initialement découvert et décrit dans le tissu adipeux, il a récemment été montré qu'il était exprimé dans le cerveau et que son activation menait à la diminution de l'activité neuronale sur des neurones en culture. Cependant, on ne sait toujours pas si HCAR1 module également l'activité neuronale dans des circuits neuronaux conservés. Dans cette étude, en utilisant la qRT-PCR, nous montrons que les produits de la transcription, l'ARNm de HCAR1, sont présents dans le cerveau humain de patients épileptiques ayant subi une chirurgie résective du foyer épileptique. Dans des tranches de cerveau de ces patients, l'activation pharmacologique de HCAR1 par l'agoniste non-métabolisé, appelé 3Cl-HBA, a diminué la fréquence de l'activité neuronale spontanée mesurée à l'aide de l'imagerie calcique, ainsi que la fréquence des courants spontanés excitateurs post-synaptiques (EPSCs). Dans le cerveau des souris, nous avons trouvé l'expression de HCAR1 dans différentes régions en utilisant une lignée de souris transgénique qui exprime une protéine fluorescente rouge sous l'influence du promoteur de HCAR1 et une technique d'hybridation *in situ* dernière génération. Nous avons constaté une forte présence du récepteur dans l'hippocampe et plus particulièrement au niveau des cellules moussues du gyrus denté. Les cellules moussues sont des actrices clés dans les circuits excitateurs de l'hippocampe. Ces cellules sont potentiellement impliquées dans l'épilepsie sachant que leur perte partielle est une caractéristique majeure de l'épilepsie du lobe temporal. Nous avons donc pour objectif d'évaluer si HCAR1 est capable de créer un effet inhibiteur dans la circuitrie du gyrus denté. En utilisant des enregistrements électrophysiologiques dans des tranches de cerveau de souris et de rat, nous avons démontré que l'activation de HCAR1 engendre une diminution de l'excitabilité, des EPSC spontanés et miniatures des cellules granuleuses, la principale connection des cellules moussues. Ce résultat confirme donc la présence d'HCAR1 sur les cellules moussues. Lorsque

nous utilisons des souris HCAR1 KO, c'est-à-dire dépourvues du récepteur, nous n'observons pas d'effet lorsque nous administrons l'agoniste de HCAR1. Dans l'ensemble, nous proposons que le lactate agissant sur HCAR1 peut être considéré comme un neuromodulateur diminuant l'activité synaptique dans le cerveau des humains et des rongeurs, ce qui fait de HCAR1 une cible intéressante pour le traitement de pathologies comme l'épilepsie.

## Introduction

### History of lactate

The history of acid lactic (HLA) or lactate ( $\text{La}^-$ ) started in 1780 with its discovery in the milk by a Swedish chemist named Carl Wilhelm Scheele (Ferguson et al., 2018). Within the physiological pH range of mammalian muscle and blood, HLA is more than 99% dissociated into lactate anion ( $\text{La}^-$ ) and protons ( $\text{H}^+$ ). Lactate exists under two enantiomers often referred as L(+) $\text{La}^-$  and D(-) $\text{La}^-$ , although perhaps more correctly as (S)- $\text{La}^-$  and (R)- $\text{La}^-$ , respectively (Cahn et al., 1956). In the human body, the L(+) form is by far the most predominant and the one produced by glycolytic activity. As a comparison, D(-) $\text{La}^-$  concentration reaches 0.013 to 0.3 mM in healthy humans (Hasegawa et al., 2003; Filiz et al., 2010), while L(+) $\text{La}^-$  concentration is between 1.0 mM at rest and 15mM after exercise (Abi-Saab et al., 2002; Offermanns, 2017). A few years later in a paper published in 1848, Berzelius described his observations indicating the presence of lactate in muscle. It will follow a series of studies reporting the presence of lactate in the mammalian body until the paper of Fletcher and Hopkins (1907) that settled the first principle of lactate. They postulated that lactate is present at low concentrations in resting muscles, whereas the concentration increase in resting anaerobic or highly stimulated muscles. Moreover, this increase disappears when fatigued muscles are placed in  $\text{O}_2$ -rich environments. From this observation, lactate production and accumulation were associated with inadequate  $\text{O}_2$  supply, leading to the conclusion that higher lactate levels were the results of hypoxia/dysoxia (Ferguson et al., 2018). In line with this idea, lactate was believed to be the cause of muscle fatigue, notably because of the acidosis arising from an increase in lactate concentration. Even though lactate increase and pH decrease seem to have an effect on muscle fatigue, some studies reported data opposing this position (Lamb and Stephenson, 2006; Westerblad, 2016). In 1926, Warburg gave his name to the Warburg effect, a phenomenon that recognized that lactate could also be produced in presence of  $\text{O}_2$  (Ferguson et al., 2018). This effect was initially described in tumor cells, known to consume more energy than normal cells. These cells were shown to produce energy using a high rate of glycolysis rather than a comparatively low rate of glycolysis followed by oxidation of pyruvate in mitochondria as found in most normal cells, even under conditions of sufficient oxygen (Li et al., 2015).

Considered a dead-end and fatigue-causing waste product of the metabolism, it is only in the 1980s that evidence started to accumulate showing that lactate could be in fact used as a metabolic fuel. It began with the studies of Brooks who demonstrated that lactate could be transferred from glycolytic cells to oxidative cells in order to sustain the latter (Brooks, 1985a, b, 2000, 2002, 2007, 2009, 2016), now known as the intracellular or cell-to-cell lactate shuttle. Extensively studied in muscles, lactate exchanges also occur in the brain and are called the astrocyte-neuron lactate shuttle (ANLS) (Pellerin and Magistretti, 1994).

In addition to its metabolic and energy donor role, lactate is now also considered a signaling molecule –a “lactohormone” (Brooks, 2009). Indeed, lactate is reported to participate in several mechanisms in which lactate seems to be a regulator rather than being just an energy substrate. For example, lactate can be oxidized into pyruvate via the lactate dehydrogenase (LDH) and act as a regulator of the cellular redox state. Lactate is shown to inhibit lipolysis and achieve its signaling role by interacting with the G-protein coupled receptor GPR81, now renamed hydroxycarboxylic acid receptor 1 (HCAR1). More recently, HCAR1 was identified in the brain and a new signaling role was attributed to lactate in the brain.

The aim of this thesis work was to better understand the signaling role of lactate in the brain, and more precisely in regions where the receptor HCAR1 is found to be expressed. To do so, we investigated neuronal activity under the activation of the receptor in rodent and human brain tissue.

## Lactate in the brain

### Brain metabolism

The brain is a huge energy burner with 20 to 25% consumed of the energy produced in the body, whereas the brain represents only 2% of the total body mass (Magistretti, 2006). The brain draws energy from glucose and oxygen delivered by the blood flow, representing 15-20% of the cardiac output (Xing et al., 2017). Glucose enters the brain after crossing the blood-brain barrier, composed of endothelial cells, pericytes, basal lamina, and the astrocytic endfeet. The concentration of glucose in the parenchymal compartment in the brain is about 1.2 mM and the human brain consumes glucose at 6.5  $\mu\text{M/s}$  (Barros et al., 2007). Glucose is the major source of

energy in the brain and provides between 30 to 36 ATPs per glucose. In mammalian brain cells, energy is sequentially produced by glycolysis, the tricarboxylic acid (TCA) cycle, and the associated oxidative phosphorylation, resulting in the oxidation of glucose into CO<sub>2</sub> and H<sub>2</sub>O. In the ANLS, astrocytes uptake glucose and transform it into lactate via aerobic glycolysis. Lactate then exits astrocytes before being taken up by neurons and transformed into pyruvate to enter the TCA cycle and associated respiratory chain (Cali et al., 2019).

During glycolysis (**Figure 1**), glucose is broken down into two molecules of pyruvate after a 10-step reaction taking place in the cytoplasm, which results in the net production of 2 ATP molecules.

These reactions are catalyzed by 10 enzymes, which are hexokinase (HK), phosphoglucose isomerase, phosphofructokinase, aldolase, triosephosphate isomerase, glyceraldehyde 3 phosphate dehydrogenase, phosphoglycerate kinase, phosphoglycerate mutase, enolase, and pyruvate kinase (Li et al., 2015). However, glucose is not necessarily completely transformed into pyruvate. After phosphorylation of glucose by the HK, the first step of the glycolysis, glucose may enter the pentose phosphate pathway (PPP). The PPP branches after the first step of glycolysis and consumes the intermediate glucose-6-phosphate to, in the end, generate NADPH and ribose 5-phosphate. These two metabolites are vital for the survival and

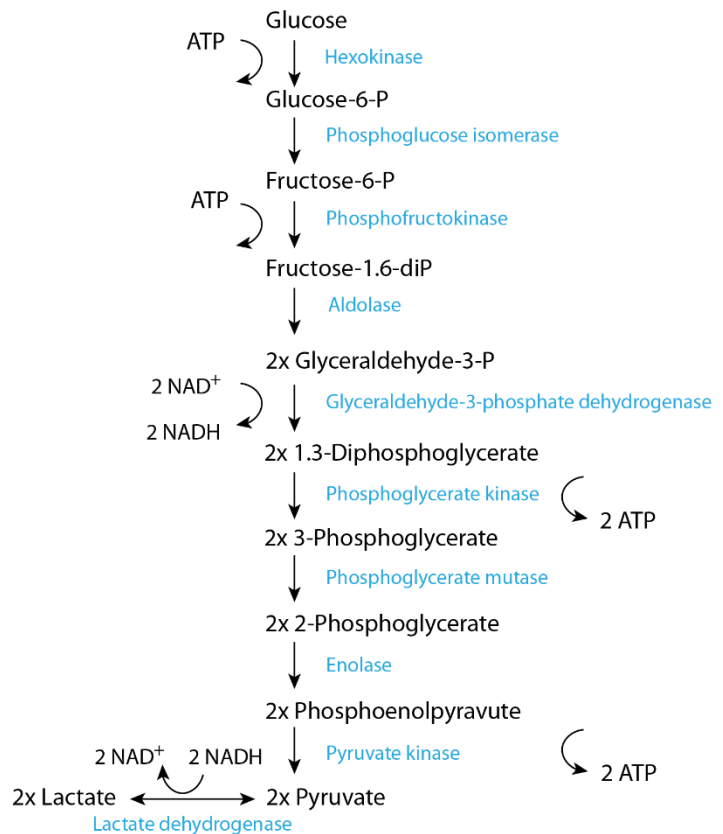


**Figure 1.** Summary scheme of the glycolytic pathway transforming one molecule of glucose into 2 pyruvate. 2 molecules of lactate is produced by the lactate dehydrogenase transforming 2 molecules of pyruvate, which in addition restore NAD<sup>+</sup> levels.

proliferation of cells and take part in the synthesis of nucleotides or aromatic amino acids, the building blocks of protein, as well as for neurotransmitters such as glutamate, GABA ( $\gamma$ -aminobutyric acid), and acetylcholine (Bouzier-Sore and Bolaños, 2015). The final step of glycolysis is not necessarily pyruvate either. Cells express high levels of LDH, an oxidoreductase that catalyzes the interconversion between pyruvate and lactate.

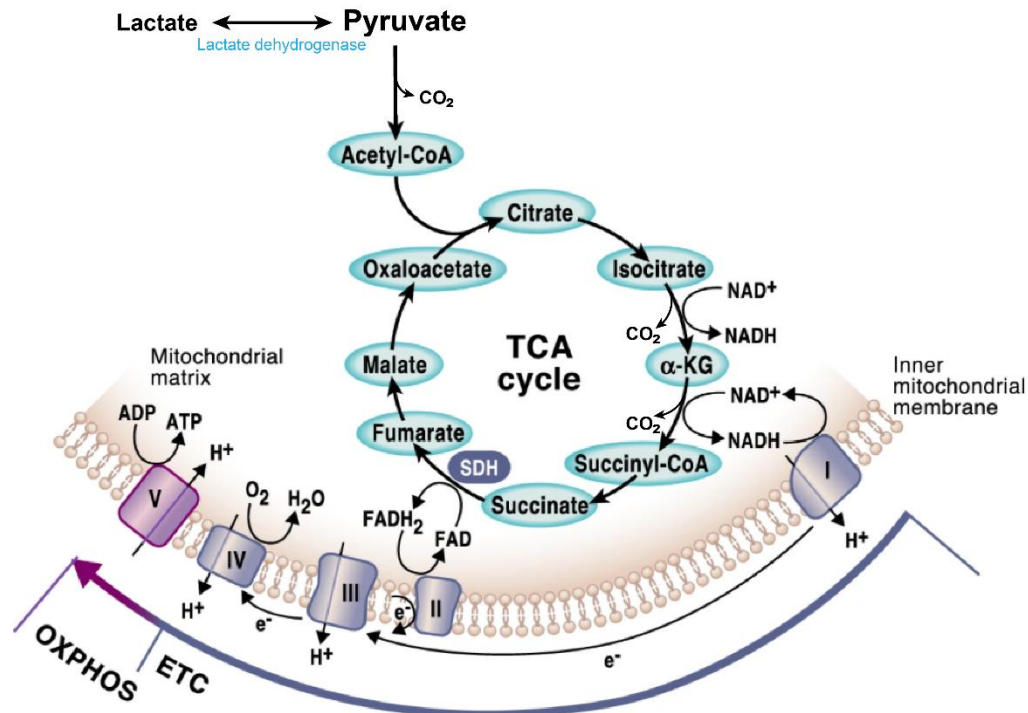


**Figure 2. Tricarboxylic acid cycle (TCA) and oxidative phosphorylation (OXPHOS).** Adapted from (Martínez-Reyes and Chandel, 2020).

In a second phase (**Figure 2**), pyruvate enters the mitochondrial matrix to be oxidized into acetyl coenzyme A (acetyl-CoA) with the help of the pyruvate dehydrogenase. At the same time, this reaction produces CO<sub>2</sub> and NADH that will be further used in the electron transport chain (ETC). Then, Acetyl-CoA enters the TCA cycle and follows an 8-step reaction leading to the production of GTP, NADH, FADH<sub>2</sub>, and coenzyme A. The TCA cycle itself does not generate ATP, but instead, 1 GTP molecule is produced per pyruvate. However, NADH and FADH<sub>2</sub>, two electron carriers, will connect with the last portion of cellular respiration, and deposit their electrons into the ETC to drive the synthesis of ATP molecules through oxidative phosphorylation.

In the brain, one finds distinctive metabolic profiles according to the diversity of cells. Such differences have been particularly investigated in neurons and astrocytes. As a first, high-level view, one can say that neurons are predominantly oxidative, therefore using pyruvate to produce energy via the TCA and the oxidative phosphorylation, whereas astrocytes are rather glycolytic and therefore mainly lactate producers (Hyder et al., 2006; Bélanger et al., 2011; Zhang et al., 2014). Following the first postulate of lactate shuttling by Brooks and his colleagues, evidence suggested that lactate could support both synaptic function, and reactivate glucose-depleted synaptic quiescence in hippocampal slices (Schurr et al., 1988; Izumi et al., 1997). A few years later, Schurr et al. demonstrated that lactate, rather than glucose (Schurr et al., 1997b), is shuttled to post-hypoxic neurons to recover functions (Schurr et al., 1997c) and that the lactate originates from glial cells (Schurr et al., 1997a). During the same period, Magistretti and Pellerin established the framework of a hypothesis that will become the prevailing contemporary viewpoints of neuroenergetics by proposing the so-called astrocyte-neuron lactate shuttle (ANLS) (Pellerin and Magistretti, 1994; Magistretti and Pellerin, 1996).

### Astrocyte-neuron lactate shuttle

During excitatory synapse communication, glutamate is the main excitatory neurotransmitter in the brain. It is released to bind its ionotropic and metabotropic receptors which further trigger activity. Then, glutamate is removed from the synaptic cleft by several high-affinity glutamate transporters present in both glial cells and presynaptic terminals. This reuptake mechanism by astrocytes induces glycolysis (Pellerin and Magistretti, 1994). This is how the ANLS model (**Figure 3**) brought a new link between metabolism and neuronal activity, in which lactate played a central role as an energy substrate for neurons (Mosienko et al., 2015). Briefly, in astrocytes, glutamate is taken up by a  $\text{Na}^+$ -dependent glutamate transporter, which carries one glutamate, three  $\text{Na}^+$ , and one  $\text{H}^+$  inward while one  $\text{K}^+$  is moved out of the cell. This co-transport results in an astrocyte intracellular  $\text{Na}^+$  concentration increase leading to an activation of the astrocytic  $\text{Na}^+/\text{K}^+$ -ATPase to restore ionic balance (Chatton et al., 2016). During this process, the  $\text{Na}^+/\text{K}^+$ -ATPase pump doubles its activity resulting in a corresponding augmentation of the metabolic cost (Chatton et al., 2000). This ATPase pump activation has an associated energy cost, which stimulates glucose uptake and utilization by astrocytes to produce ATP mainly by glycolysis.

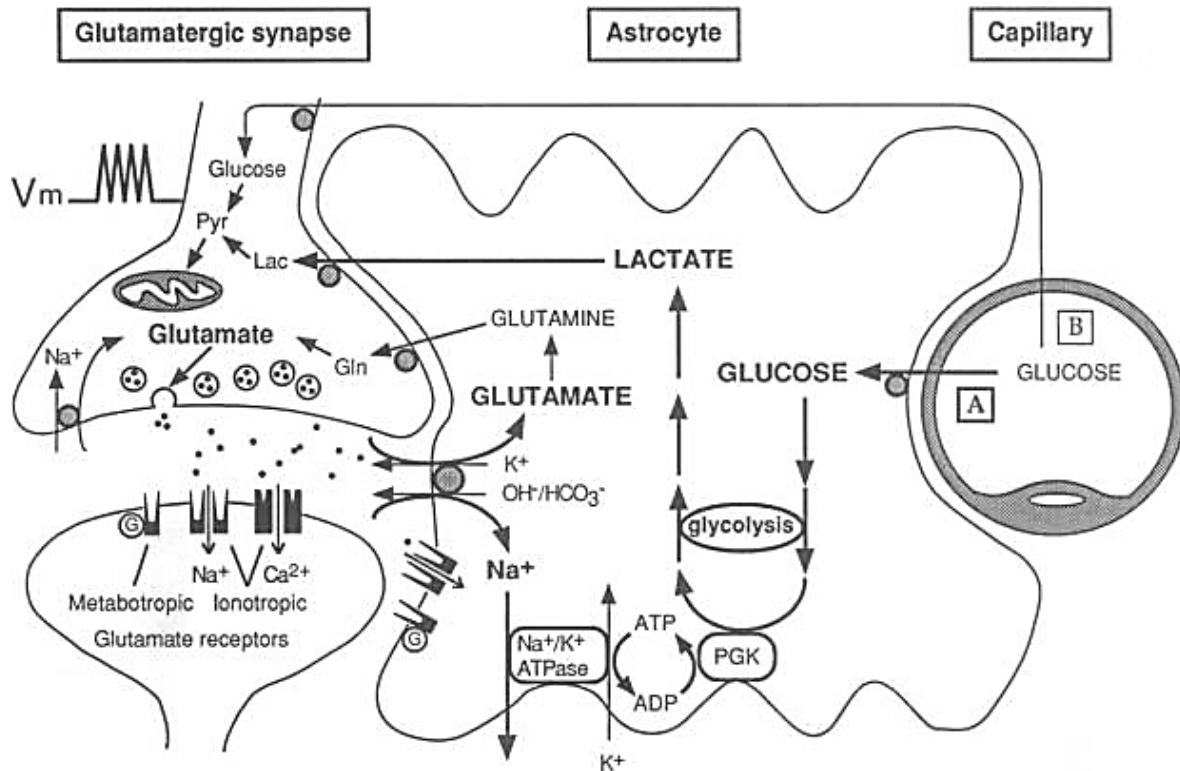


**Figure 3.** Original scheme of the ANLS model proposed by Pellerin and Magistretti (1994).

According to the ANLS, for each glutamate molecule taken up, one glucose enters astrocytes resulting in the production of two ATP and two lactate molecules through glycolysis. This process is therefore energetically balanced, as one of the ATP molecule sustain  $\text{Na}^+/\text{K}^+$ -ATPase activity, while the other provides the energy needed to convert glutamate into glutamine by the glutamine synthase. This reaction thereby replenishes the neurotransmitter pool of glutamate and completes the glutamate–glutamine cycle. Accumulation of lactate induces outward release along its concentration gradient via monocarboxylate transporters 1 (MCT1) located in the astrocytic plasma membrane (Pierre and Pellerin, 2005). Once in the extracellular space, lactate can be taken up by neighbouring neurons via MCT2 located in the neuronal plasma membrane. At this point, lactate is metabolized into pyruvate, which enters the TCA cycle and is finally used as an oxidative energy substrate by neurons. This demonstrates the presence of an astroglial metabolic network, allowing energy substrates exchange between astrocytes from their source, which is blood vessels, to the site of high energy demand and use, the neurons (Giaume et al., 2010). Since then, this hypothesis has been further supported by new experimental data (Pellerin



and Magistretti, 2012) showing, for example, in vivo evidence for lactate gradient from astrocytes to neurons, determined using genetically encoded biosensor and two-photon laser scanning microscopy (Machler et al., 2016).

The consequence of glucose utilization by astrocytes, after glutamate release by neurons, is the production and liberation of lactate in the extracellular space immediately surrounding neurons. As said, lactate was viewed as a toxic waste for brain cells and rapid clearance must be a necessary step, because local lactate accumulation would otherwise become an opposing driving force that would influence many reversible NAD<sup>+</sup>/NADH-coupled redox reactions, including continued conversion of pyruvate to lactate under oxygenated conditions (Dienel and Hertz, 2001). Lactate, even in presence of physiological glucose concentration, was shown to be preferred as an oxidative substrate over glucose by neurons (Bouzier-Sore et al., 2003; Itoh et al., 2003; Bouzier-Sore et al., 2006; Ivanov et al., 2011), although glucose is also used by neurons (Mangia et al., 2009) and was shown to be equally effective in energizing activity-dependent synaptic vesicle turnover in purified cortical neurons (Morgenthaler et al., 2006). This model is however not exclusive, it is therefore important to consider other models proposed in the literature (Dienel, 2012).

### Lactate function in the brain

In this chapter, we will go over few examples where lactate utilization is essential in several neurophysiological mechanisms such as the control of respiration (Erlichman et al., 2008), regulation of blood glucose for energy homeostasis (Lam et al., 2005; Lam et al., 2007), as well as arousal and food intake regulation (Parsons and Hirasawa, 2010). In addition, lactate metabolism has a significant function in the regulation of local cerebral blood flow in response to neuronal activity (Gordon et al., 2008), as well as fuel for the recovery of synaptic functions after hypoxia (Schurr et al., 1997b) and in neuroprotection (Berthet et al., 2009; Berthet et al., 2012). Lactate utilization is essential for the support of neuronal activity and cerebral functions in healthy and pathological conditions.

Besides this metabolic role, lactate, while in the extracellular space, may exert other actions on brain cells (Barros, 2013). The question of possible direct roles of lactate on neural function was proposed. Evidence has accumulated to support lactate-mediated signaling, which could

modulate the activity of multiple molecular targets affecting functions at the cellular and organ levels.

### Lactate, learning, and memory

Lactate has been described to be involved in learning and memory, notably for long-term memory formation (Newman et al., 2011; Suzuki et al., 2011; Descalzi et al., 2019; Harris et al., 2019). In 2011, two highly-cited papers revealed a link between lactate produced by astrocytes and learning and memory processing. Suzuki et al. (2011) reported that long-term memory formation and long-term potentiation maintenance are two mechanisms for which at least the lactate shuttle between astrocytes and neurons plays an essential role. By blocking the MCT2 neuronal lactate transporter or glycogen degradation in the hippocampus, the authors could disrupt long-term memory and decrease gene expression required for memory formation. Interestingly, administration of exogenous lactate could rescue memory formation when MCT2 was not blocked highlighting neuronal uptake of lactate as an essential process. The addition of glucose at equicaloric concentration only marginally mimicked the rescuing effect of lactate, which indicates the lactate mechanism of action was independent of its ability to act as an energy substrate (Suzuki et al., 2011). Then, Newman et al. (2011) supported the view that, in rat hippocampus, glycogenolysis in astrocytes and the subsequent production of lactate to support neuronal functions are important for the regulation of spatial working memory formation. This was later backed by a study showing that pyruvate and ketone body  $\beta$ -hydroxybutyrate can functionally replace lactate in rescuing memory impairment after glycogenolysis inhibition or astrocytic MCT1 and MCT4 inhibition by virus-mediated knockdown in rat hippocampus. However, both metabolites were unable to rescue memory impairment if neuronal MCT2 expression was suppressed using the same method, which indicates the significant role of astrocyte-derived lactate in memory processing (Descalzi et al., 2019). In addition, the authors described the importance of lactate to sustain learning-induced protein synthesis, a hallmark process required for long-term memory formation. Another study reported that the expression of synaptic plasticity-related genes such as *Arc*, *Fos-c*, and *Zif268*, which participate in different physiological processes associated with neuronal plasticity, seems to be stimulated by lactate (Yang et al., 2014). In this study, the authors demonstrated that lactate action is mediated by the

modulation of NMDA receptor activity and the downstream ERK1/2 signaling cascade, through a mechanism associated with changes in the cellular redox state. Recent *in vivo* experiments revealed the critical role of aerobic glycolysis and subsequent lactate release by astrocytes during memory acquisition rather than during retrieval and established memory in mice (Harris et al., 2019).

### Lactate and neuropathology

Lactate has also been reported to play a role in pathological conditions affecting the brain (Brooks, 2018). Different conditions, such as hypoxia, hyperglycaemia, brain trauma, or seizure, induce an increase in lactate levels in the brain (Mosienko et al., 2015). Lactate therapy has been in particular used after traumatic brain injury (TBI) (Bouzat et al., 2014), an injury that leads to high energy needs for recovery. Indeed, lactate utilization by the brain may be an alternative fuel to maximize energy functions and limit substrate reduction. Wolahan et al. (2018) investigated the impact of exogenous sodium L-lactate supplementation by constant intravenous infusion in TBI patients. The authors demonstrated an increase in total cerebral lactate uptake without changes in glucose availability or uptake, which could improve cerebral neuroenergetics by creating more ATP to support cellular recovery mechanisms (Wolahan et al., 2018).

Knowing that lactate may be beneficial for brain recovery processes, studies investigated its neuroprotective action, notably after cerebral ischemia. Berthet et al. (2009) showed that *in vitro* organotypic hippocampal slices that underwent oxygen and glucose deprivation and *in vivo* mice that underwent ischemia due to transient middle cerebral artery occlusion (MCAO), rapid superfusion and intracerebroventricular lactate injection, respectively, can protect against cell death, decrease lesion size, and improve neurological outcome (Berthet et al., 2009). The authors reported a long-term neuroprotective effect of intracerebroventricular injection of lactate in mice submitted to transient MCAO with improvement in the behavioural outcome and decrease in tissue destruction resulting in significantly smaller hemisphere atrophy at 14 days (Berthet et al., 2012). For clinically relevant utilization of lactate, they showed that intravenous injection of lactate is also able to provide neuroprotection after ischemia by decreasing lesion volume and neurological deficit 48h hours after transient MCAO in mice, as well as 24 hours after permanent MCAO (Buscemi et al., 2020). The same research group proposed that lactate, in addition to its

role as an alternative energy substrate, may exert a neuroprotective effect by acting on the HCAR1 lactate receptor in an *in vitro* model (Castillo et al., 2015). Independently of the enantiomer type, as well as the use of an HCAR1 specific agonist, a receptor-mediated signal transduction mechanism seems to confer neuroprotection. More recently, preclinical investigation used transient MCAO mice model that received an intracerebroventricular injection of lactate together with recombinant tissue plasminogen activator (rtPA), the only currently approved drug for blood clots removal in acute ischemic stroke. The authors observed a positive impact on functional outcomes and reduce harmful effects of rtPA, even though the neuroprotective effect is weaker compared to administration of lactate alone (Buscemi et al., 2020). This work offers a clearer understanding of the potential use of a lactate-based therapy for selected patients, namely patients not treated with rtPA. Currently, Prof. Lorenz Hirt started an exploratory randomized double blind placebo controlled trial on acute ischemic stroke patients, in which lactate solution or placebo will be administered (personal communication).

It has also been reported that lactate could present neuroprotective properties through coordinated mechanisms in case of excitotoxic environments. Jourdain et al. (2016) suggested that L-lactate increases the ATP production via the TCA cycle that, after putative release, stimulates specific purinergic receptors, in particular, the P2Y1 in hippocampal interneurons. P2Y1 stimulation then promotes synaptic inhibition of the neuronal network through the activation of the PI3-kinase pathway that leads to  $K_{ATP}$  channels activation (Jourdain et al., 2016).

#### Lactate and neuronal excitability

Recent studies have documented that lactate may also strongly affect neuronal excitability. In 2006, Gilbert et al. reported that elevated concentration of lactate suppresses neuronal firing *in vitro* in hippocampal slices cultures, and above all, *in vivo* in rat hippocampal pyramidal cells (Gilbert et al., 2006). The authors reported that lactate at high concentration (10mM) suppressed glucose oxidation *in vitro* but not at physiological concentration (1mM), even though glucose uptake was not altered. In addition, they postulated that the suppression of neural discharge and the glucose metabolism by lactate resides in the alteration of the redox ratio. Interestingly, GABAergic neurons of the subfornical organ, the center of the sensing responsible for the control of salt-intake behavior, seem also stimulated by lactate released from glial cells (Shimizu et al.,

2007). Another study has also demonstrated that lactate influences the activity of glucosensing neurons of the ventromedial hypothalamic neurons (VMN). Glucose-excited neurons increase, and glucose-inhibited neurons decrease, their action potential frequency as glucose increases from 0.1 to 2.5 mmol/l, however, lactate administration reversed the inhibitory effects of decreased glucose on VMN glucose-excited neurons via closure of the  $K_{ATP}$  channel. Lactate did not reverse the effects of decreased glucose on VMN glucose-inhibited neurons (Song and Routh, 2005). Orexin neurons, involved in food intake, autonomic functions such as hepatic glucose production, wakefulness, and arousal, seem to possess a mechanism that detects and controls lactate levels and/or gates brain activation accordingly (Parsons and Hirasawa, 2010). To show the capacity of orexin neurons to act as lactate sensors, the authors performed conventional whole-cell patch clamp on orexin neurons in hypothalamic slices incubated (>20 min) with different concentrations of lactate without glucose. The effect of lactate on the firing rate was found to be concentration dependent, confirming the role of lactate sensors of these neurons. Intriguingly, a recently published work using rat hippocampal slices describes distinctive firing patterns depending on the concentration of lactate in pyramidal cells (Herrera-Lopez and Galvan, 2018). However, this biphasic effect is receptor-dependent as shown by the use of a specific agonist of HCAR1. Low versus high concentration decrease and increase, respectively, the excitability of cell during injection of depolarizing current step. This receptor was mentioned for the first time to be involved in the modulation of neuronal activity in 2013 already by Bozzo et al. (2013). L-lactate (5mM) was able to reversibly decrease the calcium spiking frequency acquired during calcium imaging by more than 50% in both principal and GABAergic neurons in experiments carried out in the presence of 5mM glucose to ensure that neuronal energy metabolism needs are fulfilled. During the same period, other evidence for non-metabolic modulation of neuronal activity by lactate was described in the locus coeruleus (LC) (Tang et al., 2014). Optogenetically activated astrocytes release L-lactate which excites LC neurons and triggers the release of norepinephrine. Both in vitro and in vivo application of exogenous L-lactate in physiological concentration had an excitatory effect on the neuronal activity, independently of its role as energy substrates. This result indicates an opposite effect to what was found in our laboratory, suggesting the presence of another receptor sensitive to lactate.

These findings raise the question of whether receptor-mediated non-metabolic mechanisms of lactate could underlie some of lactate effects observed in the brain. This would confer additional roles on lactate such as that of a signaling molecule for neurons (Bergersen and Gjedde, 2012; Barros, 2013; Magistretti and Allaman, 2018).

### Hydroxycarboxylic Acid Receptors

The family of hydroxycarboxylic acid receptors is a subfamily of G-protein coupled receptors (GPCRs), composed of three receptors: initially named GPR81, GPR109A, and GPR109B and reported to be expressed in various cells and tissue (Lee et al., 2001). GPCRs are a large family of transmembrane receptors composed of 7 transmembrane domains and mediated effect through a G-protein composed of three elements,  $G\alpha$ ,  $G\beta$ , and  $G\gamma$ . In 2011, a new nomenclature was proposed for these receptors, based on the fact that all known endogenous ligands of GPR81, GPR109A, and GPR109B are hydroxycarboxylic acids. They possess similar agonists since they bind the metabolite 2-hydroxy-propanoate (lactate), the ketone body 3-hydroxy-butyrate, and the  $\beta$ -oxidation intermediate 3-hydroxy-octanoate, respectively (Cai et al., 2008). They were then classified as the hydroxy-carboxylic acid receptors (HCAR), with the individual names HCAR1 (GPR81) (**Figure 4**), HCAR2 (GPR109A), and HCAR3 (GPR109B) (Offermanns et al., 2011). The broad

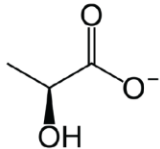
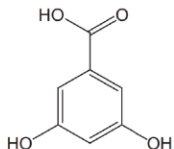
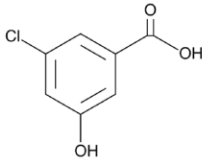
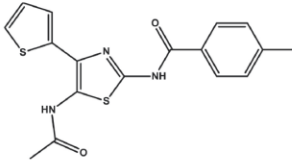
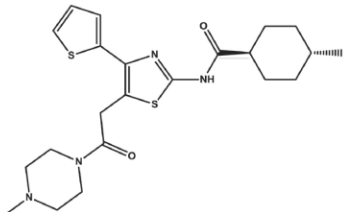
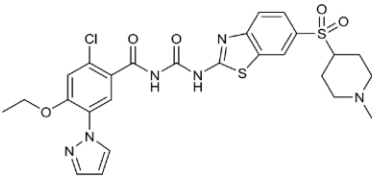
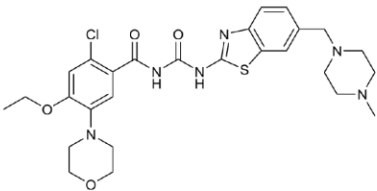


**Figure 4.** 3D structure of HCAR1 modeled by IntFOLD6 (<https://www.reading.ac.uk/bioinf/IntFOLD>) and created using Mol\* Viewer: modern web app for 3D visualization and analysis of large biomolecular structures (Sehna et al., 2021) and RCSB PDB.

expression of HCAR1 across the body tissues suggests that HCAR1 is capable to support a wide range of physiological functions. Indeed, HCAR1 has been shown to modulate metabolic processes and lipolysis in adipose tissue (Ahmed et al., 2010; Liu et al., 2012), neuronal excitability

and activity (Bozzo et al., 2013; Herrera-Lopez and Galvan, 2018; de Castro Abrantes et al., 2019; Herrera-López et al., 2020; Briquet et al., 2022), cellular development and survival (Roland et al., 2014), and inflammatory response (Hoque et al., 2014; Harun-Or-Rashid and Inman, 2018).

L-Lactate, the only known natural agonist of HCAR1 under physiological conditions, has an  $EC_{50}$  established at around 5 mM (Liu et al., 2009). The low potency of lactate as a ligand for HCAR1 (in the millimolar range) and its rapid metabolic turnover, cause a serious challenge for *in vivo* studies using lactate. It was therefore necessary to find an agonist to facilitate *in vivo* study of HCAR1 function. By screening hydroxylated carboxylic acids, Liu et al. (2012) identified a specific agonist named 3,5-dihydroxybenzoic acid (3,5-DHBA) with a  $EC_{50}$  value of  $191 \pm 26 \mu\text{M}$  in adipocytes. A few months later, 3-chloro-5-hydroxybenzoic acid (3Cl-HBA) was shown to be a more potent agonist than 3,5-DHBA with an  $EC_{50}$  value of  $\sim 22\mu\text{M}$  in mouse adipose tissue (Dvorak et al., 2012). Then, two new agonists, “Compound 1” (N-(5-acetamido-4-(2-thienyl)-1,3-thiazol-2-yl)-4-methylbenzamide) and compound 1-derived “Compound 2” (4-methyl-N-(5-(2-(4-methylpiperazin-1-yl)-2-oxoethyl)-4-(2-thienyl)-1,3-thiazol-2-yl)cyclohexanecarboxamide), were shown to have an  $EC_{50}$  value of  $810 \pm 93 \text{ nM}$  and  $58 \pm 5.4 \text{ nM}$ , respectively (Sakurai et al., 2014). More recently, new promising agonists were developed for HCAR1, named AZ1 (2-Chloro-4-ethoxy-N-[[6-[(1-methyl-4-piperidyl)sulfonyl]-1,3-benzothiazol2-yl]carbamoyl]-5-pyrazol-1-yl-benzamide) and AZ2 (2-Chloro-4-ethoxy-N-[[6-[(4-methylpiperazin-1-yl)methyl]-1,3-benzothiazol2-yl]carbamoyl]-5-morpholino-benzamide), with an  $EC_{50}$  value of 5 to 20 nM and 70 to 180 nM, respectively (Wallenius et al., 2017) (**Figure 5**). It is important to mention that there is no synthetic or natural specific antagonist available for HCAR1 rendering the investigation of its functional role more complicated.

HCAR1 agonists	Chemical structures	EC <sub>50</sub>
<b>Physiological agonist</b>		
Lactate (Cai et al., 2008)		5 mM
<b>Pharmacological agonists</b>		
3,5-DHBA (Liu et al., 2012)		190 μM
3Cl-HBA (Dvorak et al., 2012)		22 μM
Compound 1 (Sakurai et al., 2014)		810 nM
Compound 2 (Sakurai et al., 2014)		50 nM
AZ1 (Wallenius et al., 2017)		5-20 nM
AZ2 (Wallenius et al., 2017)		70-180 nM

**Figure 5.** Currently available agonist of HCAR1 and their corresponding EC<sub>50</sub>.



## Signaling pathways of HCAR1

HCAR1 is a  $G_i$ -type G protein coupled receptor (Ge et al., 2008; Ahmed et al., 2010) that modulates related signaling pathways. In adipose tissue, activation of HCAR1 leads to adenylyl cyclase (AC) activity and subsequent cAMP production decrease, and the downstream protein kinase A (PKA) activity decrease as well, resulting in lipolysis inhibition (Ahmed et al., 2010). In the brain, these observations were confirmed by pharmacological manipulations. Bozzo et al. (2013) showed that the receptor was sensitive

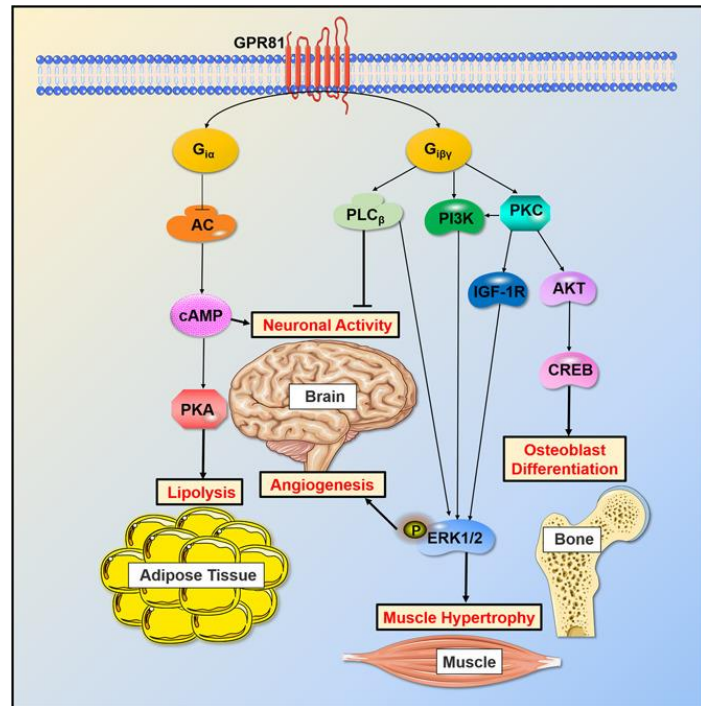


**Figure 6.** Summary of downstream pathway activation by HCAR1 from (Hu et al., 2020)

to pertussis toxin (PTX), a  $G_{i\alpha}$  subunits inhibitor, confirming the activation of this transduction cascade. Interestingly, de Castro Abrantes et al. (2019) showed that HCAR1 also interacts with the  $G_{i\beta\gamma}$  subunits, which regulates phospholipase C (PLC) to reduce neuronal excitability in a different manner than through the  $G_{i\alpha}$  pathway. Several other downstream pathways have been identified for HCAR1-mediated signaling (**Figure 6**) (Hu et al., 2020).

## Localization of HCAR1

So far, the importance of HCAR1 has been described in the adipose tissue (Ahmed et al., 2010), the gut (Ranganathan et al., 2018), the stomach (Engelstoft et al., 2013), the immune system (Hoque et al., 2014; Lerch et al., 2014), the muscles (Rooney and Trayhurn, 2011; Sun et al., 2016), the brain (Bozzo et al., 2013; de Castro Abrantes et al., 2019; Briquet et al., 2022), the kidney (Blad et al., 2011; Wallenius et al., 2017; Jones et al., 2020), the liver (Blad et al., 2011; Offermanns, 2017), the pancreas (Hoque et al., 2014) and the blood vessel (Morland et al., 2017; Sun et al., 2019). This wide expression of the receptor shows the importance of the HCAR1 in physiological functions throughout the body.

In the brain, widespread HCAR1 mRNA expression was shown using *in situ* hybridization technique, which revealed that the distribution was neuron predominant, including principal neurons in the cortex, hippocampal pyramidal and granule cells, and cerebellar granule cells, while astrocytic cells cannot be excluded (The Allen Institute for Brain Science, <http://www.brain-map.org>; GENSTAT, <http://www.gensat.org>). Moreover, quantitative Real-Time Polymerase Chain Reaction (qRT-PCR) data showed expression of HCAR1 in the cerebellum, the hippocampus, and the cortex with a relative GPR81 mRNA level ~140 fold smaller than in omental adipose tissues (Lauritzen et al., 2014). Few studies tried to precisely localize HCAR1 using immunohistochemistry (Bozzo et al., 2013; Lauritzen et al., 2014). However, because current commercial HCAR1 antibodies lack specificity (Wallenius et al., 2017; de Castro Abrantes et al., 2019), the precise expression and localization of HCAR1 in the brain are still ambiguous. When HCAR1-deficient mice became available (Ahmed et al., 2010), our lab tested nine commercial primary HCAR1 antibodies with different epitope specificities and found that none was specific for HCAR1 (de Castro Abrantes et al., 2019). During this thesis work, five additional antibodies were found not to be specific (see **Supplementary Figure 1**). We, therefore, selected different approaches by using new *in situ* hybridization technology and a transgenic mouse line that expresses a red fluorescent protein under the HCAR1 promoter (mRFP-HCAR1) (Ahmed et al., 2010) to identify HCAR1-expressing cells in the mouse brain (Briquet et al., 2022).

### HCAR1 functions in the body

As mentioned previously, HCAR1 is expressed in various tissues and not only in the brain. In this chapter, we will better understand the role of this receptor in the periphery. White and brown adipose tissue was the first tissue in which HCAR1 was described (Cai et al., 2008; Ahmed et al., 2010; Wanders et al., 2012). In adipose tissue, glucose is converted to lactate under the influence of insulin and evidence showed that lactate, through the activation of HCAR1, decreases lipolysis via the reduction of free fatty acid (FFA) and glycerol release (Ahmed et al., 2010). It is intriguing to see that HCAR1 knock-out (KO) mice lose their insulin induced anti-lipolytic effect, which suggests a possible synergic effect of insulin (Cai et al., 2008; Liu et al., 2009; Ahmed et al., 2010; Liu et al., 2012; Wallenius et al., 2017). Interestingly, it has also been demonstrated that the levels of HCAR1 expression can change depending on the diet (Wanders

et al., 2012) and together with the sex of the animal (Kwon et al., 2020), as well as a 10% weight reduction in HCAR1 KO mice compared to wild-type (WT) after high-fat diet (Ahmed et al., 2010). When WT mice are fed with high-fat diet, male, but not female, mice gain body weight and develop hyperglycemia. In addition, WT male showed a reduced expression of HCAR1 in brown adipose tissue, where HCAR1 is upregulated in female WT (Wanders et al., 2012).

Moreover, inflammation seems to also negatively control the level of expression of HCAR1. Infections and inflammation are responsible for a wide range of metabolic changes in the body, including a marked alterations in lipid metabolism characterized by an increase in serum FFA levels coming from the breakdown of triglycerides stored in adipose tissue. Feingold et al. (2011) demonstrated that, after treatment by a model of bacterial infections, HCAR1 mRNA levels were markedly decreased suggesting that HCAR1 could be involved in the regulation of the inflammatory response to some extent.

HCAR1 has also been demonstrated to be important for intestinal homeostasis through a complex interaction with the immune system, which ensures a fine balance between an immune response against pathogenic bacterial antigen and a tolerance for commensal bacterial and food antigen (Ranganathan et al., 2018). The study reports that HCAR1-mediated signaling in colonic dendritic cells and macrophage plays an important role in suppressing colonic inflammation and restoring colonic homeostasis through inhibition of pro-inflammatory cytokines (IL-6, IL-1 $\beta$ , and TNF- $\alpha$ ) and stimulation of anti-inflammatory cytokines IL-10 secretions (Ranganathan et al., 2018). HCAR1 seems therefore to be essential for maintaining a proper environment in the gut and preventing inflammation and colitis. Convergent results toward inhibition of inflammatory factors by HCAR1 were demonstrated by Madaan et al. (2017). Activation of HCAR1 by either lactate or 3,5-DHBA could reduce mice uterus inflammation during labor by inhibiting inflammatory factors such as IL-6, IL-1 $\beta$ , and MMP9 expression. At the organ level, injuries induce inflammation via the recruitment of the NLRP3 inflammasome through toll-like receptors (TLRs) signaling, also responsible for stimulation of aerobic glycolysis and subsequent generation of lactate (Hoque et al., 2014). Specifically, in macrophages and monocytes, increasing concentrations of lactate reduced TLR4-mediated induction of the inflammasome and pro-inflammatory response players by HCAR1 activation (Hoque et al., 2014).

Finally, HCAR1 has been found to be implicated in the pathogenesis of atherosclerosis (Sun et al., 2019), an inflammatory disease of the arteries characterized by the accumulation of a fatty substance called plaque between the layers of the endothelium in places where the vasculature is subject to oscillatory shear stress (OSS). It has been demonstrated that endothelial cells have up to 50% reduced expression of HCAR1 in response to OSS at both the protein and mRNA levels whereas the level of HCAR1 is increased when cells are subjected to high shear stress, demonstrating that shear stress can change the level of expression of HCAR1 (Sun et al., 2019). Interestingly, OSS-mediated downregulated HCAR1 expression can be restored by physiological concentration of lactate, and the following activation of the receptor significantly reduces oxidative stress and subsequent expression of pro-inflammatory cytokines.

### HCAR1 functions in the brain

In this introduction, I discussed several metabolic and signaling functions of lactate in the brain. However, the involvement of the receptor HCAR1 was not necessarily described. In this chapter, I will focus more specifically on HCAR1-mediated lactate functions in the brain.

Back in 2013, our group was the first to demonstrate that activation of HCAR1 in neuronal primary cultures was sufficient to decrease spontaneous calcium spiking frequency (Bozzo et al., 2013). In presence of glucose to sustain energy metabolism, a concentration of lactate (5mM) was presented to both glutamatergic and GABAergic primary neurons. Results indicated that neuronal action potential measured by calcium imaging was decreased by more than 50% in both neuronal subtypes in a reversible manner. As previously noted, L-lactate can be converted into pyruvate by the LDH and enter the TCA cycle leading to ATP production and potential membrane conductance modifications. To invalidate this possibility, pyruvate (5mM), as well as glucose (0.5 and 10mM) were applied and results indicated a negligible decrease of neuronal activity (7%) and no influence, respectively. In addition, D-lactate, the poorly metabolized stereoisomer of L-lactate, showed a similar decrease in neuronal activity, indicating one more time the involvement of HCAR1. Finally, pharmacological activation of HCAR1 by the specific agonist 3,5-DHBA was shown to inhibit neuronal activity by 33%. Following this work that showed HCAR1-mediated signaling in the brain, our group continued to investigate the lactate receptor and characterized associated intracellular pathways influencing neuronal activity. In the study of de Castro Abrantes

et al. (2019), to which I had the chance to contribute, we found using whole-cell patch clamp that the activation of HCAR1 with 3Cl-HBA decreased miniature excitatory post-synaptic current (mEPSC) frequency, increased paired-pulse ratio, decreased firing frequency, and modulated membrane intrinsic properties of primary neurons. Together, these results indicated that HCAR1 seems to influence neuronal activity of primary cortical neurons both pre- et post-synaptically. Moreover, using pharmacological manipulations, the study confirmed that downstream effectors of the  $G_i$ -protein intracellular pathways were involved. The increased activity due to forskolin application, an AC activator, was reversed by HCAR1 activation. Interestingly, control experiments using HCAR1 KO mice indicating a higher increased neuronal activity upon forskolin application suggesting a tonic inhibition operated by HCAR1. cAMP levels and PKA activity were also shown to be involved in the modulation of neuronal activity by HCAR1 (de Castro Abrantes et al., 2019). In another study, a similar decrease in cAMP levels was reported in hippocampal rat slices after activation of HCAR1 by either L-lactate or 3,5-DHBA, confirming that HCAR1 signaling is mediated by  $G_i$ -coupled receptor (Lauritzen et al., 2014).

Recently, papers published by the same group (Herrera-Lopez and Galvan, 2018; Herrera-López et al., 2020) investigated the role of HCAR1 in rat hippocampal pyramidal neurons of the CA1 and CA3 using whole-cell patched clamp. The authors showed that lactate induces a biphasic effect on neuronal excitability of CA1 pyramidal cells (Herrera-Lopez and Galvan, 2018). Lower concentrations of lactate (5mM) or 3,5-DHBA (0.56mM) reduced the firing frequency, whereas higher concentrations (30mM and 3.1mM respectively) increased the action potential discharge. As observed in primary neuronal culture, experiments in acute slices showed that activation of the receptors seems to modulate intrinsic properties of CA1 pyramidal cells, notably with a decreased input resistance and an increased rheobase indicating the inhibitory impact of HCAR1. In addition, observations made in the CA3 demonstrated that lactate and 3,5-DHBA induce glutamatergic potentiation on the recurrent collateral of synapse of the CA3 pyramidal neurons, however not at the mossy fiber synapses (Herrera-López et al., 2020). This form of synaptic plasticity seems therefore to be input-specific. Surprisingly, the authors reported the involvement of a lactate receptor, HCAR1 or a maybe yet unidentified  $G_s$  protein-coupled

receptor, and the  $G_{\beta\gamma}$  subunits downstream signaling cascade involving inositol-1,4,5-trisphosphate 3-kinase, PKC, and CaMKII.

Up to now, HCAR1 was shown to be involved in many mechanisms as shown by the non-exhaustive list presented above. It seems that HCAR1 participates in the regulation of the activity in different regions and types of neurons across species. In addition, the role of HCAR1 in the human brain remains unknown and needs to be investigated.

In the study presented in this thesis, we demonstrated that cortical neurons from human pharmaco-resistant patients decrease their excitability, spontaneous neuronal calcium spiking, and spontaneous EPSC (sEPSC) upon activation of HCAR1. We also describe how the activation of HCAR1 tunes down neuronal network activity in mouse and rat dentate gyrus (DG). The human and rodent results that we present here enable us to propose that HCAR1 represents a novel clinically relevant therapeutic target for pathologies characterized by network hyperexcitability dysfunction, such as epilepsy.

## Results

### Preamble

During my thesis, we aimed at better understanding the role of the receptor HCAR1. We first demonstrated in primary neurons the modulation of the neuronal activity by the receptor and described parts of its transduction cascade responsible for this modulation. I had the chance to participate in this study published in Journal of Neuroscience (de Castro Abrantes et al., 2019) (**appendix 2**). In my thesis project, we hypothesized that this modulation would be present in conserved neuronal circuits. We investigated the modulatory functions of HCAR1 in the DG, a region found to express the receptor, using an ex-vivo approach. In addition, we showed for the first time that human brain samples from epileptic patients also express the receptor and that neurons can be modulated by the activation of HCAR1. These results are published in Journal of cerebral blood flow and metabolism (Briquet et al., 2022). We also raised the question of the possibility to develop a new tool capable of measuring extracellular lactate in the brain. Indeed, such a tool would be beneficial for precisely analyzing lactate concentration fluxes within living tissues and in specific microdomains, such as the synaptic environment. To do so, we built a genetically encoded fluorescent lactate biosensor based on HCAR1 protein and a cpGFP. Despite promising results, further development remains to be done to reach a useable tool. This research is published in Biosensor (Wellbourne-Wood et al., 2022).

### Study 1

Activation of lactate receptor HCAR1 down-modulates neuronal activity in rodent and human brain tissue

#### Summary of the results

In this study, we describe how HCAR1 down-modulates the activity of human cortical neurons in acute slices prepared from brain samples from epileptic pharmacoresistant patients. We demonstrate a decrease in excitability, spontaneous neuronal calcium spiking activity, and synaptic activity upon activation of HCAR1. We further explored the role and the localization of HCAR1 in the rodent central nervous system, where it is predominantly found in the hippocampus and dentate gyrus, especially on mossy cells. In both mice and rats, we describe

how the activation of HCAR1 tunes down neuronal network activity in the dentate gyrus, a brain region critically involved in learning and memory, as well as in temporal lobe epilepsy.

### Personal contribution

In this study, I performed and analyzed the experiments performed on rodents model. Together with my colleagues, Anne-Bérengère-Rocher, Nadia Rosenberg, Haissa de Castro Abrantes, Joel Wellbourne-Wood, and I, participated in the recording of human cells. We collaborate with the group of Dr. Julien Puyal from our institute for the qRT-PCR experiments. Some immunohistochemistry and patch-clamp experiments were performed by Maxime Alessandri, a former master student, who worked under my supervision. Moreover, I contributed to the experimental design together with Anne-Bérengère Rocher et Jean-Yves Chatton. I also wrote the manuscript with Jean-Yves Chatton.



# Activation of lactate receptor HCARI down-modulates neuronal activity in rodent and human brain tissue

Marc Briquet<sup>1,\*</sup>, Anne-Bérengrère Rocher<sup>1,\*</sup>,  
Maxime Alessandri<sup>1</sup>, Nadia Rosenberg<sup>1</sup>,  
Haissa de Castro Abrantes<sup>1</sup>, Joel Wellbourne-Wood<sup>1</sup>,  
Céline Schmuziger<sup>1</sup>, Vanessa Ginet<sup>1</sup>, Julien Puyal<sup>1</sup>,  
Etienne Pralong<sup>2</sup>, Roy Thomas Daniel<sup>2</sup>, Stefan Offermanns<sup>3</sup>  
and Jean-Yves Chatton<sup>1,4</sup>

Journal of Cerebral Blood Flow &amp;

Metabolism

0(0) 1–16

© The Author(s) 2022



Article reuse guidelines:

[sagepub.com/journals-permissions](https://sagepub.com/journals-permissions)

DOI: 10.1177/0271678X221080324

[journals.sagepub.com/home/jcbfm](https://journals.sagepub.com/home/jcbfm)

## Abstract

Lactate can be used by neurons as an energy substrate to support their activity. Evidence suggests that lactate also acts on a metabotropic receptor called HCARI, first described in the adipose tissue. Whether HCARI also modulates neuronal circuits remains unclear. In this study, using qRT-PCR, we show that HCARI is present in the human brain of epileptic patients who underwent resective surgery. In brain slices from these patients, pharmacological HCARI activation using a non-metabolized agonist decreased the frequency of both spontaneous neuronal  $Ca^{2+}$  spiking and excitatory post-synaptic currents (sEPSCs). In mouse brains, we found HCARI expression in different regions using a fluorescent reporter mouse line and *in situ* hybridization. In the dentate gyrus, HCARI is mainly present in mossy cells, key players in the hippocampal excitatory circuitry and known to be involved in temporal lobe epilepsy. By using whole-cell patch clamp recordings in mouse and rat slices, we found that HCARI activation causes a decrease in excitability, sEPSCs, and miniature EPSCs frequency of granule cells, the main output of mossy cells. Overall, we propose that lactate can be considered a neuromodulator decreasing synaptic activity in human and rodent brains, which makes HCARI an attractive target for the treatment of epilepsy.

## Keywords

Dentate gyrus, electrophysiology, epilepsy, HCARI receptor, human brain slices

Received 1 October 2021; Revised 22 December 2021; Accepted 24 January 2022

## Introduction

Lactate is recognized as an energy substrate for neurons.<sup>1,2</sup> It can be provided to neurons by transport from astrocytes to the extracellular space, thereafter entering neurons through monocarboxylate transporters (MCTs),<sup>3</sup> as well as from the blood stream. The extracellular brain lactate level is estimated to be in the low millimolar range at resting state<sup>4,5</sup> and to undergo a two-fold increase during synaptic activity.<sup>6</sup> During intense physical exercise, plasma lactate, which can cross the blood-brain barrier, can rise to 10–20 mM.<sup>7</sup> Besides this metabolic role, lactate, while in the extracellular space, may exert other actions on

<sup>1</sup>Department of Fundamental Neurosciences, University of Lausanne, Lausanne, Switzerland

<sup>2</sup>Department of Neurosurgery Service, University Hospital of Lausanne and Faculty of Biology and Medicine, UNIL, Lausanne, Switzerland

<sup>3</sup>Max Planck Institute for Heart and Lung Research, Bad Nauheim, Germany

<sup>4</sup>Cellular Imaging Facility, University of Lausanne, Lausanne, Switzerland

\*These authors contributed equally to this work.

### Corresponding author:

Jean-Yves Chatton, Dept. of Fundamental Neurosciences, University of Lausanne, Rue Bugnon 9, CH-1005 Lausanne, Switzerland.

Email: [jean-yves.chatton@unil.ch](mailto:jean-yves.chatton@unil.ch)

brain cells,<sup>8</sup> notably for long-term memory formation.<sup>9–11</sup> Studies have reported that lactate can also influence the excitability of select populations of neurons via different metabolic pathways. Lactate was found to change the firing frequency of glucose-sensing neurons of hypothalamic and GABAergic neurons of the subfornical organ,<sup>12</sup> the center for the control of salt intake behavior. Studies have also demonstrated that lactate influences the activity of glucose-sensitive ventromedial hypothalamic neurons<sup>13</sup> and orexin neurons.<sup>14</sup> Lactate was shown to be necessary for inducing plasticity-related genes expression in neurons through potentiation of NMDA receptor activity.<sup>15</sup> Evidence for L-lactate-mediated excitation of neuronal activity triggering norepinephrine release was described in the locus coeruleus.<sup>16</sup> These findings raise the question of whether receptor-mediated non-metabolic mechanisms of lactate could underlie these effects in the brain. This would confer additional roles on lactate such as that of a signaling molecule for neurons.<sup>3,17</sup>

In this context, a new family of G-protein coupled receptors (GPCR) called hydroxycarboxylic acid receptors (HCAR) has recently been identified in adipocytes.<sup>18</sup> HCARs are activated by several intermediates of cellular energy metabolism. Among them, HCAR1 (named GPR81 before being orphanized) is considered to be a sensor for lactate in peripheral organs.<sup>19,20</sup> HCARs are reported to be coupled to G<sub>i</sub> proteins<sup>20</sup> and their activation has antilipolytic effects.<sup>21–23</sup> Recently, we and other labs have demonstrated that HCAR1 is present in brain cells.<sup>23–25</sup> HCAR1 expression was found to be enhanced in models of ischemic stroke 24 hours after reperfusion,<sup>26</sup> which was accompanied with a reduction of cell death.

However, because current commercial HCAR1 antibodies lack specificity,<sup>27,28</sup> the precise expression and localization of HCAR1 in the brain is still ambiguous. At the functional level, our group confirmed that HCAR1 is active at the membrane of cultured primary cortical neurons.<sup>24,27</sup> Its activation by lactate was concentration-dependent and was not consistent with a metabolic effect, considering that it was not observed with glucose and even the closely related metabolite pyruvate. Lactate and non-metabolized agonists of HCAR1 caused a reversible, concentration-dependent decrease in spiking activity, an effect that was absent in HCAR1-deficient mice (HCAR1 KO). The intracellular mechanisms involves the inhibition of the adenylyl cyclase – cAMP – protein kinase A axis which leads to a decreased synaptic vesicular release and reduction of excitability,<sup>27</sup> which was also reported in rat hippocampal CA1 neurons.<sup>29</sup>

In this study, we investigated the specific localization and function of HCAR1 in brain tissue. We report

that HCAR1 is expressed in the human and mouse brain. We used HCAR1 fluorescent reporter mice and new *in situ* hybridization technology to map the expression of HCAR1 in the mouse brain in specific neuronal population including sub-regions of the hippocampus and cerebellum. At the functional level, we show a neuromodulation caused by HCAR1 activation in the dentate gyrus (DG) of the hippocampus in mouse and rat. Importantly, this modulation is also present in fresh human cortical slices. Indeed, HCAR1 activation by non-metabolic ligands cause a decrease in firing and spontaneous excitatory postsynaptic current (sEPSCs) frequency. We therefore demonstrate that HCAR1 drives negative metabolic feedback on neuronal activity *in situ* both in rodent brain tissue and in human epileptic tissue.

### Material and methods

**Human tissue experiments.** Human tissue was made available for experiments within an experimental framework approved by the Cantonal Ethics Committee on human research (CER-VD, protocol number 207/10) and procedures. Brain tissue samples resected from patients undergoing surgery at the Service of Neurosurgery of Lausanne University Hospital (CHUV) were used for *in vitro* neuronal activity recordings. Patients provided written informed consent to participate in the study, which operated in accordance with the ethical standards of the institutional national research committee and with the 1964 Helsinki declaration and its later amendments.

Human tissue is classified as ‘epileptic’ as it originated from resected tissue of the epileptogenic locus of patients with dysplasia (or other forms of epilepsy) and who were pharmacoresistant. Brain samples were from both male (57%) and female (43%) patients with median age 18 years, and originated from frontal (n = 5), insular (n = 2), parietal (n = 1), and temporal (n = 9) cortex from both hemispheres.

**Animal tissue experiments.** All animal experimentation procedures were carried out in accordance with the recommendations of the Swiss Ordinance on Animal Experimentation, and were specifically approved for this study by the Veterinary Affairs of the Canton Vaud, Switzerland (authorizations# VD1288.6-7-8 and VD2927d) and conformed to the ARRIVE guidelines. Animals were housed at our local animal facility with *ad libitum* access to food and water (maximum 5 animals per cage) before euthanasia for brain tissue preparation. Male C57BL/6N and HCAR1 KO<sup>21</sup> mice (18–25 days old) were used for experiments. Transgenic mice (male 20 days old) that expresses monomeric red fluorescent protein (mRFP) under the

HCAR1 promoter generated and validated as previously described was used for HCAR1 localization.<sup>21</sup> This fluorescent reporter protein is not targeted to the plasma membrane but spreads in the cytoplasm, allowing us to identify the cells which endogenously express the HCAR1 transcripts. Male Sprague Dawley (30–35 days old) were used for experiments.

**qRT-PCR.** Human tissue from patient and dissected brain from C57BL/6N mice at P7 (n = 3), P14 (n = 3), and P31 (n = 6) were instantaneously frozen in liquid nitrogen. In another group of P31 mice, brain was further dissected out into different brain regions (cerebellum, hippocampus, brainstem and cortex). Extraction and purification of RNA were done using the RNeasy Mini Kit (Qiagen, Basel, Switzerland, n°74104) following the protocol from the manufacturer. RNA assay and analysis was performed with Agilent RNA 6000Nano Kit (Agilent Technologies, Santa Clara, Ca, USA, n°5067-1511). Reverse transcriptase was carried out with High-Capacity cDNA Reverse Transcription Kit (Applied biosystems, Ca, USA, n°4368814). qPCR for hydroxy-carboxylic acid receptor 1 (HCAR1) was normalized with the housekeeping gene  $\beta$ -actin for the human tissue and GAPDH for the mouse tissue. Primer pair sequences (Supplementary Table 1) was carried out in the CFX Connect™ Real-Time System (BioRad, California, USA) using the iQ SYBR® Green Supermix 2x (Bio-Rad, n°1708880) for the human tissue and in the CFX96 Touch Real-time PCR detection system (BioRad) using the Power SYBR Green PCR Master mix (BioRad) for the mouse tissue. All samples were run in triplicate. The homogeneity of the triplicates was assessed calculating the percentage of difference between them  $[(SD/mean)*100]$  and the ones that had a difference bigger than 2% were eliminated. For analysis, all Cq values were rescaled for each gene to the lowest Cq value as an internal control, converted these

rescaled Cq logarithmically into linear, relative quantities taking into account the gene specific amplification efficiency [relative quantity =  $1 + \text{efficiency}^{(Cq_{\text{internal control}} - Cq_{\text{sample}})}$ ]. Finally, arithmetical means were obtained as means from the triplicates. Expression of HCAR1 was then normalized to the reference gene.

**Immunohistochemistry.** mRFP mice were anesthetized with sodium-pentobarbital (150 mg/kg, intraperitoneally) and transcardially perfused with fresh solutions of 4% paraformaldehyde (PFA) in phosphate buffered saline (PBS) 0.1 M (pH 7.4) for 10 min. Brain extraction was followed with 24 h post-fixation at 4°C with 4% PFA. Afterwards, both hemispheres were sliced in PBS at 50  $\mu$ m with a vibratome (Leica, VT1000S).

Fixed slices were then rinsed 3 times in PBS prior to a 2-hour incubation in blocking solution (10% donkey serum and 0.1% Triton X-100 diluted in PBS) at room temperature (RT). Slices were then incubated overnight (O/N) at 4°C with primary antibodies (Table 1). Next, slices were washed 3 times in PBS and incubated 2 hours at RT with respective secondary antibodies. For nuclei staining, Hoechst (2  $\mu$ g/ $\mu$ l) a 10-minute incubation was performed. Finally, stained slices were mounted on slides using FluorSave mounting medium (Merck-Millipore, Darmstadt, Germany).

Imaging of mRFP stained sections was performed using a Zeiss LSM780 confocal laser scanning microscope (Zeiss, Oberkochen, Germany) outfitted with a 63X 1.40 NA Plan Apochromat oil immersion objective lens.

**Two-photon imaging.** Two-photon imaging of endogenously expressed mRFP in mouse acute brain slices of 300  $\mu$ m was carried out using a custom-built two-photon microscope with a 40X 0.8 N.A. water-dipping objective (Olympus, Tokyo, Japan). Fluorescence excitation was performed using a Chameleon Vision S femtosecond infrared laser

**Table 1.** Primary and secondary antibodies used in the study.

	Source	Catalogue number	Concentration
<b>Primary antibodies</b>			
Rabbit anti-mRFP	Rockland Immunochemicals	600-401-379	1:1000
Rat anti-mRFP	Chromotek	AB_2336064	1:100
Rabbit anti-GluR2/3	Merck-Millipore	07-598	1:400
Mouse anti-GFAP	Sigma-Aldrich	G3893	1:200
Mouse anti-NeuN	Merck-Millipore	MAB377	1:200
Mouse anti-GAD67	MAB5406 Merck-Millipore	MAB5406	1:1000
<b>Secondary antibodies</b>			
Donkey anti-rabbit IgG Alexa Fluor 594	Invitrogen	A21207	1:200
Donkey anti-mouse IgG Alexa Fluor 488	Invitrogen	R37114	1:200
Donkey anti-rat IgG Alexa Fluor 488	Invitrogen	A48269	1:200

including group velocity dispersion compensation (Coherent, Ca, USA). Captured emission wavelengths were  $607 \pm 70$  nm for red channel. Image acquisition was performed using custom-written software in the Labview environment. ImageJ software (RRID:SCR\_003070) was further used for downstream image processing.

**In situ hybridization – RNAscope™.** C57BL/6N mice were deeply anesthetized with sodium-pentobarbital and transcardially perfused with 50 ml of 4% PFA in 0.1 M PBS (pH 7.4). Brains were dissected out and post-fixed in 4% PFA for 24 h at 4°C. The tissues were then washed 3 times with PBS and cryoprotected in 10% (O/N at 4°C), 20% (O/N at 4°C) and 30% (O/N at 4°C) sucrose in PBS. Tissues were embedded in Tissue-TEK O.C.T. compound (Sakura Finetek, Torrance, Ca, USA) sectioned at 14  $\mu$ m with a cryostat (Leica, CM3050 S), and mounted onto Superfrost Ultra Plus slides (Thermo Fischer Scientific, Waltham, MA, USA). For *in situ* hybridization (RNAscope™, Advanced Cell Diagnostics, San Francisco, CA, USA), the manufacturer's protocol was followed. All experiments were replicated in three animals. The probes were designed by the manufacturer and available from Advanced Cell Diagnostics. The following probe was used in this study: Mm-GPR81-C1 (#4317421).

**Human: Electrophysiology and calcium imaging.** After resection, cortical tissue was quickly placed in ice-cold artificial CSF (aCSF) slicing solution continuously bubbled with 95% O<sub>2</sub>/5% CO<sub>2</sub> and that contained (mM): 110 choline chloride, 26 NaHCO<sub>3</sub>, 10 D-glucose, 11.6 ascorbic-acid, 7 MgCl<sub>2</sub>, 3.1 Na-pyruvate, 2.5 KCl, 1.25 NaH<sub>2</sub>PO<sub>4</sub>, and 0.5 CaCl<sub>2</sub>.<sup>30</sup> The tissue was then swiftly transported to the neurophysiology laboratory. Transition time from tissue resection to slice preparation was approximately 10 min. Tissue was placed in a petri dish containing ice-cold and oxygenated slicing solution for removal of the pia, if necessary, and orientation in order to slice perpendicular to the white matter. The tissue blocks were then glued on mounting plate and submerged in slicing chamber filled with ice-cold slicing solution. Slices are cut at 340  $\mu$ m and then transferred to a holding chamber in which they were stabilized for 20 min at 34°C. Subsequently, slices were stored for at least 1 h at RT before recording in aCSF containing the following (mM): 125 NaCl, 26 NaHCO<sub>3</sub>, 3 KCl, 1.25 NaH<sub>2</sub>PO<sub>4</sub>, 1 MgSO<sub>4</sub>, 2 CaCl<sub>2</sub>, 3 myo-inositol, 3 Na-pyruvate, 0.5 ascorbic acid, and 10 glucose. Recording aCSF solution was similar to holding solution with glucose reduced to 2.5 mM.

For recording, each slice was transferred in a double perfusion recording chamber submerged in recording

aCSF (34°C) and attached to the stage of a Zeiss LSM510 Meta upright microscope equipped with infrared differential interference contrast and 40X water dipping objective. Whole-cell patch-clamp recordings were made from pyramidal cells using standard  $\sim 5$  M $\Omega$  borosilicate glass pipettes filled with the internal solution containing (mM): 130 K-gluconate, 5 KCl, 5 NaCl, 1 MgCl<sub>2</sub>, 0.1 EGTA, 0.025 CaCl<sub>2</sub>, 10 HEPES; 5 Na-phosphocreatine; 4 Glucose, 4 ATP-Mg; 0.3 GTP-Na, biocytin 1 mg/ml (pH = 7.3 adjusted with KOH, 290 mOsm). Recordings were obtained in voltage- and current-clamp configuration with a Multiclamp 700B amplifier (Molecular Devices, San José, CA, USA). Data were acquired with a Digidata 1440 A (Molecular Devices), at 10 kHz sampling rate and filtered at 2 kHz, controlled with pCLAMP 10 software (RRID:SCR\_011323). Access resistance was monitored by a  $-5$  mV step (0.1 Hz). Experiments were discarded if the access resistance varied by more than 20%. Spontaneous excitatory post-synaptic events (sEPSCs) were recorded for 2 min from a holding potential of  $-80$  mV in the absence and in the presence of 3Cl-HBA (40  $\mu$ M). Stable (otherwise rejected) sEPSCs recordings were manually analyzed offline using the MiniAnalysis software (Synaptosoft Inc, USA, RRID:SCR\_002184). For each cell, the frequency and the amplitude of these synaptic events were analyzed. We further assessed cell passive properties and firing frequency in control conditions and after HCAR1 activation. A series of positive and negative current steps (30 pA increments, starting from  $-120$  pA) of 2000 ms duration were injected to measure the firing frequency. Action potential (AP) frequency was measured as the number of AP in response to 540 pA current injection. Input resistance was determined by passing current steps (2000 ms, with 30 pA increments from  $-120$  to 0 pA), and calculated as the slope of the current-voltage plot. The rheobase was determined as the minimal current amplitude able to evoke an AP, and was obtained by applying 3-sec steps of positive current (starting at 0 pA, 50 pA increments). These cell passive properties and firing frequency were recorded control conditions (baseline) and after HCAR1 activation. At the end of recordings, slices were fixed and processed with streptavidin-AlexaFluor 647 (1:500, Invitrogen, Catalog # S21374) for morphological characterization.

Neuronal activity was also monitored by calcium imaging using the membrane-permeant dyes Fluo-4 AM (Teflabs, Austin, TX, USA) or Fluo-8 AM (Abcam, Cambridge, UK), diluted at 1 mM in DMSO and applied by bolus loading using a pressure ejection system (Picospritzer II, General Valve, or Toohey Company) imaged by wide-field fluorescence or two-photon microscopy. Widefield calcium imaging



was performed with an upright epifluorescence microscope (FN1, Nikon, Tokyo, 163 Japan) using a 40X 0.8 N.A. water-immersion objective lens. Fluorescence excitation wavelengths were selected using a fast filter wheel (Sutter Instr., Novato, CA) and fluorescence was detected using an Evolve EMCCD camera (Photometrics, Tucson, AZ, USA). Digital image acquisition and time series were computer-controlled using the Metafluor software (RRID:SCR\_014294). For two-photon imaging, we used a custom-built multiphoton microscope equipped with a 40X 0.8 N.A. objective (Olympus) and a femtosecond Ti:Sapphire laser (Chameleon Vision S, Coherent) with excitation at 820 nm. Fluorescence intensity over time was recorded at 1–2 Hz and ultimately assessed using a custom image analysis software by placing regions-of-interest (ROIs) over neuronal somata.

**Mouse: Electrophysiology.** In anesthetized C57BL/6N and HCAR1 KO mice, brains were removed promptly after decapitation and submerged in ice-cold aCSF slicing solution containing (in mM): 86 NaCl, 75 sucrose, 25 NaHCO<sub>3</sub>, 25 D-glucose, 4 MgCl<sub>2</sub>, 3 KCl, 1 NaH<sub>2</sub>PO<sub>4</sub>, 1 CaCl<sub>2</sub>. All aCSF solutions were continuously bubbled with 95% O<sub>2</sub>/5% CO<sub>2</sub>. 300 μm thick sagittal acute slices were prepared using a vibratome (Leica VT-1000S). Slices were then transferred to holding chambers in oxygenated slicing solution for 15 min at 34°C. Slices were then placed for 1 h at RT in an oxygenated incubation solution containing (mM): 120 NaCl, 26 NaHCO<sub>3</sub>, 5 D-glucose, 1 MgSO<sub>4</sub>, 3.2 KCl, 1 NaH<sub>2</sub>PO<sub>4</sub>, 2 CaCl<sub>2</sub>.

For recording, each slice was transferred in the same setup described above and continuously superfused with oxygenated recording solution containing (mM): NaCl, 26 NaHCO<sub>3</sub>, 10 Na-oxamate, 5 Na-pyruvate, 2.5 D-glucose, 1 MgSO<sub>4</sub>, 3.2 KCl, 1 NaH<sub>2</sub>PO<sub>4</sub>, 2 CaCl<sub>2</sub>. Cells visualized in the granule cell layer of the dentate gyrus were targeted for recording in whole-cell configuration with borosilicate glass pipettes (6–8 MΩ) filled with internal solution containing (mM): 130 K-gluconate, 5 KCl, 5 NaCl, 1 MgCl<sub>2</sub>, 0.1 EGTA, 0.025 CaCl<sub>2</sub>, 10 HEPES; 5 Na-phosphocreatine; 4 glucose, 4 ATP-Mg; 0.3 GTP, biocytin 1 mg/ml (pH = 7.3 adjusted with KOH, 290 mOsm). Experiments were discarded if the access resistance varied by more than 20%. sEPSCs were recorded for 3 min from a holding potential of –70 mV in the absence and in the presence of 3Cl-HBA (40 μM). mEPSCs were pharmacologically isolated by having picrotoxin (100 μM) (Tocris, Bristol, UK, Catalog # 1128) and tetrodotoxin (TTX, 1 μM) (Alomone labs, Jerusalem, Israel, Catalog # T-550) present throughout the experiment while clamping the cells at –70 mV. Analyses of sEPSC and mEPSC were performed offline and verified by eye using the

MiniAnalysis software. For each cell, the frequency and the amplitude of these synaptic events were analyzed. To investigate the excitability, the maximum firing frequency reached in each condition was quantified, as well as the necessary current injected to produce this maximum firing.  $R_N$ , RMP, and rheobase were acquired and analyzed as described above. At the end of recordings, slices were fixed and processed with streptavidin-AlexaFluor 647 for cell identification and morphological characterization.

**Rat: Electrophysiology.** Sprague Dawley rats were anesthetized with isoflurane and rapidly decapitated. Once removed, brain was placed in ice-cold aCSF slicing solution containing (in mM): 210 sucrose, 2.8 KCl, 2 MgSO<sub>4</sub>, 1.25 Na<sub>2</sub>HPO<sub>4</sub>, 25 NaHCO<sub>3</sub>, 1 MgCl<sub>2</sub>, 1 CaCl<sub>2</sub> and 10 D-Glucose.<sup>29</sup> All aCSF solutions were continuously bubbled with 95% O<sub>2</sub>/5% CO<sub>2</sub>. 385 μm thick horizontal acute slices of each hemisphere were prepared using a vibratome (Leica VT-1000S). Slices were then transferred to a holding chamber for 30 min at 34°C in oxygenated aCSF containing (in mM): 125 NaCl, 2.5 KCl, 1.25 Na<sub>2</sub>HPO<sub>4</sub>, 25 NaHCO<sub>3</sub>, 4 MgCl<sub>2</sub>, 1 CaCl<sub>2</sub> and 10 glucose.<sup>29</sup> Slices were then placed for 90 min at RT before any experimental procedure.

For recording, each slice was transferred in the same setup as described for mouse experiments and continuously superfused with oxygenated recording solution containing (mM): 125 NaCl, 2.5 KCl, 1.25 Na<sub>2</sub>HPO<sub>4</sub>, 25 NaHCO<sub>3</sub>, 2 MgCl<sub>2</sub>, 2 CaCl<sub>2</sub> and 10 D-glucose, pH = 7.35–7.4. Cells visualized in the granule cell layer of the dentate gyrus were targeted for recording in whole-cell configuration with borosilicate glass pipettes (6–8 MΩ) filled with internal solution containing (mM): 135 K-gluconate, 10 KCl, 5 NaCl, 1 EGTA, 10 HEPES, 10 phosphocreatine; 2 Mg-ATP, 0.4 Na-GTP, biocytin 1 mg/ml (pH = 7.3 adjusted with KCl, 290 mOsm). Experiments were discarded if the access resistance varied by more than 20%. sEPSCs were recorded for 3 min from a holding potential of –70 mV in the absence and in the presence of 3Cl-HBA (40 μM). Analyses of sEPSC were performed offline and verified by eye using the MiniAnalysis software. For each cell, the frequency and the amplitude of these synaptic events were analyzed. Excitability and intrinsic properties were analyzed the same way as the mouse one. At the end of recording, slices were fixed and processed with streptavidin-Alexa Fluor 647 for cell identification and morphological characterization.

**Experimental design, data analysis, and statistical significance.** Data analysis was performed using Clampfit (Molecular Devices, RRID:SCR\_011323) and Prism

(GraphPad, San Diego, USA; RRID:SCR\_002798). Most data are represented using scatter plots showing mean  $\pm$  SD and individuals values. We employed the following statistical tests: Student's t test, one sample t test (when compared to the percentage of baseline) and one-way repeated measure ANOVA. Unless otherwise specified, tests are paired and two-tailed. Parametric or non-parametric tests were performed according to data normality verified with the Shapiro-Wilk test. *Post hoc* corrections for multiple comparisons were performed when appropriate (after one-way ANOVA). Significance was conventionally set as \*\*\* $P < 0.001$ , \*\* $P < 0.01$  and \* $P < 0.05$ .

**Chemicals and drugs.** 3Cl-HBA was obtained from Sigma-Aldrich (Catalog #16795) or Cayman chemicals (Catalog #16795). Other chemicals were from Sigma-Aldrich.

## Results

### Characterization of HCAR1 brain expression

Limited data is available on HCAR1 expression and functions in the brain. In addition, the reported non-specificity of HCAR1 antibodies led us to select different approaches to identify HCAR1-expressing cells in the mouse brain.<sup>27</sup>

First, we looked for the presence of HCAR1 mRNA using qRT-PCR. Figure 1(a) shows that HCAR1 mRNA was found in hippocampus, cortex, brain stem, and cerebellum of wild-type mice. Hemi-brain samples prepared from mice at different ages (P7, P14, and P31) displayed the same levels of HCAR1 transcripts, which indicates that HCAR1 transcription is not age-dependent (Figure 1(b),  $P = 0.95$ , one-way ANOVA). As expected, no cDNA could be amplified from brain samples of HCAR1 KO mice (Supplementary Figure 1).

The distribution of HCAR1 expressing cells was then investigated using a reporter mouse line expressing mRFP under the HCAR1 promoter.<sup>21</sup> Results suggest that HCAR1 is expressed in specific brain regions of the mRFP reporter mice. Using 2-photon imaging of endogenous mRFP signal in fresh mouse acute brain slices (Figure 2(a)), we found expression of mRFP in the granule cell (GC) layer and the hilus of the DG, in the CA3 region, and in the cerebellum. We then acquired immunofluorescent confocal images of mRFP signal to enable counterstaining of cell nuclei. HCAR1 positive cells are found in the hippocampus and the cerebellum. Hippocampal expression is highest in the hilar area of the DG and in the pyramidal cells from CA3 (Figure 2 (b)). In the cerebellum, the Purkinje cell (PC) layer and the molecular layer have the strongest expression.

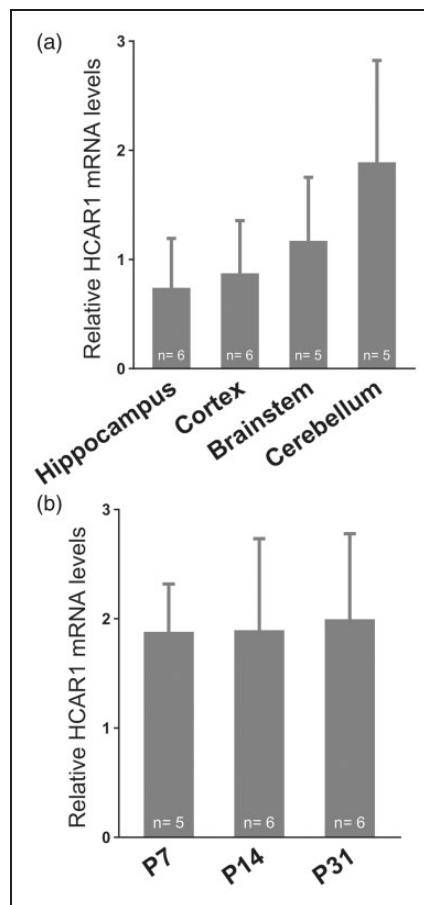


**Figure 1.** HCAR1 mRNA transcript expression in different mouse brain regions and across age. (a) HCAR1 mRNA detection in selected regions after dissection of 1-month old mice. (b) HCAR1 mRNA detection in brains from mice at post-natal day 7, 14, 31. Results are expressed relative to GAPDH expression as means  $\pm$  SD. The number of experiments are indicated in the graph.

Finally, we carried out *in situ* hybridization assays (Figure 2(c)). In the hippocampus, HCAR1 transcripts were observed throughout the DG, while more abundantly expressed in the hilus and in the CA3 region. In the cerebellum, HCAR1 transcript was found in the GC and the PC layers. To further phenotype the cellular expression of HCAR1 in the DG, our main region of interest, co-staining with cellular markers was performed (Figure 3(a)). We confirmed the neuronal identity of HCAR1-mRFP positive cell using the neuronal marker NeuN. The absence of colocalization with GAD67 and GFAP staining indicates that mRFP positive cell are not hilar GABAergic neurons and astroglial cells. HCAR1-positive cells of the hilus colocalized with GluR2/3, a specific marker for the mossy cells (MCs) in the DG<sup>31</sup> (Figure 3(b)). This specific hilar HCAR1 expression pattern prompted to further explore its functional role in the DG network.

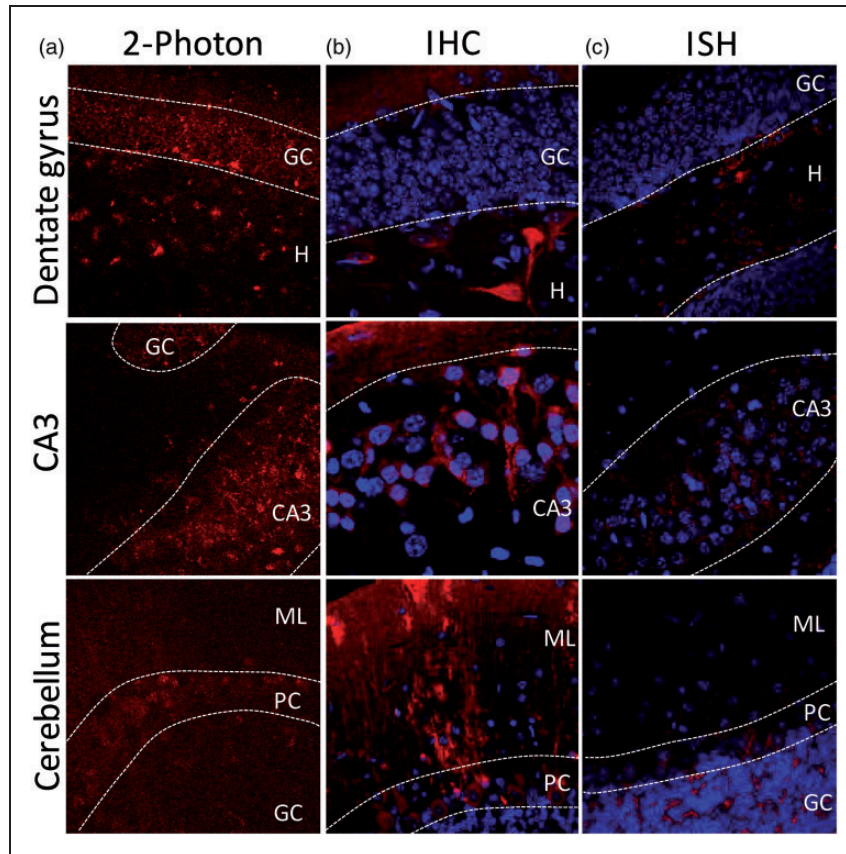


**Figure 2.** HCARI positive cells in dentate gyrus, CA3 and cerebellum. Analysis of brain tissue from reporter mouse line expressing mRFP under the HCARI promoter revealed scattered mRFP-positive cells in several regions of the brain. (a) Using a 2-photon microscope, endogenous mRFP signal on fresh 300  $\mu\text{m}$  acute slice was found in the GC layer and the hilus of the DG, in the CA3, and in the Purkinje cell layer of the cerebellum. (b) Using anti-mRFP immunohistochemistry to reveal HCARI-mRFP positive cells, mRFP expression was found in the hilus of the DG as well as in the inner molecular layer, in the CA3, and in the Purkinje, molecular, and granule cell layer of the cerebellum. Alexa 680 secondary antibody staining is shown in red and nuclei (Hoechst) in blue. (c) Using in situ hybridization (RNAscope<sup>TM</sup>), HCARI mRNA transcript was found in the hilus and in the GC layer of the DG, in the CA3, and mainly in the granule and Purkinje cell layer. HCARI transcript is shown in red and nuclei (DAPI) in blue. GC = granule cell layer, H = hilus, ML = molecular layer, PC = Purkinje cell.

### *HCARI influences synaptic events at GCs synapses in the mouse brain*

First, we used organotypic hippocampal slices to assess HCARI-dependent neuronal activity modulation. By using calcium imaging, we observed a down-modulation of neuronal activity by 42% (Supplementary Figure 2;  $n = 107$  cells,  $P < 0.0001$ , one-way ANOVA) after HCARI activation by 3Cl-HBA, a non-metabolized HCARI agonist.<sup>22</sup>

In the DG, MCs mediate an intrinsic excitatory loop, receiving powerful inputs from a relatively small number of GCs and providing highly distributed excitatory outputs to a large numbers of GCs.<sup>32</sup> As we found localization of HCARI mainly in MCs (Figure 3(b)), we hypothesized that HCARI activation by 3Cl-HBA may modulate synaptic events at

GCs. We thus decided to dissect the functional role of HCARI in the DG network of acute slices by performing whole-cell patch clamp recordings of GCs, which receive inputs from MCs. We first recorded sEPSC from neurons of the GC layer (Figure 4(a)). We found that HCARI activation significantly altered the frequency of events, as indicated by a rightward shift in interevent cumulative probability distributions (Figure 4(b);  $P < 0.0001$ , K-S test). The mean frequency was decreased by 36% (Figure 4(c);  $P = 0.0087$ , one sample t test), but not the amplitude (Figure 4(d);  $P = 0.9$ , one sample t test). Importantly, this modulation was not observed in cells from HCARI KO mice (Figure 4(b),  $P = 0.18$ , K-S test; Figure 4(c),  $P = 0.5$ , one sample t test; Figure 4(d);  $P = 0.98$ , one sample t test), highlighting the specificity of 3Cl-HBA effects.



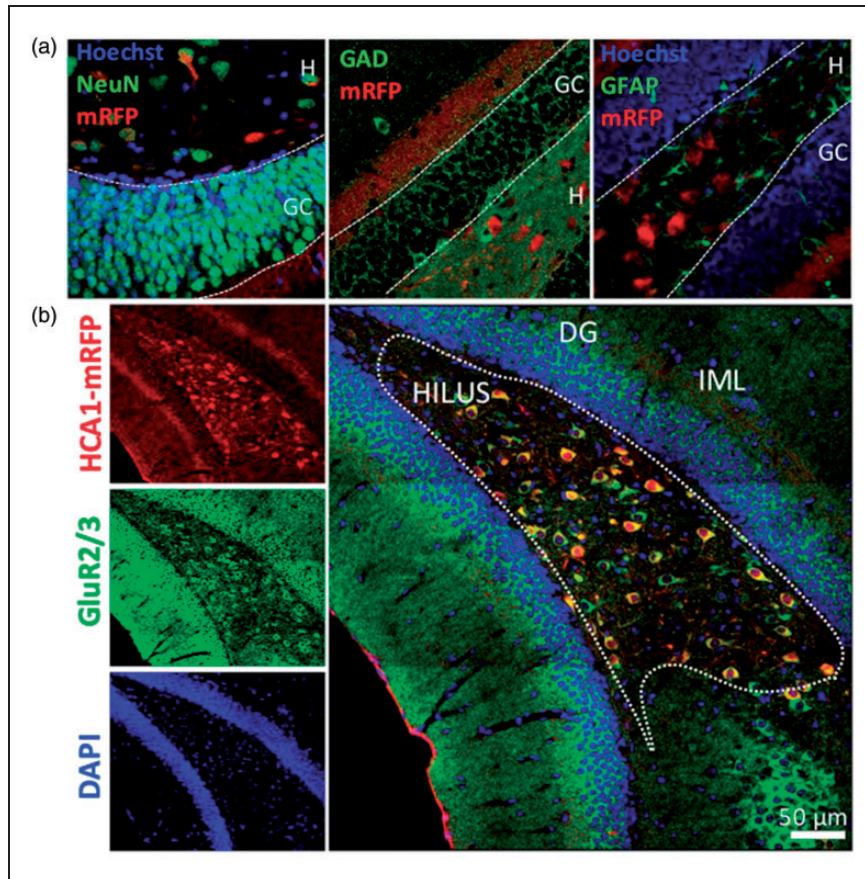


**Figure 3.** Identity and distribution of HCAR1 positive cells in the dentate gyrus. Hippocampal mRFP-positive cells were found mainly in the DG. (a) These cells colocalized with the neuronal marker NeuN, but not with the GABAergic cell marker GAD67, nor with the glial GFAP marker. (b) In the hilar region of the DG, mRFP-positive cells colocalized with the marker GluR2/3 shown to be associated with MCs. GC = granule cell layer, H = hilus, IML = inner molecular layer.

In addition, MCs also make synapses with GABAergic interneurons, which mediate feed-forward inhibition onto GCs.<sup>32</sup> Therefore, to focus on the effect of HCAR1 activation on MC-GC synapses, we recorded miniature excitatory post-synaptic currents (mEPSC) in the presence of TTX (1  $\mu$ M) and picrotoxin (100  $\mu$ M) to block inhibition and exclude any modulation coming from interneurons. We found a similar effect consisting in a shift of the cumulative probability distributions (Figure 4(e);  $P < 0.0001$ , K-S test). The frequency of mEPSCs was decreased by 53% when HCAR1 was activated compared to baseline condition (Figure 4(f);  $P = 0.009$ , one sample t test), while the amplitude was not altered (Figure 4(g);  $P = 0.63$ , one sample t test). The specificity of these effects was confirmed by the lack of agonist effects on mEPSCs recorded in neurons from HCAR1 KO mice (Figure 4(f),  $P = 0.64$ , and Figure 4(g),  $P = 0.47$ , one sample t test). These results provide evidence for a

pre-synaptic action of HCAR1 on glutamatergic neurotransmission provided by MCs.

Some of our staining approaches and the published *in situ* hybridization (the Allen Brain Atlas, <http://www.brain-map.org>) are consistent with expression of HCAR1 by GCs. We therefore tested whether HCAR1 influenced GC excitability. Increasing current injection of 30 pA steps were applied until establishment of neuronal accommodation in baseline and during activation of HCAR1. The resulting maximum frequency of AP discharge achieved is reported in Figure 4(h). Result showed that the maximum firing frequency was decreased by about 20% under HCAR1 activation ( $P = 0.019$ , paired t-test). However, HCAR1 activation did not alter neuronal accommodation since the current injected to reach the maximum firing frequency was similar in both conditions (Figure 4(i),  $P = 0.14$ , paired t-test). GCs from HCAR1 KO mice were not affected by 3Cl-



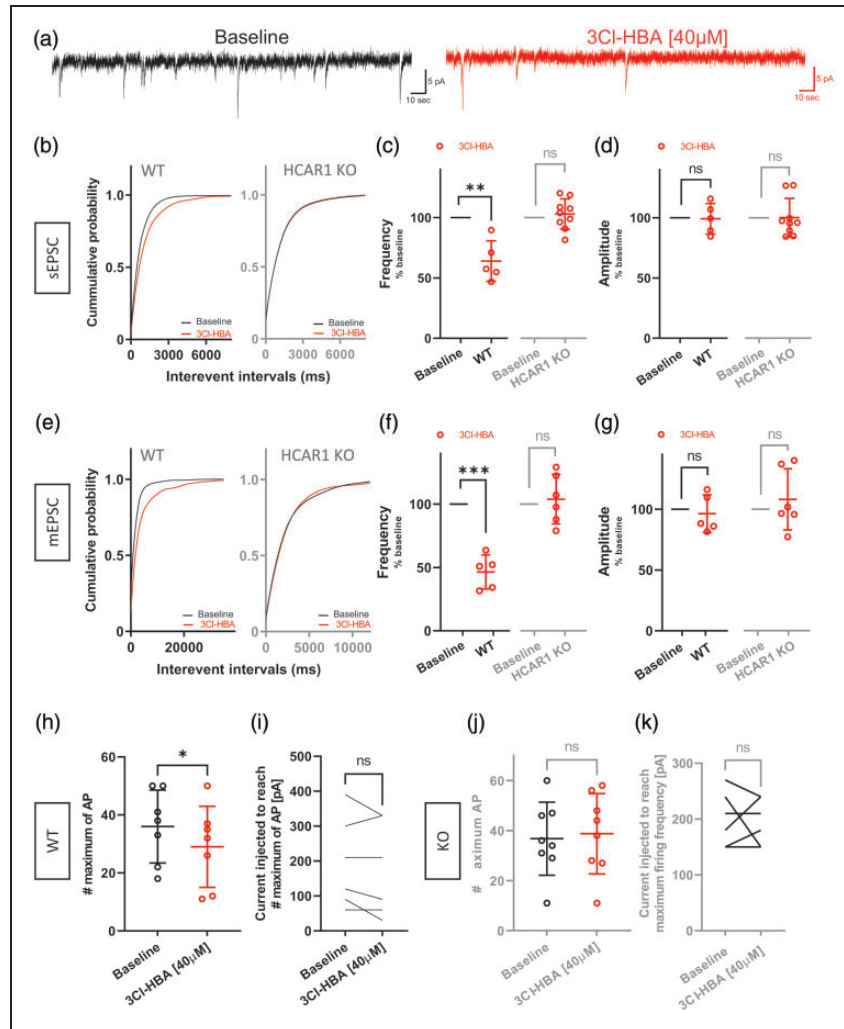


**Figure 4.** Granule cells from mice decrease spontaneous and mini EPSCs and firing frequency after activation of HCARI. (a) Example traces of sEPSCs measured during baseline condition (black) and following application of  $40\ \mu\text{M}$  3CI-HBA (red). (b) Cumulative distributions of sEPSCs frequency in WT and HCARI KO were analyzed by using Kolmogorov-Smirnov test. WT:  $P < 0.0001$  versus HCARI activation; HCARI KO:  $P = 0.18$  versus HCARI activation (c) Summary of recorded cells showing a decreased frequency of sEPSC by 36% induced by 3CI-HBA compared to baseline (one sample t,  $n = 5$ , mean =  $63.97 \pm 16.79$ ,  $P = 0.0087$ ). HCARI KO recorded cells showed no significant decrease in sEPSC frequency after 3CI-HBA (one sample t,  $n = 9$ , mean =  $103 \pm 12.58$ ,  $P = 0.5$ ) (d) sEPSC amplitude showed no statistically significant changes between baseline and 3CI-HBA application in both WT and HCARI KO (WT: one sample t,  $n = 5$ , mean =  $99.22 \pm 12.72$ ,  $P = 0.9$ ; HCARI KO: one sample t,  $n = 9$ , mean =  $100.1 \pm 16.07$ ,  $P = 0.98$ ). (e) Cumulative distributions of mEPSCs frequency in WT and HCARI KO were analyzed by using Kolmogorov-Smirnov test. WT:  $P < 0.0001$  versus HCARI activation; HCARI KO:  $P = 0.14$  versus HCARI activation. (f) Summary of recorded cells showing a decreased frequency of mEPSC by 53% induced by 3CI-HBA compared to baseline (one sample t,  $n = 5$ , mean =  $46.5 \pm 13.42$ ,  $P = 0.0009$ ). HCARI KO recorded cells showed no significant decrease in mEPSC frequency after 3CI-HBA (one sample t,  $n = 6$ , mean =  $103.9 \pm 19.55$ ,  $P = 0.64$ ) (g) mEPSC amplitude showed no statistically significant changes between baseline and 3CI-HBA application both in WT and HCARI KO (WT: one sample t,  $n = 5$ , mean =  $96.34 \pm 15.52$ ,  $P = 0.63$ ; HCARI KO: one sample t test,  $n = 6$ , mean =  $108.1 \pm 25.10$ ,  $P = 0.47$ ). (h, i) Effect of HCARI activation on neuronal firing frequency following steps of current injection in WT mice. The maximum number of action potentials evoked was significantly decreased by HCARI activation (paired t test,  $n = 7$ , Baseline: mean =  $36 \pm 12.58$ , 3CI-HBA: mean =  $29 \pm 13.98$ ,  $P = 0.019$ ), but not the current injected to reach the maximum firing frequency (paired t test,  $n = 7$ , Baseline: mean =  $184.3 \pm 121.8$ , 3CI-HBA: mean =  $162.9 \pm 127.1$ ,  $P = 0.14$ ). (j, k) In HCARI KO, activation of HCARI did not change the maximum number of AP compared to baseline (paired t test,  $n = 8$ , Baseline: mean =  $36.75 \pm 14.62$ , 3CI-HBA: mean =  $38.75 \pm 16.06$ ,  $P = 0.62$ ), nor the current injected to reach the maximum firing frequency (paired t test,  $n = 8$ , Baseline: mean =  $202.5 \pm 41.66$ , 3CI-HBA: mean =  $198.8 \pm 35.63$ ,  $P = 0.82$ ). Values are means  $\pm$  SD, \* $P < 0.05$ , \*\* $P < 0.01$ , \*\*\* $P < 0.001$  versus 3CI-HBA application.

HBA (Figure 4(j),  $P=0.62$ , paired t-test; Figure 4(k);  $P=0.82$ , paired t-test). Finally, intracellular passive properties values of GCs showed no significant differences between baseline and HCAR1 activation (Supplementary Table 2).

These results suggest a marked pre-synaptic effect on the spontaneous release of glutamate at the MC-GC synapse and a mild reduction of GC excitability suggesting an expression of HCAR1 in GCs as well.

### ***HCAR1 activation in rat brain tissue modulates MC-GC synapses***

The genetic distance between mice and rats is substantial, which goes along with significant differences at functional and behavioral levels.<sup>33</sup> As rats are widely used in biomedical research and in order to obtain comparative information on the functional involvement of HCAR1, we next decided to move to the rat brain. We investigated the DG network in rat brain acute slices using the same approach as with mice, and recorded sEPSC from GCs (Figure 5(a)). We found that HCAR1 activation by 3Cl-HBA significantly altered the frequency of events, as indicated by the cumulative probability distributions (Figure 5(b);  $P<0.0001$ , K-S test). The mean frequency of sEPSCs during HCAR1 activation was decreased by 27% compared to baseline (Figure 5(c);  $P=0.018$ , one sample t test), while no change in amplitude was observed (Figure 5(d);  $P=0.54$ , one sample t test).

We found that excitability of rat GCs was differently affected compared to mouse cells. Whereas the maximum firing frequency was not significantly different (Figure 5(e);  $P=0.13$ , paired t-test), neuronal accommodation was reached at lower injected current steps during HCAR1 activation (Figure 5(f);  $P=0.0049$ , paired t-test). Finally, basic electrophysiological properties of GCs did not show significant differences between baseline or HCAR1 activation (Supplementary Table 2).

These experiments in rat DG showed a pre-synaptic modulation of MC-GC synapses comparable with the mouse results. Overall, our results supports the functional presence of HCAR1 in the DG network and suggest a pre-synaptic location of the receptor, in line with recent papers reporting a modulation of CA1 and CA3 pyramidal cells in the rat hippocampus.<sup>29,34</sup>

### ***HCAR1 activation in epileptic human brain neurons***

By down-modulating neuronal activity in rodent brains, HCAR1 represents an interesting target for tackling conditions of exuberant activity in humans such as found in the epileptic brain. The availability of human cortical tissue resected during surgery for relief of

pharmacoresistant epilepsy gives a unique opportunity to investigate the physiology of cortical neurons and drug effects with obvious clinical relevance.

First, we probed HCAR1 expression in the human cortex using qRT-PCR measurements. Figure 6(a) shows that HCAR1 mRNA transcripts were found in all 17 brain samples from patients that we tested. Three of them showed levels that were on average about nine fold higher than the average. We did not find a correlation with either gender or age in the samples, or with any other patient's parameters available. Interestingly, these three samples originated from the temporal region.

We then performed both whole-cell patch clamp recordings and spontaneous neuronal calcium activity monitoring. Pyramidal cortical neurons were identified based on their morphology and electrical properties. The use of biocytin-containing pipette solutions followed by post-fixation and fluorescent streptavidin counter-staining of slices allowed verifying the morphology of these neurons (Figure 6(b)).

To examine neuronal modulation by HCAR1, we recorded sEPSC in control condition and under HCAR1 activation using 3Cl-HBA (Figure 6(c)). Results indicate a rightward shift of the interevent interval cumulative probability (Figure 6(d),  $P=0.0005$ , K-S test), consistent with a decrease of the frequency of synaptic events by ~40% (Figure 6(e),  $P<0.0001$ , one sample t). No significant change in amplitude (Figure 6(f),  $P=0.13$ , one sample t) or kinetics of sEPSCs was observed. Next, we looked at changes in excitability after activation of HCAR1 by injecting current steps of increasing amplitude. We quantified the number of AP discharge for 540 pA steps (Figure 6(g)), which revealed that excitability of these cells was decreased by about 12% compared to baseline after 3Cl-HBA application (Figure 6(h),  $P=0.035$ , paired t test). No change in intracellular passive properties values of human pyramidal neurons between control and 3Cl-HBA bath application was detected (Supplementary Table 2).

We also recorded neuronal spiking activity in human slices using calcium imaging. Cortical neurons displayed spontaneous spiking activity, in some cases with periodic bursting of activity presumably reflecting the epileptic nature of the tissue. We tested for the sensitivity of these human neurons to the application of HCAR1 agonist. We observed that HCAR1 agonist 3Cl-HBA caused a significant and reversible reduction in calcium spiking activity in these neurons (Figure 6(i) and (j);  $P=0.013$ , one-way ANOVA).

Taken together, these data suggest that neuronal activity is modulated by the activation of HCAR1 in acute brain slices obtained from epileptic patients. The receptor appears to act at the pre-synaptic

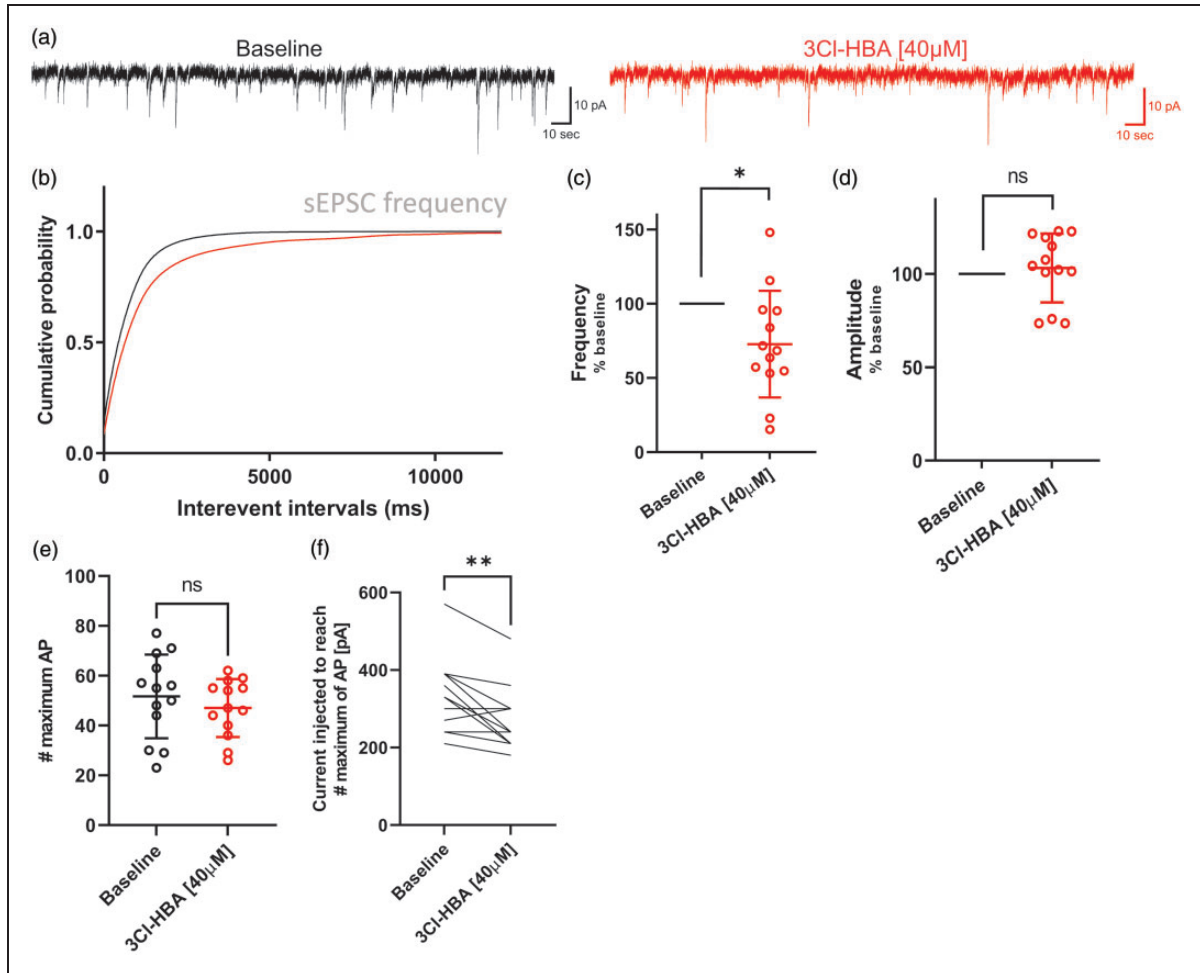


**Figure 5.** Granule cells from Sprague-Dawley rat decrease the sEPSC and firing frequency after activation of HCARI. (a) Example traces of sEPSCs measure during baseline condition (black) and following application of 40  $\mu$ M 3CI-HBA (red). (b) Cumulative distributions of sEPSCs frequency were analyzed by using Kolmogorov-Smirnov test:  $P < 0.0001$  versus HCARI activation. (c) Summary of recorded cells showing a decreased frequency of sEPSC by 27% induced by 3CI-HBA compared to baseline (one sample t,  $n = 13$ , mean =  $72.77 \pm 35.96$ ,  $P = 0.018$ ). (d) sEPSC amplitude showed no statistically significant changes between baseline and 3CI-HBA application (one sample t,  $n = 13$ , mean =  $103.2 \pm 18.38$ ,  $P = 0.0049$ ). Frequency and amplitude are shown in percentage compared to baseline. (e) Summary graph of the effect of HCARI activation on neuronal firing frequency following steps of current injection. The maximum number of action potentials evoked was calculated for each condition. No difference was observed (paired t test,  $n = 7$ , Baseline: mean =  $51.69 \pm 16.79$ , 3CI-HBA: mean =  $47 \pm 11.59$ ,  $P = 0.13$ ). (f) The current injected to reach the maximum firing frequency was calculated for each condition. HCARI activation significantly decreases the current needed for reaching the maximum firing frequency (paired t test,  $n = 13$ , Baseline: mean =  $327.7 \pm 96.79$ , 3CI-HBA: mean =  $270 \pm 80.31$ ,  $P = 0.0049$ ). Values are means  $\pm$  SD, \* $P < 0.05$ , \*\* $P < 0.01$ , \*\*\* $P < 0.001$  versus 3CI-HBA application.

level of the cortical network and affect excitability in recorded cells.

## Discussion

Evidence has accumulated over the past two decades indicating that lactate is more than a waste-product of metabolism. On the contrary, it is an important molecule used as metabolic fuel for a variety of cells and, more recently, as a signaling molecule,<sup>3,8,16,35</sup> particularly since the discovery of a selective plasma

membrane receptor coupled to G-proteins named HCARI. In the present study, we demonstrate that HCARI is expressed in rodent and human brains and that its activation leads to a decrease in neuronal activity.

The precise functional role of HCARI in neurons has remained elusive because of the lack of specific antibodies that have hampered the reliable identification of HCARI-positive cells. In this study, we instead used a mRFP reporter mouse. HCARI expressing cells was mainly found in the cerebellum and the

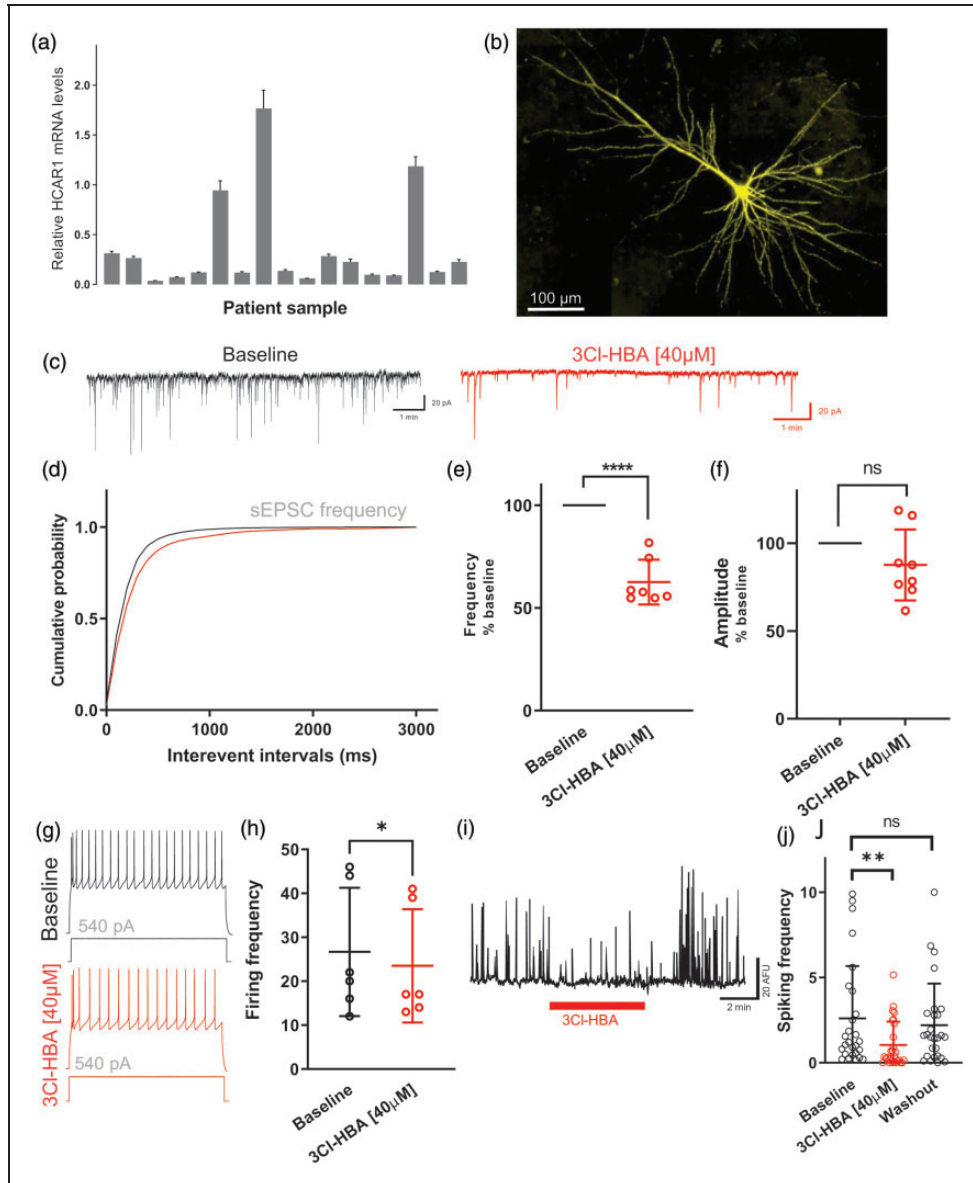


**Figure 6.** Cortical neurons from epileptic human patients decrease their spontaneous EPSC frequency following HCARI activation. (a) HCARI mRNA detection in human brain sample from 17 different pharmacoresistant epileptic patients undergoing resective surgery. Brain samples were from both male (57%) and female (43%) patients with median age 18 years, and originated from frontal ( $n = 5$ ), insular ( $n = 2$ ), parietal ( $n = 1$ ), and temporal ( $n = 9$ ) cortex from both hemispheres. Basal expression of HCARI is normalized to a reference gene ( $\beta$ -actin). All samples were run in triplicate and data is shown as means  $\pm$  SD. (b) Maximum intensity projection of a biocytin-filled recorded human cortical neuron. (c) Example traces of sEPSCs recorded during baseline condition (black) and following application of  $40 \mu\text{M}$  3CI-HBA (red). (d) Cumulative distributions of sEPSCs frequency were analyzed by using Kolmogorov-Smirnov test:  $P = 0.0005$  versus HCARI activation. (e) Summary of recorded cells showing a decreased frequency of sEPSC by  $\sim 40\%$  induced by 3CI-HBA compared to baseline (one sample  $t$ ,  $n_{\text{cells/patients}} = 7/5$ , mean =  $62.54 \pm 10.89$ ,  $P < 0.0001$ ). (f) sEPSC amplitude showed no statistically significant changes between baseline and 3CI-HBA application (one sample  $t$ ,  $n_{\text{cells/patients}} = 7/5$ , mean =  $87.65 \pm 20.2$ ,  $P = 0.13$ ). Frequency and amplitude are shown in percentage compared to baseline. (g) Representative traces from neurons recorded before and after HCARI activation obtained from a series of current injections ( $-120$  to  $540$  pA,  $2$  sec,  $30$  pA increments); the response to  $540$  pA current injection is shown. (h) Summary graph of the effect of HCARI activation on neuronal firing frequency following steps of current injection ( $n = 6$ ). The firing frequency was calculated from the number of AP evoked by  $540$  pA current injection during  $2$  seconds. Individual data and significance is shown between the baseline and 3CI-HBA conditions (paired  $t$  test,  $n_{\text{cells/patients}} = 6/5$ , Baseline: mean =  $26.67 \pm 14.62$ , 3CI-HBA: mean =  $23.5 \pm 12.9$ ,  $P = 0.035$ ). (i) Example trace of calcium spiking activity from neurons in human acute slices with application of 3CI-HBA. (j) Summary graph of spontaneous calcium spiking activity down-modulated by HCARI activation in cortical neurons from epileptic human patients (one-way ANOVA,  $n_{\text{cells/patients}} = 27/5$ , Baseline: mean =  $2.6 \pm 3.07$ , 3CI-HBA: mean =  $1.04 \pm 1.37$ , Washout: mean =  $2.21 \pm 2.44$ ,  $P = 0.013$ ). The calcium spiking activity of individual cells is shown. Values are means  $\pm$  SD;  $P < 0.05$ ,  $**P < 0.01$ ,  $***P < 0.001$  versus 3CI-HBA application.



hippocampus, where the positive cells predominantly correspond to hilar MCs. We did not find evidence for HCAR1 expression in interneurons or astrocytes. These results were confirmed using *in situ* hybridization technology (RNAscope™). MCs, via their communication with GCs, have been implicated in various forms of mnemonic functions such as associative memory,<sup>36</sup> pattern separation,<sup>37</sup> and recall of memory sequences.<sup>38</sup> Systemic administration of D-lactate and of the HCAR1 agonist 3,5-DHBA 15 min before performing inhibitory avoidance training showed memory impairments compared to saline administration, suggesting the involvement of HCAR1 signaling in learning and memory.<sup>9</sup> However, whether HCAR1 is involved in the dentate gyrus mnemonic processes is not yet known.

Previous studies by us<sup>24,27</sup> and others<sup>29,34</sup> reported evidence for a neuromodulatory action of HCAR1 on neurons. Based on our histological observations and our functional characterization in cultured neurons, we asked whether HCAR1 would act as neuromodulator of DG neurons *in situ*. Hilar MCs provide broadly distributed excitatory outputs to a large number of GCs.<sup>32</sup> Using electrophysiology recordings in the mouse hippocampus, we found that dentate GCs displayed a reduction in mEPSC and sEPSC frequency without changes in synaptic event amplitude. This result suggests presynaptic control of spontaneous neurotransmitter release at MC-GC, consistent with our description of HCAR1-expressing cells. These results could be replicated in rats, and indicate that HCAR1 is also present and functional in the DG, where GC synaptic events were markedly reduced by HCAR1 activation.

This result brings new perspectives for the understanding of neuronal activity at MC-GC synapses. These circuits are critically involved in temporal lobe epilepsy,<sup>32,39,40</sup> where MCs either become overactive and driving GC firing,<sup>41</sup> or undergo cell death, reducing the magnitude of feed-forward inhibition.<sup>42</sup> Therefore, by acting on HCAR1, lactate may be beneficial to temporal lobe epilepsy management, an idea also supported by experiments showing the capacity of 3,5-DHBA to successfully decrease spiking frequency in hippocampal subiculum neurons in an *in vitro* model of epilepsy using 4-aminopyridine.<sup>43</sup> It was also demonstrated that MCs are more susceptible to excitotoxicity than GCs,<sup>44</sup> therefore lactate could exert a dual role of metabolic neuroprotective support and of signaling molecule acting on HCAR1 to lower activity. Whether MCs metabolize lactate has not been directly addressed to our knowledge. However, the lactate transporter MCT2 appears to be present in hilar neurons,<sup>45,46</sup> suggesting that they are equipped to use lactate as a metabolic substrate. Even though most aCSF solutions used for *in vitro* slice electrophysiology

contain high concentrations of glucose (10–25 mM), we chose to use 2.5 mM glucose, as found in the brain *in vivo*,<sup>47</sup> reasoning that this low glucose level should prevent excessive lactate production by astrocytes that could interfere with HCAR1 signaling. Knowing the vulnerability of MCs,<sup>44</sup> pyruvate (3–5 mM) was supplemented throughout the experiment to support neuronal metabolic needs and to bring protective antioxidant effects, as shown before.<sup>48</sup>

We did not find unequivocal HCAR1 expression in GCs, which will need further investigations to be established. However, our experiments revealed the functional involvement of HCAR1 in diminishing mouse GC excitability. Rat GCs followed a similar trend. In support of this idea, it has been shown that paired-pulse ratio and coefficient of variation ( $CV^{-2}$ ) of CA3 pyramidal cell in rats evoked on mossy fiber stimulation are transiently decreased by lactate perfusion.<sup>34</sup> Change in the  $CV^{-2}$  is indicative of a presynaptic modulation. Because mossy fibers consist of axons projecting from GCs to CA3,<sup>49</sup> this result would be compatible with the functional presence of HCAR1 in GCs.

Overall, HCAR1 was shown to be functionally present in rodent hippocampus. In rat CA1 pyramidal neurons excitability is modulated by lactate and HCAR1 agonist.<sup>29</sup> Rat subicular neuronal activity is reduced by HCAR1 activation.<sup>43</sup> CA3 pyramidal neurons are also modulated by lactate or HCAR1 agonist; however, they appear to express another putative lactate-sensitive receptor coupled to a different effector system.<sup>34</sup> In the present study, we show that in the DG, HCAR1 is mainly present in hilar MCs and acts on GCs.

To our knowledge, we present here the first report of functional effects of HCAR1 activation in fresh human brain tissue. Indeed, while known to be present in human peripheral tissue, HCAR1 expression and activity in human brains was unknown. Rodent models, particularly mice, are widely used in biomedical research notably due to the ability to manipulate their genome and to the fact that many mechanisms and paradigms translate well between species. Nevertheless, in translational research, over 90% of neurological drug candidates with promising animal results have failed in human clinical trials,<sup>50</sup> highlighting the crucial importance to validate rodent results with human tissue. Thanks to our access to fresh brain tissue from patients undergoing surgical resections of epileptic foci, we could determine that all human tissue samples contained HCAR1 mRNA transcripts. However, we faced obvious limitations in working with human samples, which include that one cannot compare HCAR1 expression levels in healthy non-epileptic brains, and that the patient individual

epileptic condition, the medication received, and the neurosurgical procedure may also influence HCAR1 expression. By preparing acute brain slices from brain tissue blocks of patients, we found both by whole-cell patch-clamp and by calcium imaging that activating HCAR1 caused a down-modulation of spontaneous activity. However, we observed that among all cells analyzed after calcium imaging, 20% of them showed a moderate increased activity under application of the HCAR1 agonist 3Cl-HBA. This effect could be explained by the putative existence of other lactate receptors with  $G_s$  activity instead of the HCAR1  $G_i$  activity as proposed by others,<sup>16,34</sup> or could involve the additional  $G_{\beta\gamma}$  action of HCAR1 observed in primary neurons.<sup>27</sup>

In conclusion, we show consistent effects of HCAR1 activation in the rodent DG as well as human neurons from pharmaco-resistant epileptic patients. In addition to being a promising new target for the development of anti-epileptic drug treatment, we can propose that HCAR1 could serve the role of providing a metabolic readout for neurons to tune their activity according to the metabolic state during brain or physical activity.

### Funding

The author(s) disclosed receipt of the following financial support for the research, authorship, and/or publication of this article: This work was supported by the Swiss National Science Foundation [grant# 31003 A\_179399 to JYC].

### Acknowledgements

We thank Ron Stoop for the very fruitful interactions on human tissue experiments, and Mélanie Reneiro and Christiane Devenoges for technical assistance.

### Declaration of conflicting interests

The author(s) declared no potential conflicts of interest with respect to the research, authorship, and/or publication of this article.

### Authors' contributions

JYC, MB and ABR conceived and designed experiments. MB and ABR performed and analyzed electrophysiological recordings. NR, MA, HDCA, JWW, JYC contributed to electrophysiology and calcium imaging experiments. MB, ABR, MA, CS performed immunohistochemistry. VG, CS performed and VG, CS, JP analyzed qRT-PCR experiments. EP and RD provided patient samples and associated data and SO provided transgenic mouse lines. JYC and MB wrote the manuscript, which was revised and approved by all authors.

### Supplemental material

Supplemental material for this article is available online.

### References

1. Morgenthaler FD, Kraftsik R, Catsicas S, et al. Glucose and lactate are equally effective in energizing activity-dependent synaptic vesicle turnover in purified cortical neurons. *Neuroscience* 2006; 141: 157–165.
2. Rouach N, Koulakoff A, Abudara V, et al. Astroglial metabolic networks sustain hippocampal synaptic transmission. *Science* 2008; 322: 1551–1555.
3. Magistretti PJ and Allaman I. Lactate in the brain: from metabolic end-product to signalling molecule. *Nat Rev Neurosci* 2018; 19: 235–249.
4. Abi-Saab WM, Maggs DG, Jones T, et al. Striking differences in glucose and lactate levels between brain extracellular fluid and plasma in conscious human subjects: effects of hyperglycemia and hypoglycemia. *J Cereb Blood Flow Metab* 2002; 22: 271–279.
5. Dielén GA, Ball KK and Cruz NF. A glycogen phosphorylase inhibitor selectively enhances local rates of glucose utilization in brain during sensory stimulation of conscious rats: implications for glycogen turnover. *J Neurochem* 2007; 102: 466–478.
6. Hu Y and Wilson GS. A temporary local energy pool coupled to neuronal activity: fluctuations of extracellular lactate levels in rat brain monitored with rapid-response enzyme-based sensor. *J Neurochem* 1997; 69: 1484–1490.
7. Offermanns S. Hydroxy-carboxylic acid receptor actions in metabolism. *Trends Endocrinol Metab* 2017; 28: 227–236.
8. Barros LF. Metabolic signaling by lactate in the brain. *Trends Neurosci* 2013; 36: 396–404.
9. Scavuzzo CJ, Rakotovaio I and Dickson CT. Differential effects of L- and D-lactate on memory encoding and consolidation: Potential role of HCAR1 signaling. *Neurobiol Learn Mem* 2019; 168: 107151.
10. Newman LA, Korol DL and Gold PE. Lactate produced by glycogenolysis in astrocytes regulates memory processing. *PLoS One* 2011; 6: e28427.
11. Suzuki A, Stern SA, Bozdagi O, et al. Astrocyte-neuron lactate transport is required for long-term memory formation. *Cell* 2011; 144: 810–823.
12. Shimizu H, Watanabe E, Hiyama TY, et al. Glial  $Na_x$  channels control lactate signaling to neurons for brain  $[Na^+]$  sensing. *Neuron* 2007; 54: 59–72.
13. Song Z and Routh VH. Differential effects of glucose and lactate on glucosensing neurons in the ventromedial hypothalamic nucleus. *Diabetes* 2005; 54: 15–22.
14. Parsons MP and Hirasawa M. ATP-sensitive potassium channel-mediated lactate effect on orexin neurons: implications for brain energetics during arousal. *J Neurosci* 2010; 30: 8061–8070.
15. Yang J, Ruchti E, Petit JM, et al. Lactate promotes plasticity gene expression by potentiating NMDA signaling

- in neurons. *Proc Natl Acad Sci U S A* 2014; 111: 12228–12233.
16. Tang F, Lane S, Korsak A, et al. Lactate-mediated glianeuronal signalling in the mammalian brain. *Nat Commun* 2014; 5: 3284.
  17. Bergersen LH and Gjedde A. Is lactate a volume transmitter of metabolic states of the brain? *Front Neuroenergetics* 2012; 4: 5.
  18. Blad CC, Ahmed K, Ij AP, et al. Biological and pharmacological roles of HCA receptors. *Adv Pharmacol* 2011; 62: 219–250.
  19. Cai TQ, Ren N, Jin L, et al. Role of GPR81 in lactate-mediated reduction of adipose lipolysis. *Biochem Biophys Res Commun* 2008; 377: 987–991.
  20. Liu C, Wu J, Zhu J, et al. Lactate inhibits lipolysis in fat cells through activation of an orphan G-protein-coupled receptor, GPR81. *J Biol Chem* 2009; 284: 2811–2822.
  21. Ahmed K, Tunaru S, Tang C, et al. An autocrine lactate loop mediates insulin-dependent inhibition of lipolysis through GPR81. *Cell Metab* 2010; 11: 311–319.
  22. Dvorak CA, Liu C, Shelton J, et al. Identification of hydroxybenzoic acids as selective lactate receptor (GPR81) agonists with antilipolytic effects. *ACS Med Chem Lett* 2012; 3: 637–639.
  23. Liu C, Kuei C, Zhu J, et al. 3,5-Dihydroxybenzoic acid, a specific agonist for hydroxycarboxylic acid 1, inhibits lipolysis in adipocytes. *J Pharmacol Exp Ther* 2012; 341: 794–801.
  24. Bozzo L, Puyal J and Chatton JY. Lactate modulates the activity of primary cortical neurons through a receptor-mediated pathway. *PLoS One* 2013; 8: e71721.
  25. Lauritzen KH, Morland C, Puchades M, et al. Lactate receptor sites link neurotransmission, neurovascular coupling, and brain energy metabolism. *Cereb Cortex* 2014; 24: 2784–2795.
  26. Castillo X, Rosafio K, Wyss MT, et al. A probable dual mode of action for both L- and D-lactate neuroprotection in cerebral ischemia. *J Cereb Blood Flow Metab* 2015; 35: 1561–1569.
  27. de Castro Abrantes H, Briquet M, Schmuziger C, et al. The lactate receptor HCAR1 modulates neuronal network activity through the activation of Galpha and Gbeta subunits. *J Neurosci* 2019; 39: 4422–4433.
  28. Wallenius K, Thalén P, Björkman JA, et al. Involvement of the metabolic sensor GPR81 in cardiovascular control. *JCI Insight* 2017; 2: e92564.
  29. Herrera-Lopez G and Galvan EJ. Modulation of hippocampal excitability via the hydroxycarboxylic acid receptor 1. *Hippocampus* 2018; 28: 557–567.
  30. Dawitz J, Kroon T, Hjorth JJ, et al. Functional calcium imaging in developing cortical networks. *J Vis Exp* 2011; 56: 3350.
  31. Leranath C, Szeidemann Z, Hsu M, et al. AMPA receptors in the rat and primate hippocampus: a possible absence of GluR2/3 subunits in most interneurons. *Neuroscience* 1996; 70: 631–652.
  32. Hashimoto-dani Y, Nasrallah K, Jensen KR, et al. LTP at hilar mossy cell-dentate granule cell synapses modulates dentate gyrus output by increasing excitation/inhibition balance. *Neuron* 2017; 95: 928–943 e3.
  33. Ellenbroek B and Youn J. Rodent models in neuroscience research: is it a rat race? *Dis Model Mech* 2016; 9: 1079–1087.
  34. Herrera-López G, Griego E and Galván E. Lactate induces synapse-specific potentiation on CA3 pyramidal cells of rat hippocampus. *PLoS One* 2020; 15: e0242309.
  35. Sun S, Li H, Chen J, et al. Lactic acid: no longer an inert and end-product of glycolysis. *Physiology (Bethesda)* 2017; 32: 453–463.
  36. Buckmaster PS and Schwartzkroin PA. Hippocampal mossy cell function: a speculative view. *Hippocampus* 1994; 4: 393–402.
  37. Myers CE and Scharfman HE. A role for hilar cells in pattern separation in the dentate gyrus: a computational approach. *Hippocampus* 2009; 19: 321–337.
  38. Lisman JE, Talamini LM and Raffone A. Recall of memory sequences by interaction of the dentate and CA3: a revised model of the phase precession. *Neural Netw* 2005; 18: 1191–1201.
  39. Bui AD, Nguyen TM, Limouse C, et al. Dentate gyrus mossy cells control spontaneous convulsive seizures and spatial memory. *Science* 2018; 359: 787–790.
  40. Ratzliff A, Howard AL, Santhakumar V, et al. Rapid deletion of mossy cells does not result in a hyperexcitable dentate gyrus: implications for epileptogenesis. *J Neurosci* 2004; 24: 2259–2269.
  41. Ratzliff AH, Santhakumar V, Howard A, et al. Mossy cells in epilepsy: rigor mortis or vigor mortis? *Trends Neurosci* 2002; 25: 140–144.
  42. Sloviter RS. Permanently altered hippocampal structure, excitability, and inhibition after experimental status epilepticus in the rat: the “dormant basket cell” hypothesis and its possible relevance to temporal lobe epilepsy. *Hippocampus* 1991; 1: 41–66.
  43. Jorwal P and Sikdar SK. Lactate reduces epileptiform activity through HCA1 and GIRK channel activation in rat subicular neurons in an in vitro model. *Epilepsia* 2019; 60: 2370–2385.
  44. Scharfman HE. The enigmatic mossy cell of the dentate gyrus. *Nat Rev Neurosci* 2016; 17: 562–575.
  45. Pierre K, Magistretti PJ and Pellerin L. MCT2 is a major neuronal monocarboxylate transporter in the adult mouse brain. *J Cereb Blood Flow Metab* 2002; 22: 586–595.
  46. Bergersen LH, Magistretti PJ and Pellerin L. Selective postsynaptic co-localization of MCT2 with AMPA receptor GluR2/3 subunits at excitatory synapses exhibiting AMPA receptor trafficking. *Cereb Cortex* 2005; 15: 361–370.

47. Silver IA and Erecińska M. Extracellular glucose concentration in mammalian brain: continuous monitoring of changes during increased neuronal activity and upon limitation in oxygen supply in normo-, hypo-, and hyperglycemic animals. *J Neurosci* 1994; 14: 5068–5076.
48. Isopi E, Granzotto A, Corona C, et al. Pyruvate prevents the development of age-dependent cognitive deficits in a mouse model of Alzheimer's disease without reducing amyloid and tau pathology. *Neurobiol Dis* 2015; 81: 214–224.
49. Sun Y, Grieco SF, Holmes TC, et al. Local and long-range circuit connections to hilar mossy cells in the dentate gyrus. *eNeuro* 2017; 4: ENEURO.0097-17.2017.
50. Hay M, Thomas DW, Craighead JL, et al. Clinical development success rates for investigational drugs. *Nat Biotechnol* 2014; 32: 40–51.



## Supplementary Information for

# Activation of lactate receptor HCAR1 down-modulates neuronal activity in rodent and human brain tissue

Marc Briquet <sup>1</sup>, Anne-Bérengère Rocher <sup>1</sup>, Maxime Alessandri <sup>1</sup>, Nadia Rosenberg <sup>1</sup>, Haissa de Castro Abrantes <sup>1</sup>, Joel Wellbourne-Wood <sup>1</sup>, Céline Schmuziger <sup>1</sup>, Vanessa Ginet <sup>1</sup>, Julien Puyal <sup>1</sup>, Etienne Pralong <sup>2</sup>, Roy Thomas Daniel <sup>2</sup>, Stefan Offermanns <sup>3</sup>, Jean-Yves Chatton<sup>1,4,\*</sup>

<sup>1</sup>Department of Fundamental Neurosciences, University of Lausanne, Switzerland; <sup>2</sup>Department of Neurosurgery Service, University Hospital of Lausanne and faculty of Biology and medicine, UNIL, Lausanne, Switzerland; <sup>3</sup>Max Planck Institute for Heart and Lung Research, Bad Nauheim, Germany; <sup>4</sup>Cellular Imaging Facility, University of Lausanne, 1005 Lausanne, Switzerland

## Supplementary Material and Methods

**Organotypic culture.** Organotypic hippocampal slice cultures were prepared from 3 day-old WT mice. After decapitation, brains were quickly removed and plunged into ice-cold filtered dissection medium containing 50% MEM, 1% Penicillin-Streptomycin (Invitrogen, catalog # 15140122) and 10 mM Tris (Merck-Millipore, catalog # 8382). The hippocampi were rapidly and carefully dissected out and put both on Teflon-disk in order to obtain 400 µm-thick transversal section using tissue-cutter (McIlwain Tissue Chopper, TC752). Slices were placed onto porous hydrophilic LCR membrane (Merck-Millipore, catalog # FHLC04700) in the Millicell-insert (Merck-Millipore, catalog # PICM03050), which were transferred into 35mm Petri dish. Each Petri dish contained 1mL of pre-warmed culture medium composed of filtered 50 % MEM, 25% horse serum (Invitrogen, catalog # 26050-047), 25% HBSS, 7.5% NaHCO<sub>3</sub>, 1% Penicillin-Streptomycin, 36mM D-Glucose and 5mM Tris, Petri dish containing the slices were incubated during 4 days at 36°C and then transferred into a 33°C incubator for the following weeks. Culture medium was first changed after 24h and then every 3-4 days. Widefield calcium imaging was performed with an upright epifluorescence microscope (FN1, Nikon, Tokyo, 163 Japan) using a 40X 0.8 N.A water-immersion objective lens. Fluorescence excitation wavelengths were selected using a fast filter wheel (Sutter Instr., Novato, CA) and fluorescence was detected using an Evolve EMCCD camera (Photometrics, Tucson, AZ, USA). Digital image acquisition and time series were computer-controlled using the Metafluor software (RRID:SCR\_014294)

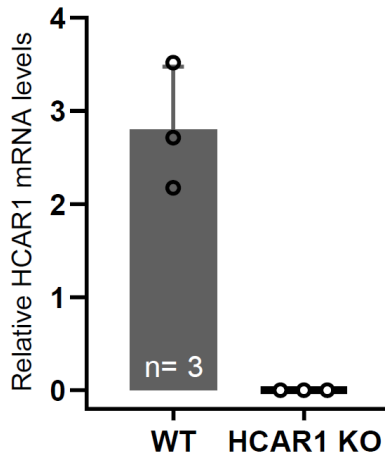
**Supplementary Table 1. Summary of primers used for qRT-PCR in human and mouse brain experiments.**

<b>Human</b>	HCAR1	GCCCAGCACTGTTTACCTTTTC	CCCCAAAAGCCCAGTGTCTAC
	$\beta$ -actin	CTGTACGCCAACACAGTGCT	GCTCAGGAGGAGCAATGATC
<b>Mouse</b>	HCAR1	GGGGACTGTGTATCTTCTGA	GAGTCTTGGTGTAGAATTTGG
	GAPDH	TCCATGACAACCTTTGGCATTG	CAGTCTTCTGGGTGGCAGTGA

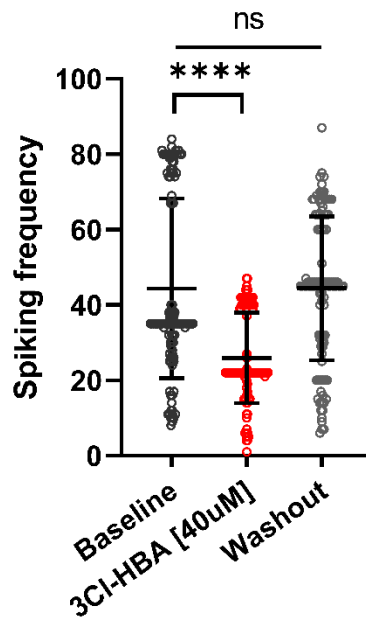
**Supplementary Table 2. HCAR1 activation did not affect passive properties of cortical human neurons and rodent GCs.**

	<b>Human</b>		<b>Mouse</b>		<b>Rat</b>	
	Baseline	3CI-HBA	Baseline	3CI-HBA	Baseline	3CI-HBA
Rheobase	351 $\pm$ 83.6	357.2 $\pm$ 71.4	52.2 $\pm$ 28.9	55.1 $\pm$ 31.6	92.9 $\pm$ 33.2	89.4 $\pm$ 41.4
RMP	-73.8 $\pm$ 3.2	-74.4 $\pm$ 2.2	-74.2 $\pm$ 11.5	-70.6 $\pm$ 10.6	-74.3 $\pm$ 4.7	-74.5 $\pm$ 5
$R_N$	68.2 $\pm$ 17.1	72.1 $\pm$ 12.2	235.9 $\pm$ 65.7	235.9 $\pm$ 56.6	207.8 $\pm$ 52	222.6 $\pm$ 59.8

All parameters were tested in all cells used for analysis. 3CI-HBA was applied at 40 $\mu$ M. Data are shown as means $\pm$ SD and analysis was done using one sample t-test. RMP, resting membrane potential;  $R_N$ , input resistance.



**Supplementary Figure 1.** HCAR1 mRNA detection in hemibrain after dissection of 1-month old mice. Results showed no expression of HCAR1 mRNA transcript in HCAR1 KO samples (WT:  $2.8 \pm 0.68$ ; KO: 0). Results are expressed relative to GAPDH expression as means  $\pm$  SD. The number of experiments are indicated in the graph.



**Supplementary Figure 2.** Hippocampal neurons from mouse organotypic slices decrease their spiking frequency after activation of HCAR1. Summary graph of spontaneous calcium spiking activity down-modulated by HCAR1 activation by 3CI-HBA (40µM) in hippocampal neurons from WT mice (one-way ANOVA,  $n = 107$  cells from 5 experiments, Baseline: mean =  $44.41 \pm 23.87$ , 3CI-HBA: mean =  $25.99 \pm 12$ , Washout: mean =  $44.44 \pm 19.13$ ,  $P < 0.0001$ ). The calcium spiking activity of individual cells is shown. Values are means  $\pm$  SD;  $P < 0.05$ ,  $**P < 0.01$ ,  $***P < 0.001$ ,  $****P < 0.0001$  versus 3CI-HBA application and washout.

## Study 2

Evaluation of hydroxycarboxylic acid receptor 1 (HCAR1) as a building block for genetically encoded extracellular lactate biosensors

### Summary of the results


In this study, we describe—to our knowledge—the first attempt at using the lactate receptor HCAR1 to build a fluorescent biosensor for extracellular lactate. We developed a set of intensimetric sensors for lactate based on HCAR1 coupled to cpGFP. Even though several methods for detecting lactate levels exist, research on lactate effects in living tissue would critically benefit from a fluorescence imaging approach. These sensors showed selective expression at the plasma membrane and responded to physiological concentrations of lactate. However, these sensors lost the original ability of HCAR1 to selectively respond to lactate versus other related small carboxylic acid molecules. Therefore, while representing a promising building block for a lactate biosensor, HCAR1 was found to be sensitive to perturbations of its structure, affecting its ability to distinguish between related carboxylic molecules.

### Personal contribution

In this study, Joel Wellbourne-Wood designed the initial sensor candidates. I performed and analyzed the expression of the different candidates, and together with Jean-Yves Chatton, developed the final candidates used in the study. Together with my colleagues, Maxime Alessandri, Francesca Binda, Maylis Touya, and I performed the experiment addressing lactate and related molecules sensitivity. Jean-Yves Chatton wrote the manuscript.

## Article

# Evaluation of Hydroxycarboxylic Acid Receptor 1 (HCAR1) as a Building Block for Genetically Encoded Extracellular Lactate Biosensors

Joel Wellbourne-Wood <sup>1,†</sup>, Marc Briquet <sup>1,†</sup>, Maxime Alessandri <sup>1,†</sup>, Francesca Binda <sup>1</sup>, Maylis Touya <sup>1</sup> and Jean-Yves Chatton <sup>1,2,\*</sup> 

<sup>1</sup> Department of Fundamental Neurosciences, University of Lausanne, 1005 Lausanne, Switzerland; joel.wellbournewood@gmail.com (J.W.-W.); marc.briquet@unil.ch (M.B.); maxime.alessandri@unil.ch (M.A.); francesca.binda@unil.ch (F.B.); maylis.touya@unil.ch (M.T.)

<sup>2</sup> Cellular Imaging Facility, University of Lausanne, 1005 Lausanne, Switzerland

\* Correspondence: jean-yves.chatton@unil.ch

† These authors contributed equally to this work.

**Abstract:** The status of lactate has evolved from being considered a waste product of cellular metabolism to a useful metabolic substrate and, more recently, to a signaling molecule. The fluctuations of lactate levels within biological tissues, in particular in the interstitial space, are crucial to assess with high spatial and temporal resolution, and this is best achieved using cellular imaging approaches. In this study, we evaluated the suitability of the lactate receptor, hydroxycarboxylic acid receptor 1 (HCAR1, formerly named GPR81), as a basis for the development of a genetically encoded fluorescent lactate biosensor. We used a biosensor strategy that was successfully applied to molecules such as dopamine, serotonin, and norepinephrine, based on their respective G-protein-coupled receptors. In this study, a set of intensimetric sensors was constructed and expressed in living cells. They showed selective expression at the plasma membrane and responded to physiological concentrations of lactate. However, these sensors lost the original ability of HCAR1 to selectively respond to lactate versus other related small carboxylic acid molecules. Therefore, while representing a promising building block for a lactate biosensor, HCAR1 was found to be sensitive to perturbations of its structure, affecting its ability to distinguish between related carboxylic molecules.

**Keywords:** lactate; genetically encoded fluorescent indicator; GPR81; HCAR1; circularly permuted green fluorescent protein



**Citation:** Wellbourne-Wood, J.; Briquet, M.; Alessandri, M.; Binda, F.; Touya, M.; Chatton, J.-Y. Evaluation of Hydroxycarboxylic Acid Receptor 1 (HCAR1) as a Building Block for Genetically Encoded Extracellular Lactate Biosensors. *Biosensors* **2022**, *12*, 143. <https://doi.org/10.3390/bios12030143>

Received: 10 February 2022

Accepted: 24 February 2022

Published: 25 February 2022

**Publisher's Note:** MDPI stays neutral with regard to jurisdictional claims in published maps and institutional affiliations.



**Copyright:** © 2022 by the authors. Licensee MDPI, Basel, Switzerland. This article is an open access article distributed under the terms and conditions of the Creative Commons Attribution (CC BY) license (<https://creativecommons.org/licenses/by/4.0/>).

## 1. Introduction

Since its discovery at the end of the 18th century and for almost two centuries, lactate has been viewed as a waste product of the metabolism generated during hypoxia, and having several adverse effects, such as muscle soreness and fatigue. However, in the 1980s, evidence started to accumulate showing that lactate could in fact be utilized as a useful metabolic fuel [1], i.e., that it could be transferred from glycolytic cells to oxidative cells for energizing respiration. Since then, several studies have indicated the valuable contribution of lactate as a metabolic substrate in tissues, including muscle [2], as a neuroprotective agent, and more recently as a signaling molecule, for reviews, see, e.g., [3]. In the central nervous system, lactate was proposed to play an important role as energy substrate for neurons [4]. Extracellular brain lactate levels are estimated to be in the low millimolar range at resting state [5,6] and to undergo a two-fold increase during synaptic activity [7]. During intense physical exercise, plasma lactate, which can cross the blood–brain barrier, can rise to 10–20 mM [8].

It has recently been found that energy substrates and metabolites of the energy metabolism have extracellular signaling properties by acting through G-protein-coupled

receptors (GPCRs) [9,10]. Lactate is the endogenous ligand of one such receptor, originally named GPR81, now known as hydroxycarboxylic acid receptor 1 (HCAR1) [11]. HCAR1 was initially described as markedly expressed in adipocytes, where its activation induces the inhibition of lipolysis through the activation of a  $G_i$ -dependent intracellular pathway [12]. Our research group demonstrated that extracellular L-lactate and non-metabolized HCAR1 agonists decrease the synaptic activity of CNS neurons [13–15].

Methods for detecting lactate levels include enzymatic assays, amperometric lactate biosensors, microdialysis, or sniffer cells-based detection [16]. Research on lactate effects in living tissue would critically benefit from a fluorescence imaging approach. Genetically encoded fluorescent indicators have been developed for a long list of analytes including, notably, cations ( $Ca^{2+}$ ,  $Zn^{2+}$ ,  $H^+$ ), intracellular metabolites (ATP, GTP, cGMP, glucose, etc.), and extracellular neurotransmitters (glutamate, dopamine, noradrenaline, etc.) [17]. A ratiometric FRET biosensor for lactate, named Laconic, has been developed [18] but is only applicable to intracellular lactate detection [19]. Recently, a genetically encoded biosensor for extracellular lactate was demonstrated that makes use of a prokaryotic lactate periplasmic binding protein TTHA0766 coupled to a circularly permuted GFP (cpGFP) that was addressed to the extracellular side of the plasma membrane [19].

In our study, we investigated whether the strategy used previously for several neurotransmitters based on their respective specific GPCRs [17] could be deployed to develop a lactate-sensitive fluorescence biosensor, and constructed an intensimetric fluorescent lactate-sensitive biosensor based on the HCAR1 lactate receptor coupled to cpGFP.

## 2. Materials and Methods

### 2.1. Engineering of Constructs

The nucleotide sequences of mouse and human HCAR1 were obtained from GenBank (KU285433.1 and KU285432.1, respectively). The gene sequences encoding cpGFP used for the constructs, having LARS as the acronym, were those published previously [20,21]. Constructs were cloned and expressed using the GenScript Biotech (Leiden, Netherlands) or the VectorBuilder (Chicago, IL, USA) platforms. Transmembrane domains of HCAR1 were determined according to the Uniprot database and implied by the published aligned sequences comparing >800 GPCRs [22]. The alignment was also compared to the alignments of other GPCR-based sensors [20]. Linker sequences (N- and C-terminal ends of cpGFP) were those used for other similar biosensors [20,21]. Amino acid sequences used are indicated in Table 1. Predictions of tertiary structures of the LARS constructs were performed using the IntFOLD tool [23] accessed through its integrated protein structure and function prediction server [24]. Three-dimensional visualizations of the constructs were created using Mol\* [25], accessed through the RCSB Protein Databank portal [26].

### 2.2. Cell Culture and Transfection

All animal experimentation procedures were carried out in accordance with the recommendations of the Swiss Ordinance on Animal Experimentation and were specifically approved for this study by the Veterinary Affairs of the Canton Vaud, Switzerland (authorizations# VD1288  $\times$  8) and conformed to the ARRIVE guidelines. Cortical astrocytes in primary culture were prepared from 1- to 3-day-old C57BL/6N mice as described previously [27]. Astrocytes were plated on coverslips and cultured for 2 weeks in DMEM (#D7777, Sigma, Schaffhausen, Switzerland) medium plus 10% FCS before experiments. HEK293 were cultured in DMEM plus 10% FCS, and plated on poly-D-lysine (#P6407, Sigma, Schaffhausen, Switzerland) coated coverslips.

Transfection with the plasmids carrying the LARS constructs was performed using Lipofectamine 2000 (#11668019, Invitrogen, Basel, Switzerland) for 5 h. For HEK293 cells, 0.5  $\mu$ g DNA was applied in Opti-MEM medium (#31985062, Gibco, Thermo Fisher Scientific, Basel, Switzerland), whereas for astrocytes, 1  $\mu$ g DNA was applied in Neurobasal medium (#21103049, Gibco, Thermo Fisher Scientific, Basel, Switzerland). HEK293 cells were transfected 1 day post-splitting and primary astrocytes were transfected at DIV 14. In

some experiments, astrocytes were loaded with the red fluorescent dye sulforhodamine 101 (SR101) applied in the bath at 1  $\mu$ M for 10 min. Cells were used 48 h after transfection, unless otherwise indicated.

**Table 1.** Summary of main construct design rationale.

Construct Name	Membrane Targeting Sequence	Linkers	Description	Results/Observations
LARS1.1	HA secretory sequence	Based on dLight 1.1 or 1.2 <sup>1</sup> N-linker: LSSLI C-linker: NHDQL	Use mouse HCAR1 gene; replace entire IC3 loop	No measurable fluorescence
LARS 1.2	HA secretory sequence	Based on dLight 1.1 or 1.2 <sup>1</sup> N-linker: LSSLI C-linker: NHDQL	Use human HCAR1 gene; replace entire IC3 loop	Some fluorescence, intracellular localization, lysosomes or ER
LARS 1.3	HA secretory sequence	Based on dLight 1.1 or 1.2 <sup>1</sup> N-linker: LSSLI C-linker: NHDQL	Using mouse HCAR1 gene; replace part of IC3 loop	Weak fluorescence, intracellular localization, lysosomes or ER
LARS 1.5 *	HA secretory sequence	Optimized linkers for B2AR and MT2R <sup>1</sup> N-linker: QLQKIDLSSLI C-linker: NHDQDIKQLQ	Use mouse HCAR1 gene; replace part of IC3 loop	Fluorescence partly intracellular and plasma membrane in several cells
LARS 1.7	HA secretory sequence	Based on dLight 1.1 or 1.2 <sup>1</sup> N-linker: LSSLI C-linker: NHDQL	Use human HCAR1 gene; replace entire IC2 loop	Weak and sparse fluorescence, intracellular localization
LARS 1.8 *	IgK secretory sequence	Optimized linkers for B2A and MT2 receptors <sup>1</sup> N-linker: QLQKIDLSSLI C-linker: NHDQDIKQLQ	Use mouse HCAR1 gene; replace part of IC3 loop; use IgK secretory sequence and mutated cpGFP of GRAB <sub>5-HT</sub> <sup>2</sup>	Robust plasma membrane fluorescence
LARS 1.10 *	IgK secretory sequence	Based on GRAB <sub>5-HT</sub> <sup>2</sup> N-linker: MFLNG C-linker: GFATA	Use mouse HCAR1 gene; replace part of IC3 loop; use IgK secretory sequence; use GRAB <sub>5-HT</sub> linkers and mutated cpGFP <sup>2</sup>	Robust fluorescence with mixed intracellular and membrane localization

\* Kept for further testing. <sup>1</sup> dLight is a dopamine biosensor [20]. <sup>2</sup> GRAB<sub>5-HT</sub> is a serotonin biosensor [21]. B2A,  $\beta$ 2-adrenergic receptor; MT2R, melatonin type 2 receptor; HA, hemagglutinin leader sequence; IgK, immunoglobulin kappa light chain leader sequence.

### 2.3. Widefield Fluorescence Imaging

Widefield imaging was performed using: (1) An upright epifluorescence microscope (FN1, Nikon, Tokyo, Japan) using a 40  $\times$  0.8 N.A. water-immersion objective lens. Fluorescence was excited using an LED light source (Lambda 421, Sutter Instr., Novato, CA, USA) and detected through a 535  $\pm$  15 nm filter (Chroma, Bellows Falls, VT, USA) using an Evolve EMCCD camera (Photometrics, Tucson, AZ, USA). (2) An epifluorescence inverted microscope (Zeiss Axiovert 100 M) equipped with a high numerical aperture fluorescence objective (40  $\times$  1.3 N.A. oil-immersion), and fast holographic monochromator (Polychrome II, Till Photonics, Planegg, Germany) coupled to a Xenon lamp for fluorescence excitation, with detection using an EMCCD camera (LUCA-R, Andor, Belfast, UK). LARS excitation spectra were obtained by driving the monochromator light source in the range 350–500 nm, with detection of fluorescence through a 535  $\pm$  20 nm filter (Chroma). Digital image acquisition and time series were computer-controlled using the Metafluor software (RRID:SCR\_014294). Experimental solutions for live imaging contained (mM): NaCl 160, KCl 5.4, HEPES 20, CaCl<sub>2</sub> 1.3, MgSO<sub>4</sub> 0.8, NaH<sub>2</sub>PO<sub>4</sub> 0.78, glucose 5 (pH 7.4) and were bubbled with air. Solutions containing lactate, pyruvate,  $\beta$ -hydroxybutyrate (BHB), or mannitol had their NaCl concentration correspondingly decreased to ensure iso-osmolarity.

### 2.4. Confocal Imaging

Cells expressing LARS constructs were observed on an LSM780 confocal microscope (Carl Zeiss, Germany) using oil immersion objectives (20 $\times$ , 40 $\times$ , or 63 $\times$  PlanApo). cpGFP

was excited at 488 nm and detected in the range 493–569 nm. SR101 was excited at 561 nm and detected in the range 569–712 nm. The GaAsP 32-channel Quasar spectral detector of the LSM780 was used to measure emission spectra of samples using 488 nm fluorescence excitation. ImageJ software (RRID:SCR\_003070) was further used for downstream image processing and analysis.

### 2.5. Two-Photon Imaging

Two-photon imaging was carried out using a custom-built two-photon microscope with a  $20 \times 0.95$  N.A. water-dipping objective (Olympus, Tokyo, Japan). Fluorescence excitation was performed using a Chameleon Vision S femtosecond infrared laser including group velocity dispersion compensation (Coherent, CA, USA). Fluorescence emission was measured at  $525 \pm 25$  nm (Semrock FF01–525/50). To measure two-photon excitation spectra, the infrared laser intensity was adjusted to yield a constant value throughout the Ti:Sapphire emission spectrum using an acousto-optic modulator (AA Opto-Electronic, Orsay, France). Image acquisition was performed using custom software in the Labview (RRID:SCR\_014325) environment.

### 2.6. Data Analysis

Bar graphs show mean  $\pm$  SEM based on quantification of individual traces, of which examples are shown. The mean fluorescence intensity in regions of interest selected around 5–6 cells (later referred to as cell groups) was measured and quantified in the image series. Graphs and nonlinear curve fitting for  $EC_{50}$  calculations were carried out using KaleidaGraph software (Synergy Software; RRID:SCR\_014980).

### 2.7. Chemicals and Drugs

Unless specified, chemicals were from Sigma-Aldrich.

## 3. Results and Discussion

### 3.1. Design and Characterization of HCAR1-Based Lactate Sensors

A major class of genetically encoded intensimetric fluorescent sensors is based on engineered chimeric seven transmembrane (7 TM) GPCR that are integral membrane proteins. The binding of the ligand to the extracellular receptor domain causes conformational changes that are transmitted to an integrated fluorescent protein, modulating its fluorescent properties. Several biosensors for neurotransmitters have cpGFP integrated on the intracellular side of the receptor protein in the third intracellular (IC3) loop [17]. We based our design on successful biosensors for dopamine, norepinephrine, melatonin [20], and for 5-hydroxytryptamine (5-HT, serotonin) [21]. The design strategies for main candidates are summarized in Table 1.

The first listed constructs (LARS1.1 and LARS1.2) did not yield any or only sparse intracellular fluorescence, possibly because of the too close proximity of cpGFP to the plasma membrane and intracellular segments of HCAR1, which prevented it from properly folding. Thus, longer stretches of the IC3 loop were kept, along with different linkers. In addition, two different membrane targeting sequences were compared: the hemagglutinin secretion motif (HA) and the immunoglobulin  $\kappa$ -chain leader sequence (IgK). IgK proved to significantly better address the protein constructs to the plasma membrane. The complete sequence of best candidate LARS1.8 is presented in Figure S1.

The three optimized sensors—LARS1.5, LARS1.8, and LARS1.10—yielded green fluorescence associated with the plasma membrane when transfected in HEK293 cells (Figure 1).

Compared to LARS1.5, LARS 1.8 and LARS1.10 were more clearly localized to the plasma membrane. Primary mouse astrocytes transfected with the LARS1.8 plasmid displayed plasma membrane expression that extended to their finest lamellipodia (Figure 2), which strongly contrasted with the distribution of the red cytosolic dye SR101 that was only visible in the thickest regions of these flat cultured astrocytes. Note that a profile plot, as



performed on HEK293 cells, would not adequately reflect membrane localization in those extremely thin cells.

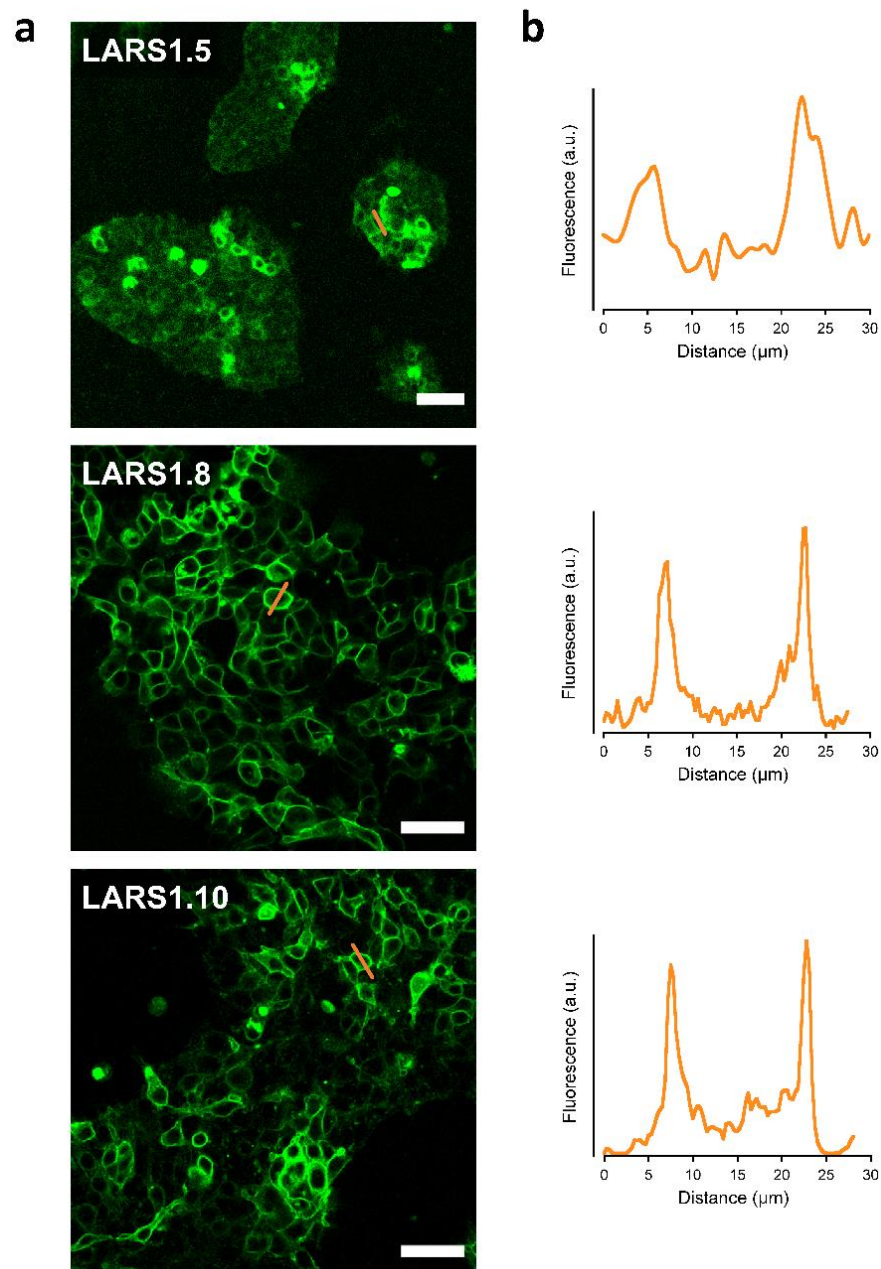


**Figure 1.** Cellular expression of candidate biosensors in HEK293 cells. Confocal images of live HEK293 cells transfected with LARS1.5, LARS1.8, and LARS1.10 and observed 48 h after transfection. Images show endogenous cpGFP fluorescence ( $\lambda_{\text{ex}} = 488 \text{ nm}$ ) (a). A representative profile plot across cells (at sites indicated by orange lines in left panel) is shown next to the candidate biosensors (b). Scale bar, 50  $\mu\text{m}$ .

In order to further support the correct folding and localization of the protein constructs, we conducted molecular modeling simulations using the IntFold [23]. Figure 3 graphically depicts the LARS1.8 construct domains and shows the predicted tertiary structure obtained for the LARS1.8 amino acid sequence. The expected transmembrane domains of the receptor part as well as cpGFP tertiary structure appear correctly folded. Similar successful predicted 3D structures were obtained for LARS1.5 and LARS1.10, and provided the indication that the constructs would be correctly inserted in the plasma membrane.

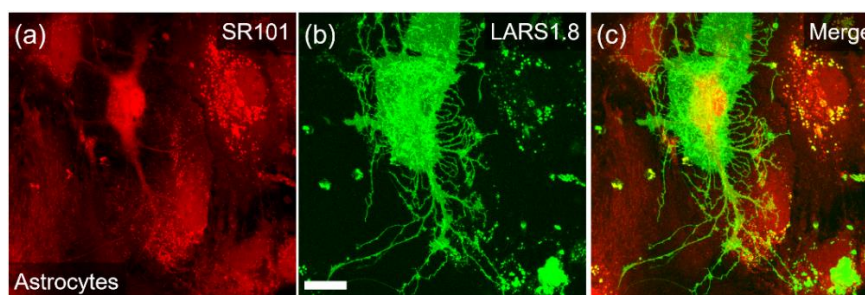


**Figure 2.** Cellular expression in primary mouse astrocytes. Confocal images of live mouse astrocytes transfected with LARS1.8 and observed 48 h after transfection. (a) SR101 dye staining ( $\lambda_{ex} = 561$  nm), (b) endogenous cpGFP fluorescence ( $\lambda_{ex} = 488$  nm), and (c) merged image. Note the cpGFP green staining extending to the finest membrane processes. Scale bar, 20  $\mu$ m.

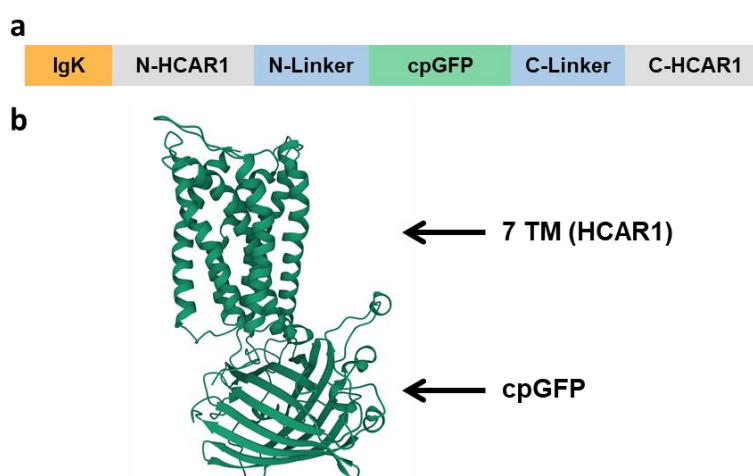


**Figure 3.** Design of candidate biosensors and predicted tertiary structure of the protein. (a) The general design of the constructs comprises a plasma membrane addressing sequence (IgK or HA) fused at the N-terminal side of the protein. cpGFP was inserted in the intracellular loop 3 and flanked with linker sequences at the N- and C-terminal side of the loop. (b) Tertiary structure prediction of LARS1.8 highlighting the seven-transmembrane domains (7 TM) of HCAR1 and the cpGFP insertion. For calculations of structure prediction, the disordered N- and C-termini of the sequence were trimmed to keep 15 amino acid residues before the start of transmembrane domain 1 and 10 residues after transmembrane domain 7 on N-terminal side. The structure prediction yielded an overall high level of confidence ( $p = 0.0024$ ).

### 3.2. Biosensor Sensitivity to Lactate

The fluorescence emission and excitation spectra of LARS1.8 recorded on live HEK293 cells are depicted in Figure 4a,b. The excitation spectrum displayed the typical  $-400$  nm and  $-490$  bands of cpGFP corresponding to the neutral and anionic form of the protein, while emission peaked at  $-515$  nm as observed with the calcium indicator series GCaMP [28]. Two-photon excitation of LARS1.8 using a pulsed femtosecond infrared laser is depicted in Figure 4c. The optimal two-photon excitation wavelength was found at 950 nm, while a second two-photon absorption band was observed at  $-1000$  nm.

LARS 1.8 was first selected for functional testing as it displayed the most clearly defined membrane expression. The fluorescence of LARS1.8 expressed in HEK293 cells was found to exhibit pronounced changes following lactate application. Interestingly, an inverse response was observed corresponding to rapid and reversible fluorescence decreases (Figure 5a). This inverse response could already be seen in the excitation spectra measured in the presence and absence of lactate (Figure 4b), which indicated that lactate caused a homogenous decrease in LARS1.8 fluorescence. The dynamic range of fluorescence

over the binding curve is in the range of 30%, providing an ample fluorescence window for sensing concentration changes. Similar inverse responses to lactate application were also observed with the LARS1.5 and LARS1.10 constructs expressed in HEK293 cells (Figure 5b). The apparent affinity of the three LARS constructs was estimated to be  $4.5 \pm 1.5$  mM,  $1.5 \pm 1.5$  mM, and  $5.6 \pm 2.1$  mM for LARS1.5, LARS1.8, and LARS1.10, respectively. These apparent  $EC_{50}$  values affinities are in the range reported for HCAR1 [12,13].

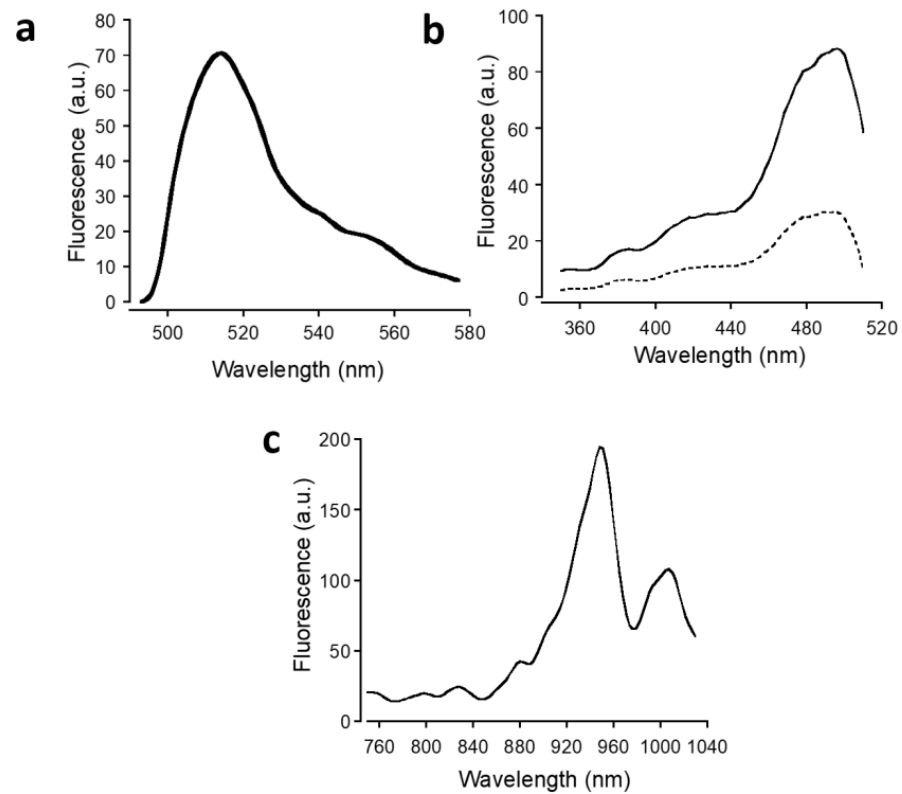


**Figure 4.** Fluorescence spectral properties. (a) In situ fluorescence emission spectrum of LARS1.8 ( $\lambda_{ex} = 488$  nm) in live HEK293 cells. (b) One-photon excitation spectra in the absence (plain line) and in the presence of lactate (10 mM, dotted line). (c) Two-photon excitation spectrum.

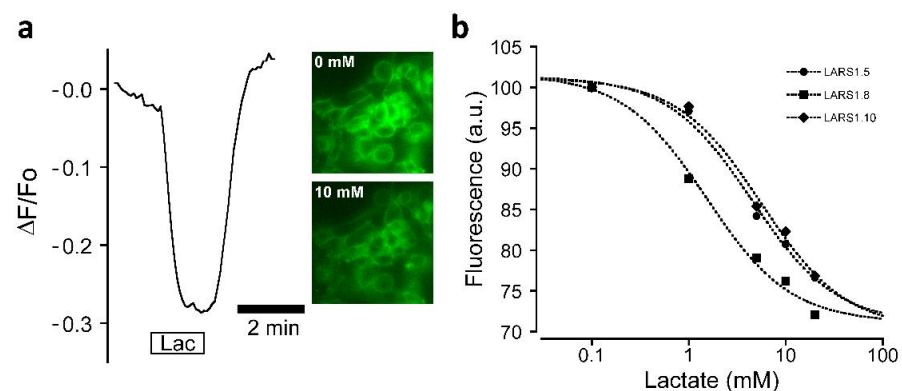


**Figure 5.** Responses of candidate biosensors to lactate application. (a) Representative fluorescent curve of LARS1.8 response to 10 mM lactate application. Widefield fluorescence images of recorded a group of HEK293 cells before and during application of lactate are shown ( $\lambda_{ex} = 490$  nm). (b) Lactate concentration dependence of LARS1.5, LARS1.8, and LARS1.10 fluorescence responses. Data points are mean values measured 6–7 groups of cells for each construct.  $EC_{50}$  values were obtained by nonlinear curve fitting using the Levenberg–Marquardt algorithm. Data are normalized to the fluorescence measured in the absence of lactate.

### 3.3. Biosensor Selectivity

In the next phase, we investigated whether the LARS constructs were able to discriminate lactate from related molecules. Figure 6 shows that LARS1.8 displayed similar responses to L-lactate, pyruvate, BHB, and D-lactate when applied at the same concentration (10 mM). The LARS1.5 construct, which differs from LARS1.8 by the membrane addressing sequence, also responded to pyruvate and BHB. As the original HCAR1 protein, from which LARS constructs are derived, has selectivity for lactate over these other molecules, one can hypothesize that the addition of cpGFP with its 11 amino acid long linkers in the third intracellular loop is perturbing the receptor such that it loses its selectivity for lactate over other hydroxycarboxylic acids. We thus tested whether LARS1.10, a construct having shorter linkers (5 amino acids) flanking cpGFP, would exhibit a different behavior. Figure 6 shows that LARS1.10 was also not able to distinguish lactate from pyruvate or BHB when applied at 10 mM. Importantly, we show that 10 mM mannitol, a molecule of similar molecular size but that is not a hydroxycarboxylic acid, did not cause significant fluorescence responses, indicating that the LARS constructs have selectivity for hydroxycarboxylic acids.

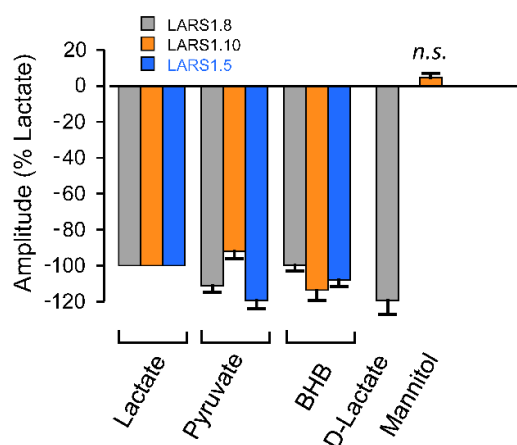


**Figure 6.** Selectivity candidate biosensor responses. The amplitude of responses of LARS1.8 ( $n = 16$  cell groups), LARS1.10 ( $n = 14$ – $17$  cell groups) and LARS1.5 ( $n = 3$  cell groups) to pyruvate (10 mM), and  $\beta$ -hydroxybutyrate (10 mM). Additionally, D-lactate (10 mM), sensitivity and lack of sensitivity to mannitol (10 mM) were observed. Responses were normalized to the response to lactate (10 mM) on the same cells.

Thus, it appears that inserting the cpGFP fluorescent protein in the third intracellular loop, as was successfully performed for several other biosensors based on GPCRs (e.g., for dopamine, norepinephrine, serotonin, etc.), had the effect of perturbing the selectivity for lactate found in the original HCAR1 protein. We postulate that the linkers flanking cpGFP were not the only culprits, as the same result was found for two linkers that differed both in their length and in their amino acid composition.

## 4. Conclusions and Outlook

Overall, in this study, we describe—to our knowledge—the first attempt at using the lactate receptor HCAR1, a  $G_i$ -coupled GPCR, to build a fluorescent biosensor for extracellular lactate. We identified that addressing the protein constructs to the plasma membrane was very efficiently achieved using the IgK leading sequence. The strategy appears promising as the candidate sensors respond to lactate at physiologically relevant concentrations with cellular resolution. Rapid fluorescence changes were observed with kinetics that are compatible with the expected kinetics of physiological lactate variations found in tissues, for instance in response to neuronal activity or to intense physical exercise. Nevertheless, further improvements of the sensors need to address the issue of selectivity. When screening for improved versions of HCAR1-based lactate sensors, as was performed

for other sensors such as the dopamine or serotonin sensors, one needs to include the double condition of maximum fluorescence change induced by lactate coupled with the lack of response to other related molecules, such as pyruvate or BHB. Ideally, variants showing fluorescence increases rather than decreases (inverse response) to lactate application would be advantageous—but not mandatory—for experiments. Compared with the recently published lactate biosensor [19] based on a bacterial extracellular lactate binding protein coupled to GFP, HCAR1-based sensors would arguably have the advantage of positioning the fluorescent protein inside the cell, protecting it from ion fluctuations that may occur in the interstitial milieu in particular in pathological situations. In addition, a biosensor based on HCAR1 that would retain the properties of the original HCAR1 protein could represent a powerful tool for the screening of new agonists or antagonist of the receptor, as well as for allosteric modulators. In conclusion, imaging approaches of lactate biosensors offer the prospect of precisely analyzing lactate concentration fluxes within living tissues, including in microdomains around cells, which will bring invaluable information for both physiological and pathological conditions.

**Supplementary Materials:** The following supporting information can be downloaded at: <https://www.mdpi.com/article/10.3390/bios12030143/s1>, Figure S1: LAR1.8 protein sequence.

**Author Contributions:** Conceptualization, J.W.-W. and J.-Y.C.; Methodology, M.B., M.A., F.B., J.-Y.C.; Formal Analysis, M.B., M.A., F.B., J.-Y.C.; Investigation, M.B., M.A., F.B., M.T., J.-Y.C.; Data Curation, M.B., M.A., F.B.; Writing—Original Draft Preparation, J.-Y.C.; Writing—Review and Editing, M.B., M.A., F.B., J.W.-W.; Project Administration, J.-Y.C.; Funding Acquisition, J.-Y.C. All authors have read and agreed to the published version of the manuscript.

**Funding:** This research was funded by the University of Lausanne, Faculty of Biology and Medicine.

**Institutional Review Board Statement:** Not applicable.

**Informed Consent Statement:** Not applicable.

**Data Availability Statement:** Not applicable.

**Conflicts of Interest:** The authors declare no conflict of interest.

## References

1. Brooks, G.A. Lactate as a fulcrum of metabolism. *Redox Biol.* **2020**, *35*, 101454. [[CrossRef](#)] [[PubMed](#)]
2. Gladden, L.B. 200th anniversary of lactate research in muscle. *Exerc. Sport Sci. Rev.* **2008**, *36*, 109–115. [[CrossRef](#)] [[PubMed](#)]
3. Barros, L.F. Metabolic signaling by lactate in the brain. *Trends Neurosci.* **2013**, *36*, 396–404. [[CrossRef](#)] [[PubMed](#)]
4. Pellerin, L.; Magistretti, P.J. Glutamate uptake into astrocytes stimulates aerobic glycolysis: A mechanism coupling neuronal activity to glucose utilization. *Proc. Natl. Acad. Sci. USA* **1994**, *91*, 10625–10629. [[CrossRef](#)]
5. Abi-Saab, W.M.; Maggs, D.G.; Jones, T.; Jacob, R.; Srihari, V.; Thompson, J.; Kerr, D.; Leone, P.; Krystal, J.H.; Spencer, D.D.; et al. Striking differences in glucose and lactate levels between brain extracellular fluid and plasma in conscious human subjects: Effects of hyperglycemia and hypoglycemia. *J. Cereb. Blood Flow Metab.* **2002**, *22*, 271–279. [[CrossRef](#)]
6. Diemel, G.A.; Ball, K.K.; Cruz, N.F. A glycogen phosphorylase inhibitor selectively enhances local rates of glucose utilization in brain during sensory stimulation of conscious rats: Implications for glycogen turnover. *J. Neurochem.* **2007**, *102*, 466–478. [[CrossRef](#)]
7. Hu, Y.; Wilson, G.S. A temporary local energy pool coupled to neuronal activity: Fluctuations of extracellular lactate levels in rat brain monitored with rapid-response enzyme-based sensor. *J. Neurochem.* **1997**, *69*, 1484–1490. [[CrossRef](#)]
8. Offermanns, S. Hydroxy-Carboxylic Acid Receptor Actions in Metabolism. *Trends Endocrinol. Metab.* **2017**, *28*, 227–236. [[CrossRef](#)]
9. Blad, C.C.; Tang, C.; Offermanns, S. G protein-coupled receptors for energy metabolites as new therapeutic targets. *Nat. Rev. Drug Discov.* **2012**, *11*, 603–619. [[CrossRef](#)]
10. Husted, A.S.; Trauelsen, M.; Rudenko, O.; Hjorth, S.A.; Schwartz, T.W. GPCR-Mediated Signaling of Metabolites. *Cell Metab.* **2017**, *25*, 777–796. [[CrossRef](#)]
11. Cai, T.Q.; Ren, N.; Jin, L.; Cheng, K.; Kash, S.; Chen, R.; Wright, S.D.; Taggart, A.K.; Waters, M.G. Role of GPR81 in lactate-mediated reduction of adipose lipolysis. *Biochem. Biophys. Res. Commun.* **2008**, *377*, 987–991. [[CrossRef](#)]
12. Liu, C.; Wu, J.; Zhu, J.; Kuei, C.; Yu, J.; Shelton, J.; Sutton, S.W.; Li, X.; Yun, S.J.; Mirzadegan, T.; et al. Lactate inhibits lipolysis in fat cells through activation of an orphan G-protein-coupled receptor, GPR81. *J. Biol. Chem.* **2009**, *284*, 2811–2822. [[CrossRef](#)]
13. Bozzo, L.; Puyal, J.; Chatton, J.-Y. Lactate modulates the activity of primary cortical neurons through a receptor-mediated pathway. *PLoS ONE* **2013**, *8*, e71721. [[CrossRef](#)]



14. De Castro Abrantes, H.; Briquet, M.; Schmuziger, C.; Restivo, L.; Puyal, J.; Rosenberg, N.; Rocher, A.B.; Offermanns, S.; Chatton, J.Y. The lactate receptor HCAR1 modulates neuronal network activity through the activation of Galpha and Gbeta subunits. *J. Neurosci.* **2019**, *39*, 4422–4433. [[CrossRef](#)]
15. Briquet, M.; Rocher, A.B.; Alessandri, M.; Rosenberg, N.; de Castro Abrantes, H.; Wellbourne-Wood, J.; Schmuziger, C.; Ginet, V.; Puyal, J.; Pralong, E.; et al. Activation of lactate receptor HCAR1 down-modulates neuronal activity in rodent and human brain tissue. *J. Cereb. Blood Flow Metab.* **2022**; *in press*.
16. Sotelo-Hitschfeld, T.; Niemeyer, M.I.; Machler, P.; Ruminot, I.; Lerchundi, R.; Wyss, M.T.; Stobart, J.; Fernandez-Moncada, I.; Valdebenito, R.; Garrido-Gerter, P.; et al. Channel-mediated lactate release by K(+)-stimulated astrocytes. *J. Neurosci.* **2015**, *35*, 4168–4178. [[CrossRef](#)]
17. Nasu, Y.; Shen, Y.; Kramer, L.; Campbell, R.E. Structure- and mechanism-guided design of single fluorescent protein-based biosensors. *Nat. Chem. Biol.* **2021**, *17*, 509–518. [[CrossRef](#)]
18. San Martin, A.; Ceballo, S.; Ruminot, I.; Lerchundi, R.; Frommer, W.B.; Barros, L.F. A genetically encoded FRET lactate sensor and its use to detect the Warburg effect in single cancer cells. *PLoS ONE* **2013**, *8*, e57712. [[CrossRef](#)]
19. Nasu, Y.; Murphy-Royal, C.; Wen, Y.; Haidey, J.N.; Molina, R.S.; Aggarwal, A.; Zhang, S.; Kamiyo, Y.; Paquet, M.E.; Podgorski, K.; et al. A genetically encoded fluorescent biosensor for extracellular L-lactate. *Nat. Commun.* **2021**, *12*, 7058. [[CrossRef](#)]
20. Patriarchi, T.; Cho, J.R.; Merten, K.; Howe, M.W.; Marley, A.; Xiong, W.H.; Folk, R.W.; Broussard, G.J.; Liang, R.; Jang, M.J.; et al. Ultrafast neuronal imaging of dopamine dynamics with designed genetically encoded sensors. *Science* **2018**, *360*, eaat4422. [[CrossRef](#)]
21. Wan, J.; Peng, W.; Li, X.; Qian, T.; Song, K.; Zeng, J.; Deng, F.; Hao, S.; Feng, J.; Zhang, P.; et al. A genetically encoded sensor for measuring serotonin dynamics. *Nat. Neurosci.* **2021**, *24*, 746–752. [[CrossRef](#)] [[PubMed](#)]
22. Cvicsek, V.; Goddard, W.A., 3rd; Abrol, R. Structure-Based Sequence Alignment of the Transmembrane Domains of All Human GPCRs: Phylogenetic, Structural and Functional Implications. *PLoS Comput. Biol.* **2016**, *12*, e1004805. [[CrossRef](#)] [[PubMed](#)]
23. McGuffin, L.J.; Adiyaman, R.; Maghrabi, A.H.A.; Shuid, A.N.; Brackenridge, D.A.; Nealon, J.O.; Philomina, L.S. IntFOLD: An integrated web resource for high performance protein structure and function prediction. *Nucleic Acids Res.* **2019**, *47*, W408–W413. [[CrossRef](#)] [[PubMed](#)]
24. Available online: <https://www.reading.ac.uk/bioinf/IntFOLD> (accessed on 9 February 2022).
25. Sehnal, D.; Bittrich, S.; Deshpande, M.; Svobodova, R.; Berka, K.; Bazgier, V.; Velankar, S.; Burley, S.K.; Koca, J.; Rose, A.S. Mol\* Viewer: Modern web app for 3D visualization and analysis of large biomolecular structures. *Nucleic Acids Res.* **2021**, *49*, W431–W437. [[CrossRef](#)]
26. 3D View. Available online: <https://www.rcsb.org/3d-view> (accessed on 9 February 2022).
27. Sorg, O.; Magistretti, P.J. Vasoactive intestinal peptide and noradrenaline exert long-term control on glycogen levels in astrocytes: Blockade by protein synthesis inhibition. *J. Neurosci.* **1992**, *12*, 4923–4931. [[CrossRef](#)]
28. Barnett, L.M.; Hughes, T.E.; Drobizhev, M. Deciphering the molecular mechanism responsible for GCaMP6m's Ca<sup>2+</sup>-dependent change in fluorescence. *PLoS ONE* **2017**, *12*, e0170934. [[CrossRef](#)]

001 METDTLLLWVLLLWVPGSTGDTSLYKKVGTGMDNGSCCLIEGEPISQVM  
051 PPLLLLVFVLGALGNGIALCGFCFHMKTWKSSTIYLFNLAVADFLLMICL  
101 PLRTDYLLRRRHWFQDIACRLVLFKLMNRAGSIVFLTVVAVDRYFKVV  
151 HPHHMVNAISNRATAATACVLWTLVILGTVYLLMESHLCVQGTLSSECF  
201 IMESANGWHDVMFQLEFFLPLTIILFCSVNVVWVSLRRQLQKIDLSLIN  
251 YIKADKQKNGIKANFHIRHNIEDGGVQLAYHYQQNTPIGDGPVLLPDNHY  
301 LSVQSKLSKDPNEKRDHMLLEFVTAAGITLGMDELYKGGTGGQESMSSK  
351 GEELFTGVVPIILVELDGDVNGHKFSVSGEGEGDATTGKLTCLKFICTTGKL  
401 PVPWPTLVTTLTYGVCFSRYPDHMKQHDFFKSAMPEGYIQERTIFFKDD  
451 GNYKTRAEVKFEGDTLVNRIELKGIDFKEDGNILGHKLEYNNHDQLDIKQ  
501 LQARMRRATRFIMVVASVFITCYLPSVLARLYFLWTVPTSACDPSVHTAL  
551 HVTLSFTYLNSMLDPLVYYFSSPSLPKFYTKLTICSLKPKRPGRTKTRRS  
601 EEMPISNLCSKSSIDGANRSQRPSDGQWDLQVC\*

**Figure S1. LAR1.8 protein sequence.** The construct comprises a IgK sequence (orange) fused to mouse HCAR1 sequence (grey). cpGFP (green) is inserted in the HCAR1 protein using two sets of linkers (blue).

## Discussion and Perspectives

In this section, I will further develop some aspects discussed in the published articles.

### HCAR1 localization in the brain

In our study, we aimed at better identifying the localization of the receptor in the brain and at cellular level to delineate its implication in physiological functions. As mentioned in the introduction, we had to find a method for overcoming the antibody specificity problem we are facing. We reported so far 14 unspecific antibodies that are commercially available (9 in de Castro Abrantes et al. (2019) and 5 in Supplementary Figure 1 by comparing the staining in WT and HCAR1 KO mice. Interestingly, Madaan et al. (2019) were able to show HCAR1 antibody specificity in the retina. The researchers reported that HCAR1 is specifically expressed on Müller cells, principal glial cells of the retina assuming similar functions that astrocytes, oligodendrocytes, and ependymal cells of the central nervous system, of WT mice. The specificity was confirmed by Western blot since immunoreactivity to HCAR1 was present in retinal homogenates from WT mice, but absent in retinas of HCAR1 KO mice. To our knowledge, this was the first study that show HCAR1 antibody selectivity in glia cells. Regrettably, the antibody used did not show specificity in our brain slices indicating that antibodies are recognizing a somewhat different receptor in the brain that are absent from the retina. In addition, the authors contacted confirmed that they experienced the same problem with brain slices (personal communication). In addition to HCAR2 and HCAR3, the orphan receptor GPR31 and the 5-oxo-6,8,11,14-eicosatetraenoic acid (5-oxo-EETE) receptor OXER1 are the receptors most closely related to HCAR1 with a conserved arginine residue in transmembrane helix 3 serving as an anchor point for the carboxylic group present in the respective agonists (Ahmed et al., 2009). Nevertheless, GPCR antibodies are known to lack specificity and many of them are reported to be unspecific (Michel et al., 2009). For example, one study reported that antibodies raised against either  $\beta_2$ - or  $\beta_3$ -adrenoceptors recognize similar band patterns on immunoblots from cells expressing any of the nine adrenoceptors subtypes (Pradidarcheep et al., 2008) or another one showed that double knock-out mice lacking both muscarinic 2 ( $M_2$ ) and  $M_3$  receptors are still stained positive for  $M_2$  and  $M_3$  receptor antibodies (Jositsch et al., 2009).



To work around this issue, we used a transgenic mouse line that expresses a red fluorescent protein (mRFP) under the promoter of HCAR1. HCAR1 expressing cells were mainly found in the cerebellum and the hippocampus, where the positive cells predominantly correspond to hilar MCs. This technique still presents limitations such as the fact that the reporter protein is not targeted to the plasma membrane, therefore, preventing us to determine the precise localization of HCAR1 using co-staining of membrane or synaptic proteins.

In addition, we used fluorescent RNAscope *in situ* hybridization as an alternative technical approach. This novel technology uses a unique probe design strategy that allows simultaneous signal amplification and background suppression to achieve single-molecule visualization while preserving tissue morphology. Thus, we confirmed the presence of HCAR1 RNA in the hippocampus, at the level of the hilus, the CA3, as well as in the cerebellum.

Despite the fact that several techniques were used to better understand the localization of HCAR1, especially in the hippocampus, we observed some remaining ambiguous results. Indeed, the HCAR1 staining was very clear on mossy cells (MCs) with all techniques used. However, the presence of HCAR1 in granule cells (GCs) is more ambiguous. The IHC of mRFP and ISH did not present obvious cellular staining of GCs. The 2-photon imaging of mRFP in fresh acute slices exhibited endogenous red fluorescence in the granule cell layer. However, the 2-photon imaging mode did not include other counterstains and the localization of the signal in the granule cell layer was therefore less detailed. We cannot exclude that some of the positive cells are close to but not within the granule cell layer, or that part of the red fluorescence corresponds to fibers of MCs crossing the granule cell layer. The question of HCAR1 expression by GCs needs further investigation.

Furthermore, we did not observe the presence of HCAR1 in hippocampal astrocytes using the mRFP mouse line. No colocalization was found with GFAP, a marker used for astrocyte staining. Intriguingly, HCAR1 has been found in astrocytes by different groups (Lauritzen et al., 2014; Órdenes et al., 2021). Lauritzen et al. (2014) revealed the presence of HCAR1 in astrocytes and at capillaries after performing double-labeling for HCAR1 and the astrocyte marker GS (glutamine synthetase) in the hippocampus and the cerebellum. Moreover, Órdenes et al. (2021) showed

that HCAR1 immunoreactivity in the arcuate nucleus (ARC) of the basal hypothalamus was detected mainly in astrocyte-like cells, and HCA1R co-localized with GFAP. However, these results are based on immunohistochemical observations using anti-HCAR1 antibodies known to be unspecific (de Castro Abrantes et al., 2019; Briquet et al., 2022) without control using the HCAR1 KO line. We therefore remain skeptical about the presence of HCAR1 in astrocytes.

In conclusion, the need to find a specific antibody for HCAR1 is crucial for further investigations of specific brain and cellular structures.

### HCAR1 activation in rodent hippocampus

Previous studies by us (Bozzo et al., 2013; de Castro Abrantes et al., 2019) and others (Herrera-Lopez and Galvan, 2018; Herrera-López et al., 2020) reported evidence for a neuromodulatory action of HCAR1 on neurons. Thus, as mentioned in the previous section, we showed the presence of the lactate receptor in MCs of the dentate gyrus of the hippocampus. Therefore, we asked whether HCAR1 activation is able to modulate neuronal activity in both mouse and rat hippocampal acute slices. By using whole-cell patch clamp recordings, we showed that HCAR1 activation by its agonist 3Cl-HBA decreases spontaneous and miniature EPSCs frequency at MC-GC synapses without changes in amplitude. This result strongly suggests that the receptor is expressed at the pre-synaptic terminal (i.e. at the MCs membrane) to weaken the glutamatergic tone on GCs and make GCs less likely to fire an action potential. This result is consistent with previous observations on primary neurons, in which the spontaneous activity was decreased after activation of HCAR1 (de Castro Abrantes et al., 2019).

This finding brings a new component to the understanding of the DG complex circuitry regulation, especially at the MC-GC synapses. Hilar MCs are prominent cell types of the hilus of the DG and are proposed to play a central role in the DG network, acting as circuit integrators (Sun et al., 2017). MCs receive convergent excitatory inputs from axons of the dentate GCs and from local inhibitory hilar interneurons (Sun et al., 2017). MCs project their axons to the ipsi- and contralateral inner molecular layer of the DG, where they make synapses into GCs proximal dendrites (Scharfman, 2016). MCs not only contact GC locally, but also project from the point of origin both septally and temporally, i.e. along the longitudinal axis of the hippocampus. Thus,

single MCs may innervate the majority of the DG, establishing an estimated 35,000 synapses in the inner molecular layer GC dendrites (Buckmaster et al., 1996). Therefore, activation of MCs may cause monosynaptic excitation as well as disynaptic inhibition of GCs, and the balance of excitation/inhibition recruited by MC is of critical importance for hippocampal processing. Obviously, more investigations are needed to understand the precise role of HCAR1 in this balance. Even though, our hypothesis is that HCAR1, by sensing lactate, could act as a metabolic sensor of neuronal activity and therefore prevent excessive firing by downregulating glutamate release at MC-GC synapses.

### Epilepsy

The DG is implicated in several neurological diseases and psychiatric disorders, such as epilepsy and especially temporal lobe epilepsy (TLE), a type of epilepsy acquired after brain injury where seizures often involve the hippocampus (Botterill et al., 2019). In TLE, the role of MCs has been particularly puzzling and remains paradoxical, consisting of two distinct theories that need to be clarified. In TLE, MCs are typically damaged and GCs present abnormal activity. Moreover, it has been proposed that the loss of MCs conducts to GCs hyperactivity, which is excitotoxic for hippocampal neurons (Sloviter et al., 2003) because DG-GABAergic neurons called “basket cells” lose MC afferent input, causing disinhibition of GCs according to the so-called hypothesis “the dormant basket cells” (Sloviter, 1991; Sloviter, 1994). A second hypothesis called “the irritable MC” also exists that postulates that surviving MCs developed an overactive state, which promotes GC hyperexcitability (Ratzliff et al., 2002). In the context of the second hypothesis, understanding to which extent HCAR1-dependant inhibition is able to reduce MC overactivity is critical for further antiepileptic drugs development. One could also postulate that lactate, known to increase during strong neuronal activity (Barros and Deitmer, 2010), can operate as a metabolic and neuroprotective substrate and as an inhibitory signaling molecule sensing high neuronal activity.

### Memory

The DG is often considered the first step in information processing that is coupled with episodic memory (Amaral et al., 2007). In particular, MCs, via their communication with GCs, have been implicated in various forms of learning and memory, including associative memory

(Buckmaster and Schwartzkroin, 1994), pattern separation (Myers and Scharfman, 2009), and recall of memory sequences (Lisman et al., 2005). HCAR1 has been shown to be directly implicated in memory mechanisms.

Interestingly, numerous studies have shown that lactate modulates behaviour and memory (Newman et al., 2011; Suzuki et al., 2011), but very few investigated the role of HCAR1, now known to be expressed in the hippocampus. The group of Scavuzzo et al. (2020) used D-lactate and 3,5-DHBA, which offer experimental tools capable of testing whether lactate effects occur through a metabolic or signaling mechanism, to test the modulatory role of lactate on memory and especially during the consolidation phase. To do so, the researchers performed systemic administration of L-, D-lactate, or 3,5-DHBA 15 min *before* performing inhibitory avoidance (IA) training or *after* the foot shock received during IA. The results seem to show that learning and subsequent memory are impaired when HCAR1 agonists are injected *prior* IA. On the other hand, if non-metabolized agonist administration takes place after the foot shock, results rather pointed to an enhancement of long-term memory retention suggesting a memory promoting effect of HCAR1 signaling. The authors argue in favor of a different role of lactate metabolism over lactate signaling across memory stages (Scavuzzo et al., 2020). These results are rather in opposition to previous literature (Suzuki et al., 2011; Harris et al., 2019) where L-lactate is reported to be detrimental to long-term memory formation. Harris et al. (2019) investigated the role of lactate production in spatial learning and memory in mice performing the Morris water maze (MWM) task. Using dichloroacetate (DCA) administration, a chemical inhibitor showed to reduce lactate production via aerobic glycolysis, the authors observed impaired learning illustrated by an increased latency time to reach the platform while performing the MWM. In contrast to the study of Scavuzzo et al. (2020), administration of DCA before the probe trial (i.e. trial after 4 days of training) does not interfere with memory retrieval (Harris et al., 2019).

In conclusion, lactate seems to participate in the mnemonic process with a certain degree of signaling role via the receptor HCAR1. In addition to our findings in the DG circuitry, more experiments should be performed to precisely delineate whether HCAR1 is involved in the dentate gyrus mnemonic processes.

## Neurogenesis

Adult neurogenesis is the continuous formation of new neurons in the adult brain. It is an exciting phenomenon that occurs in the lateral subventricular zone (SVZ) and in the DG of the hippocampus. However, adult neurogenesis in the human brain is a controversial topic among researchers in the field of neuroscience. Recent publications showed that human hippocampal neurogenesis drops sharply in children to undetectable levels in adults (Sorrells et al., 2018), and finally, by using single-cell RNA-seq rather than traditional markers, Franjic et al. (2022) concluded that adult neurogenesis is absent in the human adult brain. In contrast, their analysis identified neurogenic lineage in the mouse, pig, and macaques, meaning that adult neurogenesis does not seem to be conserved across all mammalian species.

Lactate has been shown in rodents to play an undeniable role in adult neurogenesis and evidence of the involvement of HCAR1 is emerging in few studies (Nicola and Okun, 2021). Adult neurogenesis is a dynamic process regulated by different factors such as stress, learning, dietary interventions, and physical exercise, consequently making lactate a potential influencer of adult neurogenesis. Indeed, different molecular pathways, such as angiogenesis (Morland et al., 2017), neuronal excitability, and plasticity in which lactate acts as a modulator are interconnected with neurogenesis and promote the survival of newly formed neurons (Lev-Vachnisch et al., 2019). In addition, since we reported the presence of the receptor in the hippocampal region and especially in the dentate gyrus, the influence of HCAR1 on adult neurogenesis continues to gain importance.

The group of Pöttsch et al. (2021) studied the effect of L-lactate on hippocampal neural precursor cells (NPCs) behavior *in vitro*. They reported that physiological concentrations of L-lactate increase DG-derived NPC proliferation together with a shortened generation time. Interestingly, neither D-lactate nor pyruvate was able to stimulate NPC proliferation. However, L-lactate did not affect NPC differentiation. Thus, we could speculate on the involvement of the signaling role of lactate via HCAR1 in hippocampal adult neurogenesis. Increasing concentrations of 3,5-DHBA did not induce proliferation of NPCs, suggesting that HCAR1 is not involved or that its activation alone is not sufficient to elicit the effect (Pöttsch et al., 2021). In support of this

result, exercise, but not lactate, has been shown to increase neurogenesis *in vivo* in a similar manner in WT and HCAR1-KO mice (Lambertus et al., 2021).

Moreover, besides the hippocampus, the SVZ is the second niche for adult neurogenesis. *In vitro*, SVZ-derived NPC did not change in behavior upon L-lactate stimulation (Pöttsch et al., 2021), a result in contradiction with the findings of Lambertus et al. (2021). The latter showed that injection of L-lactate five days a week for seven weeks increased neurogenesis in WT mice. Remarkably, lactate injection in HCAR1-KO mice did not increase neurogenesis above control levels, indicating a HCAR1-dependant mechanism.

In conclusion, HCAR1 seems not involved in hippocampal neurogenesis or HCAR1 activation is relevant only together with the substrate effects of L-lactate, despite evidence of its expression in this region. In the SVZ, opposite results make the hypothesis difficult to postulate. However, HCAR1, shown to also be expressed in this region, may be required to elicit neurogenesis.

## HCAR1 – dual mode of action ?

In this section, I will discuss contrasting neuronal modulation following HCAR1 activation reported in the literature (**Figure 7**). We have shown across three studies that HCAR1 activation leads to a downmodulation of neuronal activity *in vitro* and *ex vivo*. The first observation demonstrated that physiological concentration of lactate (5mM) decreases spontaneous activity of primary cortical neurons by around 40% compared to control (Bozzo et al., 2013). Interestingly, to exclude any metabolic effect of lactate that could lead to this decrease, we used non-metabolized HCAR1 selective agonists: 3,5-DHBA (1mM) and 3CI-HBA (40 $\mu$ M). Both agonists

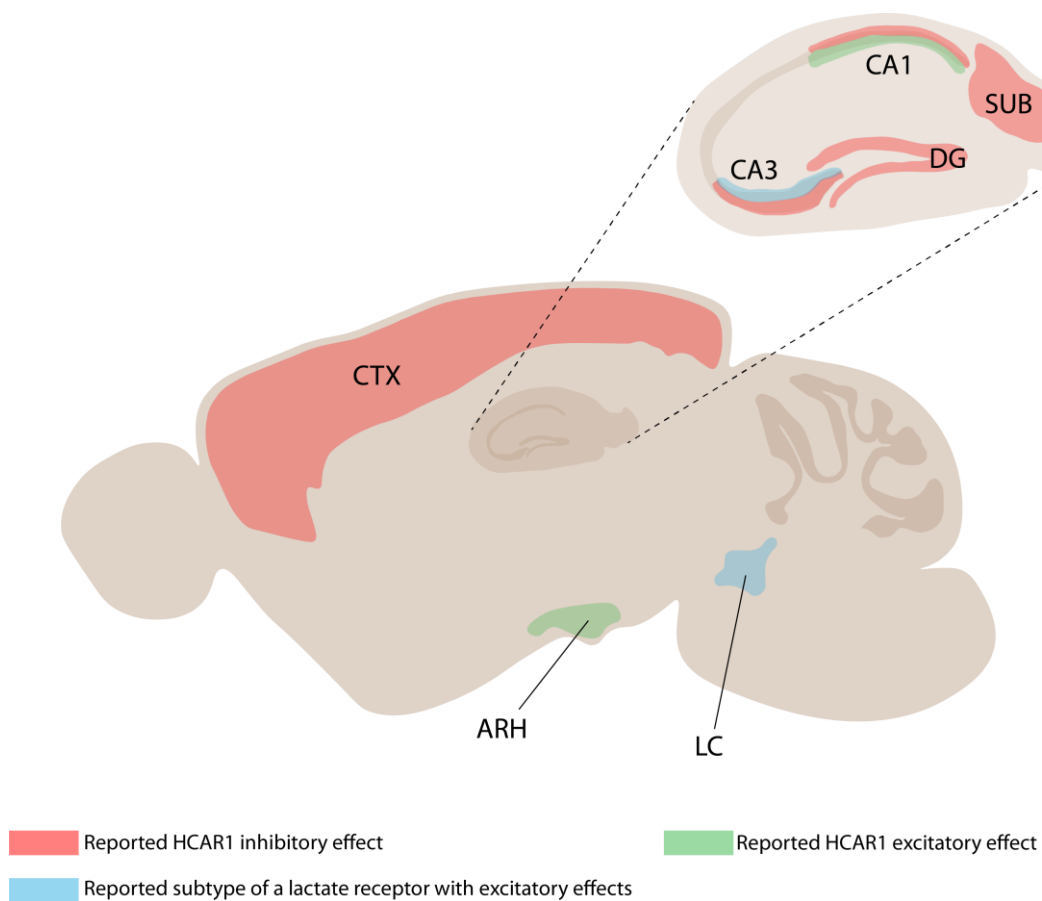


**Figure 7.** Summary of studies reporting neuromodulatory action of HCAR1 or of a putative subtype of the lactate receptor still to be identified. These studies include both rat and mouse observations. CTX: cortex (Bozzo et al., 2013), SUB: subiculum (Jorwal and Sikdar, 2019), ARH: arcuate hypothalamic nucleus (Órdenes et al., 2021), LC: locus coeruleus (Tang et al., 2014), DG: dentate gyrus (Briquet et al., 2022), CA1 (Herrera-Lopez and Galvan, 2018), and CA3 (Herrera-López et al., 2020).

showed that selective activation of HCAR1 is sufficient to decrease spontaneous  $\text{Ca}^{2+}$  activity in WT primary neurons *in vitro* (de Castro Abrantes et al., 2019). In addition, the use of HCAR1-KO animals was of prime importance to prove HCAR1 effect on neuronal activity, considering the absence of HCAR1 antagonists. Application of either lactate or HCAR1 agonist in HCAR1-KO did not elicit any modulation of spontaneous activity in primary neurons. These results were of capital importance to attest to the effect of lactate as a signaling molecule. As mentioned in the introduction, HCAR1 is a G-protein coupled receptor and seems to signal through different mechanisms leading to this down-modulation. We hypothesized that, on the one hand, lactate binding to HCAR1 would signal through the  $G_{\alpha}$  subunit, inhibiting AC, which leads to the reduction of cAMP levels, and consequently decreases neuronal exocytosis through PKA-dependent and PKA-independent mechanisms (Seino and Shibasaki, 2005). On the other hand, the  $G_{\beta\gamma}$  subunit would modulate the opening of ionic channels. For instance,  $G_{\beta\gamma}$  subunit is known to trigger the opening of  $\text{K}^{+}$  channels responsible for membrane hyperpolarization, and to repress  $\text{Ca}^{2+}$  influx via the closure of voltage-gated calcium channels, leading to the decrease of exocytosis (Blackmer et al., 2001).

In my thesis, I showed that 3CI-HBA was able to decrease sEPSCs and mEPSCs frequency by about 40% in the DG GCs of mice and rats. This modulation was not observed in HCAR1-KO mouse slices, no KO rats for the receptor was available, therefore supporting the role of HCAR1 as a neuronal activity down-modulator in conserved circuitry of acute slices.

Some studies in the current literature argue that HCAR1 may rather have an excitatory effect on neuronal activity. A recent study showed that rat CA1 pyramidal neurons respond to L-lactate in a biphasic way (Herrera-Lopez and Galvan, 2018). In that study, 5mM L-lactate decreased the intrinsic excitability of these neurons, however; at a concentration of 30mM, L-lactate increased neuronal firing frequency. The same was demonstrated using 0.56mM and 3.1mM 3.5-DHBA, respectively. One question raised by this experiment is related to the  $\text{IC}_{50}$  of HCAR1 for both lactate and 3.5-DHBA. Bozzo et al. (2013) showed that the  $\text{IC}_{50}$  value of L-lactate, for the decrease in spontaneous neuronal  $\text{Ca}^{2+}$  activity, is 4.2mM for both principal and GABAergic neurons. Liu et al. (2012) showed that the  $\text{IC}_{50}$  value of 3.5-DHBA is about 150 $\mu\text{M}$ . Therefore, do these



supraphysiological/supramaximal concentrations (30mM lactate and 3.1mM 3,5-DHBA) represent a meaningful behavior of the receptor?

Similar observations of excitatory effects of lactate were reported for noradrenergic neurons of the LC (Tang et al., 2014). Both in vitro application of exogenous L-lactate and in vivo optogenetically activated astrocytes releasing L-lactate depolarized LC neurons in a metabolic independent manner and mediated by AC and PKA. Knowing that HCAR1 is described to be an inhibitory  $G_i$ -coupled receptor inhibiting AC, these results rather suggest that LC neurons might express either a variant of this receptor with a different coupling mechanism or yet another receptor that recognizes L-lactate and signals via activation of AC. Further studies are necessary to test this hypothesis. To our knowledge, no further information has been published on the occurrence of a different lactate receptor in the LC.

Following the same trend, Órdenes et al. (2021) studied lactate effects on rat hypothalamic POMC neurons. These cells are capable of integrating peripheral signals of the body energy status and are involved in regulating feeding behavior and glucose homeostasis. POMC neurons were shown to depolarize when exposed to 15mM L-lactate. The authors suggest that this modulation is independent of its transport via MCT2, indicating that the underlying mechanism is rather non-metabolic. Furthermore, POMC neurons showed depolarization when exposed to 3Cl-HBA (40 $\mu$ M), indicating a possible excitatory role of the HCAR1. Unlike the hypothesis mentioned before arguing for the presence of different excitatory subtypes of HCAR1, Órdenes et al. (2021) demonstrated that in presence of pertussis toxin, a  $G_i$  protein inhibitor, POMC neurons showed a significant reduction in their response to 3Cl-HBA supporting the HCAR1 role in neuronal modulation.

A possible explanation for this excitatory modulation could come from the following observations we made. We asked whether HCAR1 is capable of functionally interacting with other  $G_i$ -coupled receptors, such as the adenosine A1 receptor, the  $GABA_B$ , and the  $\alpha_{2A}$ -adrenoreceptor (de Castro Abrantes et al., 2019). To answer this question, we monitored in vitro neuronal activity during HCAR1 activation and subsequent co-activation with one of the  $G_i$ -coupled receptors. The subsequent co-activation showed an additive inhibition of the neuronal activity. It was expected

that if the activation of HCAR1 and the other  $G_i$ -coupled receptors are independent, reversing the order of the receptor activation should result in the same combined inhibition of neuronal activity. We thus tested this hypothesis by first stimulating one of the  $G_i$ -coupled receptors and immediately after coactivating HCAR1. Unexpectedly, when one of the  $G_i$ -coupled receptors was first activated, the subsequent coactivation of HCAR1 partially reversed the inhibition induced. This type of cooperation was not reproduced when selecting pairs among these three GPCRs. This effect was shown to be mediated by the  $G_{i\beta\gamma}$  subunit and PLC, and only when HCAR1 is activated in sequence with another receptor. This observation highlights the complexity of the mechanism and could provide an explanation for the different actions of HCAR1 on neuronal activity described in the literature. In addition, it implies that the outcome of its activation in vivo will depend on whether other receptors of this class are active at any given time.

Overall, it appears that lactate may have either inhibitory or excitatory effects when acting in a non-metabolic way with neurons in different parts of the brain. Nevertheless, at present time the only lactate receptor non ambiguously described remains HCAR1.

## Human tissue

Epilepsy is a chronic noncommunicable disorder of the brain that affects about 50 million people worldwide (Beghi, 2019). It is defined by an enduring predisposition to generate epileptic seizures, along with the associated cognitive, psychological, and social consequences (Fisher et al., 2017). An epileptic seizure is a transient behavioural change that might be objective signs or subjective symptoms, caused by abnormal excessive or synchronous neuronal activity in the brain. Despite the fact that a significant number of antiepileptic drugs were developed and approved over the past 20 years, one third of the population with epilepsy have drug-resistant epilepsy and therefore do not respond to common pharmacological treatments (Picot et al., 2008). In this regard, the field is in urgent need of new targets to tackle pharmacoresistance. In this context, we had a unique opportunity collaborate with the CHUV and a neurosurgeon, Prof. Roy Thomas Daniel, to have access to fresh brain samples. The tissue is classified as "epileptic" originating from resected tissue of the epileptogenic locus of patients with dysplasia (or other forms of epilepsy) and who were pharmacoresistant.

In the human brain, we showed that HCAR1 mRNA transcripts were found in all 17 brain samples from epileptic patients that we tested. Interestingly, three of them showed levels that were on average about ninefold higher than the average. We did not find a correlation with either gender or age in the samples, or with any other patient's parameters available. Interestingly, these three samples originated from the temporal region. In support to this observation, the human brain atlas has shown using transcriptomic datasets that HCAR1 is present in the human brain, even though the expression level seems rather low compared to other cell types such as germinal cells (early and late spermatids) or epithelial cells (club cells of the lungs) (<https://www.proteinatlas.org/ENSG00000196917-HCAR1/celltype>). In addition, we faced obvious limitations such as the fact that no healthy brains tissues is available for comparison, the different medications received by the patients, or even the surgical procedure itself could affect HCAR1 expression.

Knowing that HCAR1 is expressed by neurons in the human brain of pharmaco-resistant epileptic patients, we showed for the first time that HCAR1 agonist was sufficient to decrease neuronal activity recorded by whole cell patch clamp or live calcium imaging. This result opens doors for further characterization of HCAR1 in the human epileptic brain.

## References

- Abi-Saab WM, Maggs DG, Jones T, Jacob R, Srihari V, Thompson J, Kerr D, Leone P, Krystal JH, Spencer DD, During MJ, Sherwin RS (2002) Striking differences in glucose and lactate levels between brain extracellular fluid and plasma in conscious human subjects: effects of hyperglycemia and hypoglycemia. *J Cereb Blood Flow Metab* 22:271-279.
- Ahmed K, Tunaru S, Offermanns S (2009) GPR109A, GPR109B and GPR81, a family of hydroxy-carboxylic acid receptors. *Trends Pharmacol Sci* 30:557-562.
- Ahmed K, Tunaru S, Tang C, Muller M, Gille A, Sassmann A, Hanson J, Offermanns S (2010) An autocrine lactate loop mediates insulin-dependent inhibition of lipolysis through GPR81. *Cell Metab* 11:311-319.
- Amaral DG, Scharfman HE, Lavenex P (2007) The dentate gyrus: fundamental neuroanatomical organization (dentate gyrus for dummies). *Progress in brain research* 163:3-22.
- Barros LF (2013) Metabolic signaling by lactate in the brain. *Trends Neurosci* 36:396-404.
- Barros LF, Deitmer JW (2010) Glucose and lactate supply to the synapse. *Brain research reviews* 63:149-159.
- Barros LF, Bittner CX, Loaiza A, Porras OH (2007) A quantitative overview of glucose dynamics in the gliovascular unit. *Glia* 55:1222-1237.
- Beghi E (2019) Global, regional, and national burden of epilepsy, 1990-2016: a systematic analysis for the Global Burden of Disease Study 2016. *The Lancet Neurology* 18:357-375.
- Bélanger M, Allaman I, Magistretti PJ (2011) Brain energy metabolism: focus on astrocyte-neuron metabolic cooperation. *Cell Metab* 14:724-738.
- Bergersen LH, Gjedde A (2012) Is lactate a volume transmitter of metabolic states of the brain? *Front Neuroenergetics* 4:5.
- Berthet C, Castillo X, Magistretti PJ, Hirt L (2012) New evidence of neuroprotection by lactate after transient focal cerebral ischaemia: extended benefit after intracerebroventricular injection and efficacy of intravenous administration. *Cerebrovasc Dis* 34:329-335.
- Berthet C, Lei H, Thevenet J, Gruetter R, Magistretti PJ, Hirt L (2009) Neuroprotective role of lactate after cerebral ischemia. *J Cereb Blood Flow Metab* 29:1780-1789.
- Blackmer T, Larsen EC, Takahashi M, Martin TF, Alford S, Hamm HE (2001) G protein betagamma subunit-mediated presynaptic inhibition: regulation of exocytotic fusion downstream of Ca<sup>2+</sup> entry. *Science* 292:293-297.
- Blad CC, Ahmed K, AP IJ, Offermanns S (2011) Biological and pharmacological roles of HCA receptors. *Adv Pharmacol* 62:219-250.
- Botterill JJ, Lu YL, LaFrancois JJ, Bernstein HL, Alcantara-Gonzalez D, Jain S, Leary P, Scharfman HE (2019) An Excitatory and Epileptogenic Effect of Dentate Gyrus Mossy Cells in a Mouse Model of Epilepsy. *Cell reports* 29:2875-2889.e2876.
- Bouzat P, Sala N, Suys T, Zerlauth JB, Marques-Vidal P, Feihl F, Bloch J, Messerer M, Levivier M, Meuli R, Magistretti PJ, Oddo M (2014) Cerebral metabolic effects of exogenous lactate supplementation on the injured human brain. *Intensive Care Med* 40:412-421.
- Bouzier-Sore AK, Bolaños JP (2015) Uncertainties in pentose-phosphate pathway flux assessment underestimate its contribution to neuronal glucose consumption: relevance for neurodegeneration and aging. *Front Aging Neurosci* 7:89.
- Bouzier-Sore AK, Voisin P, Canioni P, Magistretti PJ, Pellerin L (2003) Lactate is a preferential oxidative energy substrate over glucose for neurons in culture. *J Cereb Blood Flow Metab* 23:1298-1306.
- Bouzier-Sore AK, Voisin P, Bouchaud V, Bezanson E, Franconi JM, Pellerin L (2006) Competition between glucose and lactate as oxidative energy substrates in both neurons and astrocytes: a comparative NMR study. *Eur J Neurosci* 24:1687-1694.

- Bozzo L, Puyal J, Chatton JY (2013) Lactate modulates the activity of primary cortical neurons through a receptor-mediated pathway. *PLoS one* 8:e71721.
- Briquet M, Rocher AB, Alessandri M, Rosenberg N, de Castro Abrantes H, Wellbourne-Wood J, Schmuziger C, Ginet V, Puyal J, Pralong E, Daniel RT, Offermanns S, Chatton JY (2022) Activation of lactate receptor HCAR1 down-modulates neuronal activity in rodent and human brain tissue. *J Cereb Blood Flow Metab*.
- Brooks GA (1985a) Lactate: Glycolytic End Product and Oxidative Substrate During Sustained Exercise in Mammals — The “Lactate Shuttle”. In, pp 208-218. Berlin, Heidelberg: Springer Berlin Heidelberg.
- Brooks GA (1985b) Anaerobic threshold: review of the concept and directions for future research. *Med Sci Sports Exerc* 17:22-34.
- Brooks GA (2000) Intra- and extra-cellular lactate shuttles. *Med Sci Sports Exerc* 32:790-799.
- Brooks GA (2002) Lactate shuttles in nature. *Biochem Soc Trans* 30:258-264.
- Brooks GA (2007) Lactate: link between glycolytic and oxidative metabolism. *Sports Med* 37:341-343.
- Brooks GA (2009) Cell-cell and intracellular lactate shuttles. *J Physiol* 587:5591-5600.
- Brooks GA (2016) Energy Flux, Lactate Shuttling, Mitochondrial Dynamics, and Hypoxia. *Advances in experimental medicine and biology* 903:439-455.
- Brooks GA (2018) The Science and Translation of Lactate Shuttle Theory. *Cell Metab* 27:757-785.
- Buckmaster PS, Schwartzkroin PA (1994) Hippocampal mossy cell function: a speculative view. *Hippocampus* 4:393-402.
- Buckmaster PS, Wenzel HJ, Kunkel DD, Schwartzkroin PA (1996) Axon arbors and synaptic connections of hippocampal mossy cells in the rat in vivo. *J Comp Neurol* 366:271-292.
- Buscemi L, Blochet C, Price M, Magistretti PJ, Lei H, Hirt L (2020) Extended preclinical investigation of lactate for neuroprotection after ischemic stroke. *Clin Transl Neurosci* 4:2514183X20904571.
- Cahn RS, Ingold CK, Prelog V (1956) The specification of asymmetric configuration in organic chemistry. *Experientia* 12:81-94.
- Cai TQ, Ren N, Jin L, Cheng K, Kash S, Chen R, Wright SD, Taggart AK, Waters MG (2008) Role of GPR81 in lactate-mediated reduction of adipose lipolysis. *Biochem Biophys Res Commun* 377:987-991.
- Calì C, Tauffenberger A, Magistretti P (2019) The Strategic Location of Glycogen and Lactate: From Body Energy Reserve to Brain Plasticity. *Frontiers in cellular neuroscience* 13:82.
- Castillo X, Rosafio K, Wyss MT, Drandarov K, Buck A, Pellerin L, Weber B, Hirt L (2015) A probable dual mode of action for both L- and D-lactate neuroprotection in cerebral ischemia. *J Cereb Blood Flow Metab* 35:1561-1569.
- Chatton JY, Marquet P, Magistretti PJ (2000) A quantitative analysis of L-glutamate-regulated Na<sup>+</sup> dynamics in mouse cortical astrocytes: implications for cellular bioenergetics. *Eur J Neurosci* 12:3843-3853.
- de Castro Abrantes H, Briquet M, Schmuziger C, Restivo L, Puyal J, Rosenberg N, Rocher AB, Offermanns S, Chatton JY (2019) The lactate receptor HCAR1 modulates neuronal network activity through the activation of Galpha and Gbeta subunits. *J Neurosci* 39:4422-4433.
- Descalzi G, Gao V, Steinman MQ, Suzuki A, Alberini CM (2019) Lactate from astrocytes fuels learning-induced mRNA translation in excitatory and inhibitory neurons. *Commun Biol* 2:247.
- Dienel GA (2012) Brain lactate metabolism: the discoveries and the controversies. *J Cereb Blood Flow Metab* 32:1107-1138.
- Dienel GA, Hertz L (2001) Glucose and lactate metabolism during brain activation. *J Neurosci Res* 66:824-838.
- Dvorak CA, Liu C, Shelton J, Kuei C, Sutton SW, Lovenberg TW, Carruthers NI (2012) Identification of Hydroxybenzoic Acids as Selective Lactate Receptor (GPR81) Agonists with Antilipolytic Effects. *ACS Med Chem Lett* 3:637-639.

- Engelstoft MS et al. (2013) Seven transmembrane G protein-coupled receptor repertoire of gastric ghrelin cells. *Mol Metab* 2:376-392.
- Erlichman JS, Hewitt A, Damon TL, Hart M, Kuraszcz J, Li A, Leiter JC (2008) Inhibition of monocarboxylate transporter 2 in the retrotrapezoid nucleus in rats: a test of the astrocyte-neuron lactate-shuttle hypothesis. *J Neurosci* 28:4888-4896.
- Feingold KR, Moser A, Shigenaga JK, Grunfeld C (2011) Inflammation inhibits GPR81 expression in adipose tissue. *Inflammation research : official journal of the European Histamine Research Society [et al]* 60:991-995.
- Ferguson BS, Rogatzki MJ, Goodwin ML, Kane DA, Rightmire Z, Gladden LB (2018) Lactate metabolism: historical context, prior misinterpretations, and current understanding. *European journal of applied physiology* 118:691-728.
- Filiz AI, Aladag H, Akin ML, Sucullu I, Kurt Y, Yucel E, Uluutku AH (2010) The role of d-lactate in differential diagnosis of acute appendicitis. *J Invest Surg* 23:218-223.
- Fisher RS, Cross JH, French JA, Higurashi N, Hirsch E, Jansen FE, Lagae L, Moshé SL, Peltola J, Roulet Perez E, Scheffer IE, Zuberi SM (2017) Operational classification of seizure types by the International League Against Epilepsy: Position Paper of the ILAE Commission for Classification and Terminology. *Epilepsia* 58:522-530.
- Fletcher WM, Hopkins FG (1907) Lactic acid in amphibian muscle. *J Physiol* 35:247-309.
- Franjic D et al. (2022) Transcriptomic taxonomy and neurogenic trajectories of adult human, macaque, and pig hippocampal and entorhinal cells. *Neuron* 110:452-469.e414.
- Ge H, Weizmann J, Reagan JD, Gupte J, Baribault H, Gyuris T, Chen JL, Tian H, Li Y (2008) Elucidation of signaling and functional activities of an orphan GPCR, GPR81. *J Lipid Res* 49:797-803.
- Giaume C, Koulakoff A, Roux L, Holcman D, Rouach N (2010) Astroglial networks: a step further in neuroglial and gliovascular interactions. *Nat Rev Neurosci* 11:87-99.
- Gilbert E, Tang JM, Ludvig N, Bergold PJ (2006) Elevated lactate suppresses neuronal firing in vivo and inhibits glucose metabolism in hippocampal slice cultures. *Brain Res* 1117:213-223.
- Gordon GR, Choi HB, Rungta RL, Ellis-Davies GC, MacVicar BA (2008) Brain metabolism dictates the polarity of astrocyte control over arterioles. *Nature* 456:745-749.
- Harris RA, Lone A, Lim H, Martinez F, Frame AK (2019) Aerobic Glycolysis Is Required for Spatial Memory Acquisition But Not Memory Retrieval in Mice. *eNeuro* 6:ENEURO.0389-0318.2019.
- Harun-Or-Rashid M, Inman DM (2018) Reduced AMPK activation and increased HCAR activation drive anti-inflammatory response and neuroprotection in glaucoma. *J Neuroinflammation* 15:313.
- Hasegawa H, Fukushima T, Lee JA, Tsukamoto K, Moriya K, Ono Y, Imai K (2003) Determination of serum D-lactic and L-lactic acids in normal subjects and diabetic patients by column-switching HPLC with pre-column fluorescence derivatization. *Anal Bioanal Chem* 377:886-891.
- Herrera-Lopez G, Galvan EJ (2018) Modulation of hippocampal excitability via the hydroxycarboxylic acid receptor 1. *Hippocampus* 28:557-567.
- Herrera-López G, Griego E, Galván E (2020) Lactate induces synapse-specific potentiation on CA3 pyramidal cells of rat hippocampus. *PLoS one* 15:e0242309.
- Hoque R, Farooq A, Ghani A, Gorelick F, Mehal WZ (2014) Lactate reduces liver and pancreatic injury in Toll-like receptor- and inflammasome-mediated inflammation via GPR81-mediated suppression of innate immunity. *Gastroenterology* 146:1763-1774.
- Hu J, Cai M, Liu Y, Liu B, Xue X, Ji R, Bian X, Lou S (2020) The roles of GPR81 as a metabolic sensor and inflammatory mediator. *J Cell Physiol* 235:8938-8950.
- Hyder F, Patel AB, Gjedde A, Rothman DL, Behar KL, Shulman RG (2006) Neuronal-glia glucose oxidation and glutamatergic-GABAergic function. *J Cereb Blood Flow Metab* 26:865-877.

- Itoh Y, Esaki T, Shimoji K, Cook M, Law MJ, Kaufman E, Sokoloff L (2003) Dichloroacetate effects on glucose and lactate oxidation by neurons and astroglia in vitro and on glucose utilization by brain in vivo. *Proc Natl Acad Sci U S A* 100:4879-4884.
- Ivanov A, Mukhtarov M, Bregestovski P, Zilberter Y (2011) Lactate Effectively Covers Energy Demands during Neuronal Network Activity in Neonatal Hippocampal Slices. *Front Neuroenergetics* 3:2.
- Izumi Y, Benz AM, Katsuki H, Zorumski CF (1997) Endogenous monocarboxylates sustain hippocampal synaptic function and morphological integrity during energy deprivation. *The Journal of neuroscience : the official journal of the Society for Neuroscience* 17:9448-9457.
- Jones NK, Stewart K, Czopek A, Menzies RI, Thomson A, Moran CM, Cairns C, Conway BR, Denby L, Livingstone DEW, Wiseman J, Hadoke PW, Webb DJ, Dhaun N, Dear JW, Mullins JJ, Bailey MA (2020) Endothelin-1 Mediates the Systemic and Renal Hemodynamic Effects of GPR81 Activation. *Hypertension* 75:1213-1222.
- Jorwal P, Sikdar SK (2019) Lactate reduces epileptiform activity through HCA1 and GIRK channel activation in rat subicular neurons in an in vitro model. *Epilepsia* 60:2370-2385.
- Jositsch G, Papadakis T, Haberberger RV, Wolff M, Wess J, Kummer W (2009) Suitability of muscarinic acetylcholine receptor antibodies for immunohistochemistry evaluated on tissue sections of receptor gene-deficient mice. *Naunyn Schmiedebergs Arch Pharmacol* 379:389-395.
- Jourdain P, Allaman I, Rothenfusser K, Fiumelli H, Marquet P, Magistretti PJ (2016) L-Lactate protects neurons against excitotoxicity: implication of an ATP-mediated signaling cascade. *Sci Rep* 6:21250.
- Kwon E, Yoo T, Joung HY, Jo YH (2020) Hydrocarboxylic acid receptor 1 in BAT regulates glucose uptake in mice fed a high-fat diet. *PLoS one* 15:e0228320.
- Lam TK, Gutierrez-Juarez R, Pocai A, Rossetti L (2005) Regulation of blood glucose by hypothalamic pyruvate metabolism. *Science* 309:943-947.
- Lam TK, Gutierrez-Juarez R, Pocai A, Bhanot S, Tso P, Schwartz GJ, Rossetti L (2007) Brain glucose metabolism controls the hepatic secretion of triglyceride-rich lipoproteins. *Nat Med* 13:171-180.
- Lamb GD, Stephenson DG (2006) Point: lactic acid accumulation is an advantage during muscle activity. *J Appl Physiol* 100:1410-1412; discussion 1414.
- Lambertus M, Øverberg LT, Andersson KA, Hjelden MS, Hadzic A, Haugen ØP, Storm-Mathisen J, Bergersen LH, Geiseler S, Morland C (2021) L-lactate induces neurogenesis in the mouse ventricular-subventricular zone via the lactate receptor HCA1. *Acta Physiologica* 231:e13587.
- Lauritzen KH, Morland C, Puchades M, Holm-Hansen S, Hagelin EM, Lauritzen F, Attramadal H, Storm-Mathisen J, Gjedde A, Bergersen LH (2014) Lactate receptor sites link neurotransmission, neurovascular coupling, and brain energy metabolism. *Cereb Cortex* 24:2784-2795.
- Lee DK, Nguyen T, Lynch KR, Cheng R, Vanti WB, Arkhitko O, Lewis T, Evans JF, George SR, O'Dowd BF (2001) Discovery and mapping of ten novel G protein-coupled receptor genes. *Gene* 275:83-91.
- Lerch MM, Conwell DL, Mayerle J (2014) The anti-inflammasome effect of lactate and the lactate GPR81-receptor in pancreatic and liver inflammation. *Gastroenterology* 146:1602-1605.
- Lev-Vachnisch Y, Cadury S, Rotter-Maskowitz A, Feldman N, Roichman A, Illouz T, Varvak A, Nicola R, Madar R, Okun E (2019) L-Lactate Promotes Adult Hippocampal Neurogenesis. *Front Neurosci* 13:403.
- Li XB, Gu JD, Zhou QH (2015) Review of aerobic glycolysis and its key enzymes - new targets for lung cancer therapy. *Thorac Cancer* 6:17-24.
- Lisman JE, Talamini LM, Raffone A (2005) Recall of memory sequences by interaction of the dentate and CA3: a revised model of the phase precession. *Neural Netw* 18:1191-1201.
- Liu C, Wu J, Zhu J, Kuei C, Yu J, Shelton J, Sutton SW, Li X, Yun SJ, Mirzadegan T, Mazur C, Kamme F, Lovenberg TW (2009) Lactate inhibits lipolysis in fat cells through activation of an orphan G-protein-coupled receptor, GPR81. *J Biol Chem* 284:2811-2822.

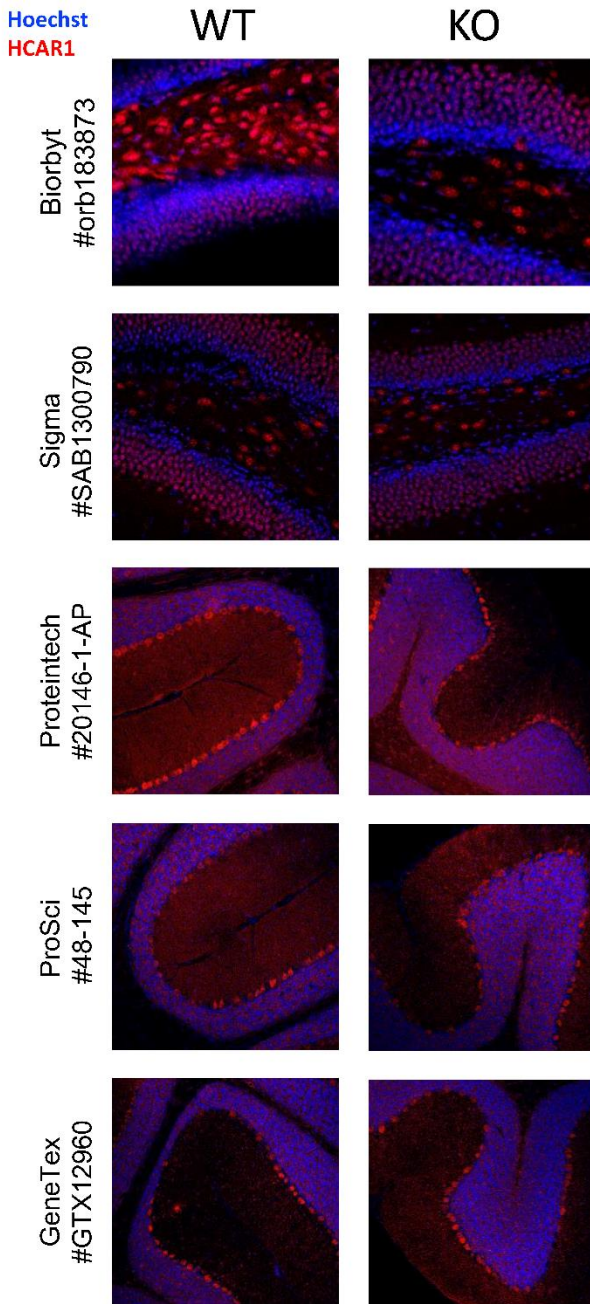
- Liu C, Kuei C, Zhu J, Yu J, Zhang L, Shih A, Mirzadegan T, Shelton J, Sutton S, Connelly MA, Lee G, Carruthers N, Wu J, Lovenberg TW (2012) 3,5-Dihydroxybenzoic acid, a specific agonist for hydroxycarboxylic acid 1, inhibits lipolysis in adipocytes. *J Pharmacol Exp Ther* 341:794-801.
- Machler P, Wyss MT, Elsayed M, Stobart J, Gutierrez R, von Faber-Castell A, Kaelin V, Zuend M, San Martin A, Romero-Gomez I, Baeza-Lehnert F, Lengacher S, Schneider BL, Aebischer P, Magistretti PJ, Barros LF, Weber B (2016) In Vivo Evidence for a Lactate Gradient from Astrocytes to Neurons. *Cell Metab* 23:94-102.
- Madaan A, Nadeau-Vallée M, Rivera JC, Obari D, Hou X, Sierra EM, Girard S, Olson DM, Chemtob S (2017) Lactate produced during labor modulates uterine inflammation via GPR81 (HCA(1)). *American journal of obstetrics and gynecology* 216:60.e61-60.e17.
- Madaan A, Chaudhari P, Nadeau-Vallée M, Hamel D, Zhu T, Mitchell G, Samuels M, Pundir S, Dabouz R, Howe Cheng CW, Mohammad Nezhady MA, Joyal JS, Rivera JC, Chemtob S (2019) Müller Cell-Localized G-Protein-Coupled Receptor 81 (Hydroxycarboxylic Acid Receptor 1) Regulates Inner Retinal Vasculature via Norrin/Wnt Pathways. *Am J Pathol* 189:1878-1896.
- Magistretti PJ (2006) Neuron-glia metabolic coupling and plasticity. *J Exp Biol* 209:2304-2311.
- Magistretti PJ, Pellerin L (1996) Cellular bases of brain energy metabolism and their relevance to functional brain imaging: evidence for a prominent role of astrocytes. *Cereb Cortex* 6:50-61.
- Magistretti PJ, Allaman I (2018) Lactate in the brain: from metabolic end-product to signalling molecule. *Nat Rev Neurosci* 19:235-249.
- Mangia S, Simpson IA, Vannucci SJ, Carruthers A (2009) The in vivo neuron-to-astrocyte lactate shuttle in human brain: evidence from modeling of measured lactate levels during visual stimulation. *J Neurochem* 109 Suppl 1:55-62.
- Martínez-Reyes I, Chandel NS (2020) Mitochondrial TCA cycle metabolites control physiology and disease. *Nat Commun* 11:102.
- Michel MC, Wieland T, Tsujimoto G (2009) How reliable are G-protein-coupled receptor antibodies? *Naunyn Schmiedebergs Arch Pharmacol* 379:385-388.
- Morgenthaler FD, Kraftsik R, Catsicas S, Magistretti PJ, Chatton JY (2006) Glucose and lactate are equally effective in energizing activity-dependent synaptic vesicle turnover in purified cortical neurons. *Neuroscience* 141:157-165.
- Morland C, Andersson KA, Haugen Ø P, Hadzic A, Kleppa L, Gille A (2017) Exercise induces cerebral VEGF and angiogenesis via the lactate receptor HCAR1. *Nat Commun* 8:15557.
- Mosienko V, Teschemacher AG, Kasparov S (2015) Is L-lactate a novel signaling molecule in the brain? *J Cereb Blood Flow Metab* 35:1069-1075.
- Myers CE, Scharfman HE (2009) A role for hilar cells in pattern separation in the dentate gyrus: a computational approach. *Hippocampus* 19:321-337.
- Newman LA, Korol DL, Gold PE (2011) Lactate produced by glycogenolysis in astrocytes regulates memory processing. *PLoS One* 6:e28427.
- Nicola R, Okun E (2021) Adult Hippocampal Neurogenesis: One Lactate to Rule Them All. *Neuromolecular Med* 23:445-448.
- Offermanns S (2017) Hydroxy-Carboxylic Acid Receptor Actions in Metabolism. *Trends Endocrinol Metab* 28:227-236.
- Offermanns S, Colletti SL, Lovenberg TW, Semple G, Wise A, AP IJ (2011) International Union of Basic and Clinical Pharmacology. LXXXII: Nomenclature and Classification of Hydroxy-carboxylic Acid Receptors (GPR81, GPR109A, and GPR109B). *Pharmacol Rev* 63:269-290.
- Órdenes P, Villar PS, Tarifeño-Saldivia E, Salgado M, Elizondo-Vega R, Araneda RC, García-Robles MA (2021) Lactate activates hypothalamic POMC neurons by intercellular signaling. *Sci Rep* 11:21644.
- Parsons MP, Hirasawa M (2010) ATP-sensitive potassium channel-mediated lactate effect on orexin neurons: implications for brain energetics during arousal. *J Neurosci* 30:8061-8070.



- Pellerin L, Magistretti PJ (1994) Glutamate uptake into astrocytes stimulates aerobic glycolysis: A mechanism coupling neuronal activity to glucose utilization. *Proc Natl Acad Sci U S A* Vol. 91:pp. 10625-10629.
- Pellerin L, Magistretti PJ (2012) Sweet sixteen for ANLS. *J Cereb Blood Flow Metab* 32:1152-1166.
- Picot MC, Baldy-Moulinier M, Daures JP, Dujols P, Crespel A (2008) The prevalence of epilepsy and pharmaco-resistant epilepsy in adults: a population-based study in a Western European country. *Epilepsia* 49:1230-1238.
- Pierre K, Pellerin L (2005) Monocarboxylate transporters in the central nervous system: distribution, regulation and function. *J Neurochem* 94:1-14.
- Pöttsch A, Zocher S, Bernas SN, Leiter O, Rünker AE, Kempermann G (2021) L-lactate exerts a proliferative effect on adult hippocampal precursor cells in vitro. *iScience* 24:102126.
- Pradidarcheep W, Labruyère WT, Dabhoiwala NF, Lamers WH (2008) Lack of Specificity of Commercially Available Antisera: Better Specifications Needed. *J Histochem Cytochem* 56:1099-1111.
- Ranganathan P, Shanmugam A, Swafford D, Suryawanshi A, Bhattacharjee P, Hussein MS (2018) GPR81, a Cell-Surface Receptor for Lactate, Regulates Intestinal Homeostasis and Protects Mice from Experimental Colitis. *J Immunol* 200:1781-1789.
- Ratzliff AH, Santhakumar V, Howard A, Soltesz I (2002) Mossy cells in epilepsy: rigor mortis or vigor mortis? *Trends Neurosci* 25:140-144.
- Roland CL, Arumugam T, Deng D, Liu SH, Philip B, Gomez S, Burns WR, Ramachandran V, Wang H, Cruz-Monserrate Z, Logsdon CD (2014) Cell surface lactate receptor GPR81 is crucial for cancer cell survival. *Cancer research* 74:5301-5310.
- Rooney K, Trayhurn P (2011) Lactate and the GPR81 receptor in metabolic regulation: implications for adipose tissue function and fatty acid utilisation by muscle during exercise. *Br J Nutr* 106:1310-1316.
- Sakurai T, Davenport R, Stafford S, Grosse J, Ogawa K, Cameron J, Parton L, Sykes A, Mack S, Bousba S, Parmar A, Harrison D, Dickson L, Leveridge M, Matsui J, Barnes M (2014) Identification of a novel GPR81-selective agonist that suppresses lipolysis in mice without cutaneous flushing. *Eur J Pharmacol* 727:1-7.
- Scavuzzo CJ, Rakotovo I, Dickson CT (2020) Differential effects of L- and D-lactate on memory encoding and consolidation: Potential role of HCAR1 signaling. *Neurobiol Learn Mem* 168:107151.
- Scharfman HE (2016) The enigmatic mossy cell of the dentate gyrus. *Nat Rev Neurosci* 17:562-575.
- Schurr A, West CA, Rigor BM (1988) Lactate-supported synaptic function in the rat hippocampal slice preparation. *Science* 240:1326-1328.
- Schurr A, Payne RS, Miller JJ, Rigor BM (1997a) Glia are the main source of lactate utilized by neurons for recovery of function posthypoxia. *Brain Res* 774:221-224.
- Schurr A, Payne RS, Miller JJ, Rigor BM (1997b) Brain lactate, not glucose, fuels the recovery of synaptic function from hypoxia upon reoxygenation: an in vitro study. *Brain Res* 744:105-111.
- Schurr A, Payne RS, Miller JJ, Rigor BM (1997c) Brain lactate is an obligatory aerobic energy substrate for functional recovery after hypoxia: further in vitro validation. *J Neurochem* 69:423-426.
- Sehnal D, Bittrich S, Deshpande M, Svobodová R, Berka K, Bazgier V, Velankar S, Burley S, Koča J, Rose A (2021) Mol\* Viewer: modern web app for 3D visualization and analysis of large biomolecular structures. *Nucleic Acids Res* 49:W431-w437.
- Seino S, Shibasaki T (2005) PKA-dependent and PKA-independent pathways for cAMP-regulated exocytosis. *Physiological reviews* 85:1303-1342.
- Shimizu H, Watanabe E, Hiyama TY, Nagakura A, Fujikawa A, Okado H, Yanagawa Y, Obata K, Noda M (2007) Glial Nax channels control lactate signaling to neurons for brain [Na<sup>+</sup>] sensing. *Neuron* 54:59-72.

- Sloviter RS (1991) Permanently altered hippocampal structure, excitability, and inhibition after experimental status epilepticus in the rat: the "dormant basket cell" hypothesis and its possible relevance to temporal lobe epilepsy. *Hippocampus* 1:41-66.
- Sloviter RS (1994) The functional organization of the hippocampal dentate gyrus and its relevance to the pathogenesis of temporal lobe epilepsy. *Ann Neurol* 35:640-654.
- Sloviter RS, Zappone CA, Harvey BD, Bumanglag AV, Bender RA, Frotscher M (2003) "Dormant basket cell" hypothesis revisited: relative vulnerabilities of dentate gyrus mossy cells and inhibitory interneurons after hippocampal status epilepticus in the rat. *J Comp Neurol* 459:44-76.
- Song Z, Routh VH (2005) Differential effects of glucose and lactate on glucosensing neurons in the ventromedial hypothalamic nucleus. *Diabetes* 54:15-22.
- Sorrells SF, Paredes MF, Cebrian-Silla A, Sandoval K, Qi D, Kelley KW, James D, Mayer S, Chang J, Auguste KI, Chang EF, Gutierrez AJ, Kriegstein AR, Mathern GW, Oldham MC, Huang EJ, Garcia-Verdugo JM, Yang Z, Alvarez-Buylla A (2018) Human hippocampal neurogenesis drops sharply in children to undetectable levels in adults. *Nature* 555:377-381.
- Sun J, Ye X, Xie M, Ye J (2016) Induction of triglyceride accumulation and mitochondrial maintenance in muscle cells by lactate. *Sci Rep* 6:33732.
- Sun Y, Grieco SF, Holmes TC, Xu X (2017) Local and Long-Range Circuit Connections to Hilar Mossy Cells in the Dentate Gyrus. *eNeuro* 4:ENEURO.0097-0017.2017.
- Sun Z, Han Y, Song S, Chen T, Han Y, Liu Y (2019) Activation of GPR81 by lactate inhibits oscillatory shear stress-induced endothelial inflammation by activating the expression of KLF2. *IUBMB life* 71:2010-2019.
- Suzuki A, Stern SA, Bozdagi O, Huntley GW, Walker RH, Magistretti PJ, Alberini CM (2011) Astrocyte-neuron lactate transport is required for long-term memory formation. *Cell* 144:810-823.
- Tang F, Lane S, Korsak A, Paton JF, Gourine AV, Kasparov S, Teschemacher AG (2014) Lactate-mediated glia-neuronal signalling in the mammalian brain. *Nat Commun* 5:3284.
- Wallenius K, Thalén P, Björkman JA, Johannesson P, Wiseman J, Böttcher G, Fjellström O, Oakes ND (2017) Involvement of the metabolic sensor GPR81 in cardiovascular control. *JCI Insight* 2:e92564.
- Wanders D, Graff EC, Judd RL (2012) Effects of high fat diet on GPR109A and GPR81 gene expression. *Biochem Biophys Res Commun* 425:278-283.
- Wellbourne-Wood J, Briquet M, Alessandri M, Binda F, Touya M, Chatton JY (2022) Evaluation of Hydroxycarboxylic Acid Receptor 1 (HCAR1) as a Building Block for Genetically Encoded Extracellular Lactate Biosensors. *Biosensors* 12.
- Westerblad H (2016) Acidosis Is Not a Significant Cause of Skeletal Muscle Fatigue. *Med Sci Sports Exerc* 48:2339-2342.
- Wolohan SM, Mao HC, Real C, Vespa PM, Glenn TC (2018) Lactate supplementation in severe traumatic brain injured adults by primed constant infusion of sodium L-lactate. *J Neurosci Res* 96:688-695.
- Xing CY, Tarumi T, Liu J, Zhang Y, Turner M, Riley J, Tinajero CD, Yuan LJ, Zhang R (2017) Distribution of cardiac output to the brain across the adult lifespan. *J Cereb Blood Flow Metab* 37:2848-2856.
- Yang J, Ruchti E, Petit JM, Jourdain P, Grenningloh G, Allaman I, Magistretti PJ (2014) Lactate promotes plasticity gene expression by potentiating NMDA signaling in neurons. *Proc Natl Acad Sci U S A* 111:12228-12233.
- Zhang Y, Chen K, Sloan SA, Bennett ML, Scholze AR, O'Keefe S, Phatnani HP, Guarnieri P (2014) An RNA-sequencing transcriptome and splicing database of glia, neurons, and vascular cells of the cerebral cortex. *J Neurosci* 34:11929-11947.

## Appendix 1



**Supplementary Figure 1.** Summary of the 5 new antibodies raised against HCAR1 tested on WT and HCAR1 KO mice. None of them showed selectivity for the receptor HCAR1.

## Appendix 2

The lactate receptor HCAR1 modulates neuronal activity through the activation of  $G\alpha$  and  $G\beta\gamma$  subunits

### **Summary of the results**

In this study, we characterized the mechanism behind HCAR1 activation in neurons, using mouse primary cortical neurons from WT and HCAR1 KO mice. First, using calcium imaging, we demonstrated that lactate modulation of neuronal activity is a metabolism independent mechanism, since activation of HCAR1 in HCAR1 KO neurons did not induce any changes on spontaneous neuronal activity. Using whole-cell patch-clamp, we found that activation of HCAR1 with 3CI-HBA decreased mEPSC frequency, increased paired-pulse ratio, decreased firing frequency, and modulated membrane intrinsic properties. We observed that HCAR1 signaling involves AC inhibition, decrease of cAMP levels, and decrease of PKA activity. We found that HCAR1 interacts with adenosine A1,  $GABA_B$ , and  $\alpha_2$ -adrenergic receptors, through a mechanism involving both its  $G_{i\alpha}$  and  $G_{i\beta\gamma}$  subunits, resulting in a complex modulation of neuronal network activity. We conclude that HCAR1 activation in neurons causes a down-modulation of neuronal activity through presynaptic mechanisms and by reducing neuronal excitability.

### **Personal contribution**

In this study, I performed the experiments concerning the interactions between HCAR1, A1R and  $GABA_B$ R (Figure 5).

# The Lactate Receptor HCAR1 Modulates Neuronal Network Activity through the Activation of $G_{\alpha}$ and $G_{\beta\gamma}$ Subunits

Haïssa de Castro Abrantes,<sup>1</sup> Marc Briquet,<sup>1</sup> Céline Schmuziger,<sup>1</sup> Leonardo Restivo,<sup>1</sup> Julien Puyal,<sup>1</sup> Nadia Rosenberg,<sup>1</sup> Anne-Bérengère Rocher,<sup>1</sup> Stefan Offermanns,<sup>3</sup> and Jean-Yves Chatton<sup>1,2</sup>

<sup>1</sup>Department of Fundamental Neuroscience, <sup>2</sup>Cellular Imaging Facility, University of Lausanne, 1005 Lausanne, Switzerland, and <sup>3</sup>Department of Pharmacology, Max-Planck-Institute for Heart and Lung Research, 61231 Bad Nauheim, Germany

The discovery of a G-protein-coupled receptor for lactate named hydroxycarboxylic acid receptor 1 (HCAR1) in neurons has pointed to additional nonmetabolic effects of lactate for regulating neuronal network activity. In this study, we characterized the intracellular pathways engaged by HCAR1 activation, using mouse primary cortical neurons from wild-type (WT) and HCAR1 knock-out (KO) mice from both sexes. Using whole-cell patch clamp, we found that the activation of HCAR1 with 3-chloro-5-hydroxybenzoic acid (3Cl-HBA) decreased miniature EPSC frequency, increased paired-pulse ratio, decreased firing frequency, and modulated membrane intrinsic properties. Using fast calcium imaging, we show that HCAR1 agonists 3,5-dihydroxybenzoic acid, 3Cl-HBA, and lactate decreased by 40% spontaneous calcium spiking activity of primary cortical neurons from WT but not from HCAR1 KO mice. Notably, in neurons lacking HCAR1, the basal activity was increased compared with WT. HCAR1 mediates its effect in neurons through a  $G_{i\alpha}$ -protein. We observed that the adenylyl cyclase–cAMP–protein kinase A axis is involved in HCAR1 downmodulation of neuronal activity. We found that HCAR1 interacts with adenosine A1, GABA<sub>B</sub>, and  $\alpha_{2A}$ -adrenergic receptors, through a mechanism involving both its  $G_{i\alpha}$  and  $G_{i\beta\gamma}$  subunits, resulting in a complex modulation of neuronal network activity. We conclude that HCAR1 activation in neurons causes a downmodulation of neuronal activity through presynaptic mechanisms and by reducing neuronal excitability. HCAR1 activation engages both  $G_{i\alpha}$  and  $G_{i\beta\gamma}$  intracellular pathways to functionally interact with other  $G_i$ -coupled receptors for the fine tuning of neuronal activity.

**Key words:** GPR81; HCAR1; intracellular pathway; lactate; neurons; spontaneous activity

## Significance Statement

Expression of the lactate receptor hydroxycarboxylic acid receptor 1 (HCAR1) was recently described in neurons. Here, we describe the physiological role of this G-protein-coupled receptor (GPCR) and its activation in neurons, providing information on its expression and mechanism of action. We dissected out the intracellular pathway through which HCAR1 activation tunes down neuronal network activity. For the first time, we provide evidence for the functional cross talk of HCAR1 with other GPCRs, such as GABA<sub>B</sub>, adenosine A1- and  $\alpha_{2A}$ -adrenergic receptors. These results set HCAR1 as a new player for the regulation of neuronal network activity acting in concert with other established receptors. Thus, HCAR1 represents a novel therapeutic target for pathologies characterized by network hyperexcitability dysfunction, such as epilepsy.

## Introduction

Lactate has long been considered a waste product of cellular metabolism. In the CNS, this concept was challenged in the 1990s when lactate was proposed to play an important role as energy

substrate for neurons (Pellerin and Magistretti, 1994). Since then, several studies indicated the valuable contribution of lactate as a metabolic fuel in several cell types, as a neuroprotective agent, as well as its role as a signaling molecule (for review, see Gladden, 2004; Barros, 2013).

The extracellular level of lactate in the brain is estimated to be in the low-millimolar range at the resting state (Abi-Saab et al., 2002). It has also been reported that physical exercise increases L-lactate plasma levels up to 10–20 mM (Offermanns, 2017). Under these conditions, the brain becomes a net consumer of lactate (Dalsgaard et al., 2004). Upon synaptic activity, lactate level undergoes a twofold increase (Dienel et al., 2007). The main cell type locally producing lactate in the brain is likely to be astrocytes, as recently reported in the *in vivo* mouse brain (Mächler et al., 2016), although this notion was recently challenged (Díaz-García

Received Aug. 10, 2018; revised March 19, 2019; accepted March 22, 2019.

Author contributions: H.d.C.A., L.R., N.R., A.-B.R., and J.-Y.C. designed research; H.d.C.A., M.B., C.S., J.P., A.-B.R., and J.-Y.C. performed research; S.O. contributed unpublished reagents/analytic tools; H.d.C.A., M.B., C.S., L.R., J.P., A.-B.R., and J.-Y.C. analyzed data; H.d.C.A. and J.-Y.C. wrote the paper.

This work was supported by the Swiss National Science Foundation (Grant #31003A\_179399). The Epac2-camps plasmid was provided by Jean-Pierre Hornung (University of Lausanne, Lausanne, Switzerland). We thank Joel Wellbourne-Wood for critical reading of the manuscript and Christiane Devenoges for the genotyping.

The authors declare no competing financial interests.

Correspondence should be addressed to Jean-Yves Chatton at jean-yves.chatton@unil.ch.

https://doi.org/10.1523/JNEUROSCI.2092-18.2019

Copyright © 2019 the authors

et al., 2017). The recent discovery of a new mechanism for lactate release from astrocytes through a  $K^+$ -sensitive channel (Sotelo-Hitschfeld et al., 2015) indicates that lactate can be rapidly mobilized and may possibly lead to a transient elevation of its extracellular concentration to high levels in microdomains close to neuronal membranes, including synapses.

Recent studies indicated that energy substrates and metabolites of the energy metabolism had extracellular signaling properties by acting through the activation of G-protein-coupled receptors (GPCRs; Blad et al., 2012; Husted et al., 2017). One of them, originally named GPR81, now known as hydroxycarboxylic acid receptor 1 (HCAR1), has lactate as an endogenous ligand (Cai et al., 2008). HCAR1 was initially described as being markedly expressed in adipocytes, where its activation induces the inhibition of lipolysis through the activation of a  $G_i$ -dependent intracellular pathway (Liu et al., 2009). Our research group was the first to demonstrate that L-lactate and a HCAR1 agonist decreases spiking activity of cortical neurons in a pertussis-sensitive manner (Bozzo et al., 2013). In the locus ceruleus, L-lactate had rather an excitatory effect, suggesting the involvement of a different receptor, possibly  $G_s$  coupled, yet to be identified (Tang et al., 2014). The aim of the present study was to explore the downstream effectors of HCAR1 activation and clarify the mechanisms through which this receptor modulates neuronal activity in mouse cortical neurons.

We focused on the investigation of the intracellular pathway mediated by the activation of  $G_i$ -coupled receptors, which classically inhibits the adenylyl cyclase (AC) as a first phase of the intracellular cascade that contributes to the decrease in neuronal activity (Seino and Shibasaki, 2005). To explore these aspects, we compared the modulatory effects of HCAR1 activation on neuronal activity of primary neurons from both wild-type (WT) and HCAR1 knock-out (KO) mice, using electrophysiological recordings and calcium imaging. Our study indicates that HCAR1 activation engages the AC–cAMP–protein kinase A (PKA) pathway and has a presynaptic effect, which is accompanied by a decrease in neuronal excitability. We further discovered that HCAR1 interacts with other  $G_i$ -coupled receptors to fine-tune neuronal activity through a complex bimodal mechanism that involves the  $G_{\beta\gamma}$  subunit and activation of phospholipase C (PLC). This interaction adds a higher level of complexity to the functional outcome of HCAR1 activation.

## Materials and Methods

**Ethics statement.** All experimental procedures were performed in accordance with the recommendations of the Swiss Ordinance on Animal Experimentation and were specifically approved for this study by the Veterinary Affairs of the Canton Vaud, Switzerland (authorizations #1288.6 and #1288.7).

**Animals.** HCAR1 KO and monomeric red fluorescent protein (mRFP)-HCAR1 mouse lines were obtained from Max-Planck-Institute for Heart and Lung Research (Bad Nauheim, Germany). The generation and validation of these lines have been previously described (Ahmed et al., 2010). The genotype of all animals used for the experiments was confirmed using PCR analysis.

**Behavioral analysis.** The assessment of general behavior along with neurological and motor functions was performed in WT and HCAR1 KO male mice (8 and 15 weeks). In a first phase, mice went through a basic neurological screening to assess their general behavior/appearance, muscle tone, and motor function. Mice were placed in a transparent Plexiglas box and observed for 5 min by an experimenter blind to the genotype of the animals. Mice were checked for stereotyped behavior, convulsions, compulsive licking, self-destructive biting, and retropulsion. Next, the grasping reflex was tested by suspending the mouse by the tail and giving a Yes/No score for hindpaw clasping over three consecutive trials. The

grip strength was assessed by placing the animal on a grid and gently pulling its tail; the mean score of three trials per animal was used for analysis. In the second phase, home-cage behavior was monitored in PhenoTyper cages (Noldus; RRID:SCR\_004074) that allow the automated scoring of parameters related to locomotion, stereotypic behavior, feeding, and nesting. Briefly, mice were individually placed inside the PhenoTyper cage for 1 d with water and food *ad libitum*. A shelter was placed in one corner of the cage for automated scoring of nesting behavior. An infrared camera tracked the mouse movements throughout the 1 d session, allowing the monitoring of the above parameters. All the behavior data were collected and analyzed using EthoVision XT 14 software (Noldus; RRID:SCR\_000441).

**Cell culture and transfection.** Mouse primary cultures from cortical neurons were prepared from embryonic day 17 (E17) embryos, both male and female, from WT, HCAR1 KO, or mRFP-HCAR1 C57BL/6N mouse lines. After removing the meninges, extracted cortices were incubated in 2 ml of HBSS with 10 mg/ml Trypsin (Worthington Biochemical) for 20 min at 37°C, and then mechanically dissociated in Neurobasal culture medium (Invitrogen) supplemented with 10% FCS. Dissociated cells were filtered using a 40  $\mu$ m nylon mesh cell strainer and resuspended in Neurobasal culture medium complemented with 2% SM1 (STEMCELL Technologies), 20 mM GlutaMAX (Invitrogen), and 0.02 mM glutamate. Cells were plated at a density of 20,000 cells/cm<sup>2</sup> in 12- and 20-mm-diameter glass coverslips, coated with poly-D-lysine and laminin (Sigma-Aldrich). Half of the culture medium was exchanged every 5 d by a maturation medium composed of BrainPhys medium (STEMCELL Technologies) and 2% SM1. Cells were used at day *in vitro* (DIV) 12–18.

Transfection with the plasmid carrying the cAMP fluorescent resonance energy transfer (FRET)-based biosensor (Epac2-camps; Nikolaev et al., 2004) was performed using Lipofectamine 2000 (Invitrogen) by adding 3  $\mu$ g of DNA for 5–6 h. Cells were transfected at DIV 10–12 and used 48 h after transfection.

**DNA extraction and PCR.** Tissue was collected from phalanges of WT and HCAR1 KO E17 embryos used for the primary culture preparation. The tissue was incubated in the digestion buffer as follows (in mM): NaCl 100, Tris 10, EDTA 25, 0.5% SDS, and 5% Proteinase K (Roche), for 2 h at 57°C. After three steps of centrifugation, the pellet was dried out and resuspended in TE (Tris and EDTA) buffer (Tris-HCl, 10 mM, pH 7.5; EDTA, 0.1 mM). The DNA was amplified using the T-Personal Thermocycler (Biometra). The following two sets of primers were used to amplify the targets sequences: HCAR1: forward, TTCTGCTTTCACATG AAGACC; reverse, CAGAACAAGATGATTGTCAGG; and Neomycin: forward, GCAGCGCATCGCTTCTATC; reverse, GATATCAGGTG GACAAGTCC.

**Quantitative RT-PCR.** Brains from WT ( $n = 3$ ) and HCAR1 KO ( $n = 3$ ) mice (1 month old) were dissected in 1 mM  $MgCl_2$  RNase-free PBS, then frozen in liquid nitrogen, and kept at  $-80^\circ C$  until use. RNA extraction from tissue or cultured neurons was performed using the commercial RNeasy Mini Kit (Qiagen), and 1  $\mu$ g/ $\mu$ l was used for reverse transcription to cDNA with the High capacity cDNA Reverse Transcription Kit (Applied Biosystems). The cDNA was amplified by quantitative RT-PCR (qRT-PCR) using the Power SYBR Green PCR Master Mix (Bio-Rad), with specific primers for the target genes at 200 nM (HCAR1: GGGGACTGTGTATCTTCTGA, GAGTCTGGGTGATAGAATTTGG; GAPDH: TCCATGACAACCTTTGGCATTG, CAGTCTTCTGGGTGG CAGTGA). Samples were run in triplicate, and negative controls were run for each target gene. All reactions were performed on a CFX96 Touch Real-Time PCR Detection System (Bio-Rad). Relative mRNA expression was quantified by using the comparative CT method, and results are shown as the fold change using the 2CT formula (Livak and Schmittgen, 2001).

**Immunohistochemistry.** Primary cortical neurons from mRFP-HCAR1 mice ( $n = 2$ ) grown on coverslips were fixed with 4% paraformaldehyde in PBS for 15 min on ice. Cells were preincubated with 15% serum and 0.05% Triton X-100 and subsequently incubated overnight with the primary mouse anti-NeuN antibody (1:200; catalog #MAB377, EMD Millipore) and rabbit anti-mRFP (1:100; catalog #600–401-379, Rockland Immunochemicals). Cells were incubated with the appropriate secondary antibodies (i.e., 1:200; Alexa Fluor 488-conjugated donkey anti-



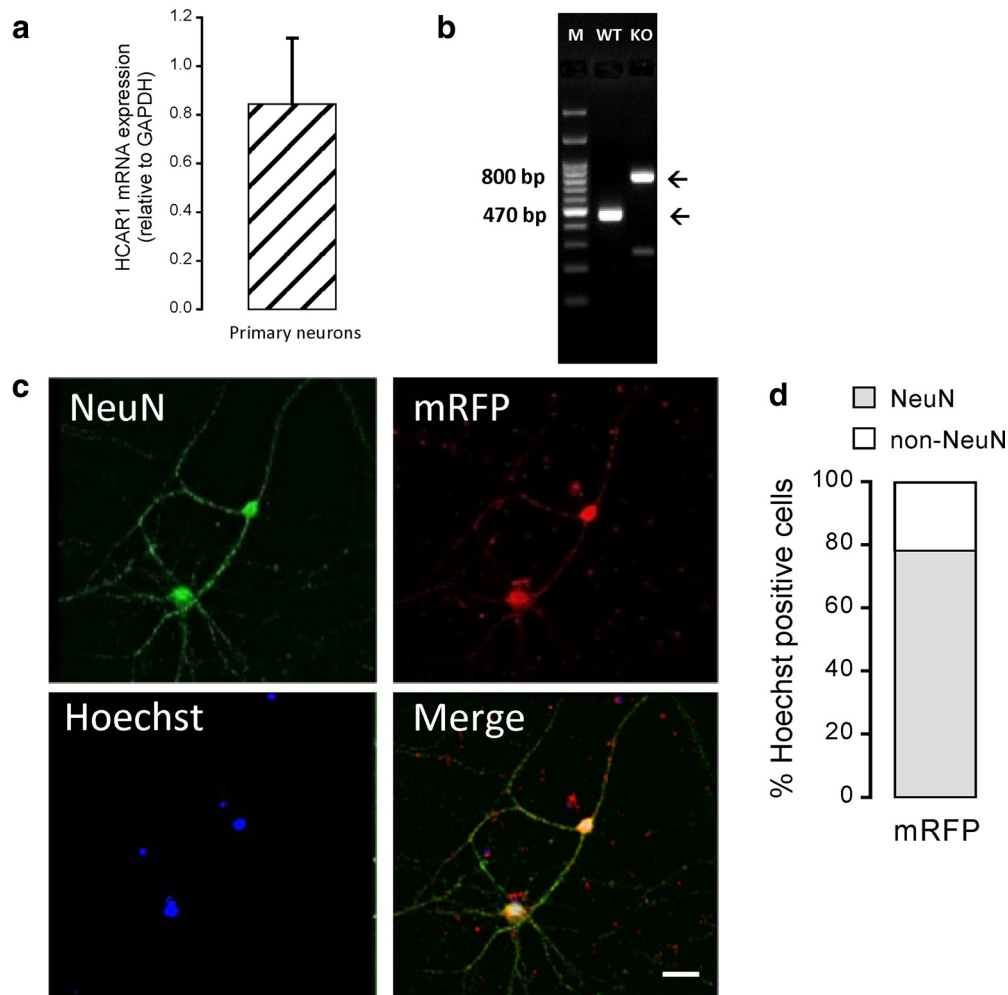


**Figure 1.** HCAR1 expression in primary mouse neurons. **a**, HCAR1 mRNA expression level in primary neurons ( $n = 4$  experiments). HCAR1 mRNA transcript levels were normalized relative to that of the housekeeping gene GAPDH. **b**, Representative PCR image of HCAR1 gene expression in WT versus HCAR1 KO animals. WT and HCAR1 KO embryonic tissue were obtained from animals used to originate neuronal primary cultures. A WT band at 470 bp and a HCAR1 KO band at 800 bp can be observed. **c**, Representative confocal images of primary cortical neurons immunostained for NeuN (green) and mRFP-HCAR1 (red), along with Hoechst nuclear staining (blue) and the overlay image. **d**, Quantification of mRFP-, NeuN-, and mRFP-NeuN-positive cells shown as the percentage of Hoechst-positive cells ( $n = 5$  experiments, repeated 3 times per experiment). Scale bar, 40  $\mu\text{m}$ .

mouse IgG; catalog #ab105105, Abcam) and Alexa Fluor 594-conjugated donkey anti-rabbit IgG (1:200; catalog #ab150076, Abcam). Brain sections from 1-month-old WT ( $n = 6$ ) and HCAR1 KO ( $n = 5$ ) mice were obtained from mice anesthetized with sodium-pentobarbital (150 mg/kg, i.p.) and transcardially perfused with 4% paraformaldehyde. The brains were sliced in a sagittal or coronal plane using a vibratome (VT1000S, Leica), or were cryoprotected in 30% sucrose and sliced using a microtome (HM 400, Microm); in both cases, 30- $\mu\text{m}$ -thick slices were obtained. Slices were preincubated with 15% donkey serum and 0.3% Triton X-100 and subsequently were incubated with the primary antibody overnight (Table 1-1, available at <https://doi.org/10.1523/JNEUROSCI.2092-18.2019.t1-1>). In sequence, slices were incubated with the appropriate secondary antibody (Table 1-2, available at <https://doi.org/10.1523/JNEUROSCI.2092-18.2019.t1-2>).

Nuclei were stained using Hoechst stain (Invitrogen). Negative controls were performed in the absence of primary antibodies. Coverslips and slices were mounted in FluorSave Mounting Medium (EMD Millipore). Coverslips were analyzed using the Leica TCS SP5 Confocal Microscope (Leica). Brain sections were analyzed using the Zeiss LSM 710 Confocal Microscope (Zeiss).

**Western blot.** Western blot was performed as previously described (Grishchuk et al., 2011), using WT ( $n = 4$ ) and HCAR1 KO ( $n = 4$ ) cortex, hippocampus, and cerebellum. Briefly, the different brain regions were dissected and then stored at  $-20^\circ\text{C}$  in lysis buffer, containing the

following (in mM): HEPES 20, pH 7.4, NaCl 10,  $\text{MgCl}_2$  3, EGTA 2.5, dithiothreitol 0.1, NaF 50,  $\text{Na}_3\text{VO}_4$  1, 1% Triton X-100, and a protease inhibitor cocktail (catalog #1187350001, Roche). Protein concentration was determined using a Bradford assay. Proteins (30–40  $\mu\text{g}$ ) were separated on 12% polyacrylamide gels and analyzed by immunoblotting. Primary antibodies (Table 1-1, available at <https://doi.org/10.1523/JNEUROSCI.2092-18.2019.t1-1>) were diluted in blocking buffer with 0.001% PBS Tween-20 and incubated overnight at  $4^\circ\text{C}$ . Secondary antibodies (Table 1-2, available at <https://doi.org/10.1523/JNEUROSCI.2092-18.2019.t1-2>) were diluted in blocking buffer and incubated for 1 h. Protein bands were visualized with the Odyssey Infrared Imaging System (LI-COR) or by using the enhanced chemiluminescence (ECL) method, using 200  $\mu\text{l}$  of ECL substrate (SuperSignal West Dura Extended Duration Substrate, Thermo Fisher Scientific). Odyssey version 1.2 software (LI-COR) or LAS 4000 Mini Luminescent Image Analyzer (FujiFilm) were used for analysis. Values were normalized with respect to actin.

**Live-cell microscopy.** Intracellular calcium imaging was performed on an upright epifluorescence microscope (model FN1, Nikon) using a  $40\times$ , 0.8 numerical aperture (NA), water-immersion objective lens. Fluorescence excitation wavelengths were selected using a fast filter wheel (Sutter Instrument) and fluorescence was detected using an Evolve Electron Multiplying CCD (EMCCD) Camera (Photometrics). Digital image acquisition and time series were computer controlled using MetaFluor software (Molecular Devices; RRID:SCR\_014294). Up to eight individ-

**Table 1. Anti-HCAR1 primary antibody specificity**

Anti-HCAR1 primary antibody (source, reference)	Epitope	IHC		WB	
		WT	HCAR1 KO	WT	HCAR1 KO
Santa Cruz Biotechnology, SC-32647	C-terminal, extracellular domain of human HCAR1	§	§	+	+
Santa Cruz Biotechnology, SC-32648	C-terminal, cytoplasmic domain of human HCAR1	+	+	–	–
Sigma-Aldrich, SAB1300090	Mouse GPR81-S296, aa 276–329	+	+	+	+
Sigma-Aldrich, SAB1300793	Rat GPR81-R320, aa 286–332	+	+	§	§
Sigma-Aldrich, SAB1300089	Human GPR81–296, aa 310–353	+	+	+	+
Sigma-Aldrich, SAB1300792	Mouse GPR81-R203, aa 193–230	+	+	§	§
Sigma-Aldrich, SAB1300791	Mouse GPR81-C7, aa 7–36	+	+	–	–
Novus Biologicals, NLS2095	19 aa peptide from C-terminus of human HCAR1	+	+	§	§
Novus Biologicals, NBP1–51956	C-QQLARQARMKKATR (internal region)	+	+	§	§

Experiments were performed in brain slices of cortex, hippocampus, and cerebellum. +, positive signal/band; –, negative/absence of signal/band; IHC, immunohistochemistry; WB, Western blot; §, not tested. See Table 1-1, available at <https://doi.org/10.1523/JNEUROSCI.2092-18.2019.t1-1>, and Table 1-2, available at <https://doi.org/10.1523/JNEUROSCI.2092-18.2019.t1-2>.

ual neurons were simultaneously analyzed in the field of view. Intracellular calcium was measured using Fluo-8 AM (5  $\mu$ M; Abcam) loaded for 15 min at 37°C, in a HEPES-buffered balanced solution containing the following (in mM): NaCl 160, KCl 5.4, HEPES 20, CaCl<sub>2</sub> 1.3, MgSO<sub>4</sub> 0.8, NaH<sub>2</sub>PO<sub>4</sub> 0.78, and glucose 20, pH 7.4 (adjusted with NaOH), supplemented with 0.1% Pluronic F127 (Thermo Fisher Scientific). Fluorescence was excited at 490 nm and detected at >515 nm, with an acquisition rate of 6–7 Hz. Fluorescence intensity was measured over time in regions of interest delineating neuronal soma using MetaFluor software. Calcium transients were analyzed using Mini Analysis version 6.0.3 (Synaptosoft; RRID: SCR\_002184), which includes an algorithm for the detection of complex and multiple events, giving the possibility to detect overlapping or closely occurring peaks, thus allowing the analysis of the frequency of spontaneous calcium spikes under different experimental conditions.

FRET measurements of intracellular cAMP levels were measured in cells expressing Epac2-camps 48 h after transfection on an epifluorescence inverted microscope (Zeiss) equipped with an image splitter (DV2, Photometrics), using a high numerical aperture fluorescence objective (40 $\times$ , 1.3 NA, oil-immersion). Fluorescence excitation wavelengths were selected via fast holographic monochromator (Polychrome II, Till Photonics) coupled to a xenon lamp, and fluorescence was detected using an EMCCD camera (LUCA-R, Andor). Digital image acquisition was performed using the MetaFluor software. One individual neuron was imaged in the selected field of view. Fluorescence was excited at 430 nm, and detected at 475 and 530 nm for cyan fluorescent protein (CFP) and yellow fluorescent protein (YFP), respectively, with an acquisition rate of 0.2 Hz. Regions of interest were selected from single cell YFP and CFP images. The FRET ratios (CFP/YFP) were computed using MetaFluor software. Decrease in FRET ratio signal reflects a decrease in the intracellular cAMP levels.

**Electrophysiological recordings.** Patch-clamp recordings were made using borosilicate glass pipettes (5–6 M $\Omega$ ) filled with intracellular solution containing the following (in mM): K-gluconate 135, NaCl 5, Naphosphocreatine 5, MgCl<sub>2</sub> 1, EGTA 1, HEPES 10, Mg-ATP 2, and Na<sub>3</sub>-GTP 0.4, pH 7.2 (adjusted with KOH). Recordings were made with a MultiClamp 700B amplifier (Molecular Devices). Data were acquired with a Digidata 1440A digitizer (Molecular Devices), at 10 kHz sampling rate, controlled with pCLAMP 10 software (RRID:SCR\_011323), and analyzed with Clampfit (RRID:SCR\_011323) and Mini Analysis (RRID:SCR\_002184). The criterion for experiment inclusion was based on the verification of stable access resistance and leak current (<200 pA at –70 mV in control solution).

mEPSCs were recorded at –70 mV in voltage clamp in gap-free mode. A stabilization period of 5 min was routinely allowed after establishment of the whole-cell configuration. Experiments were performed in presence of 1  $\mu$ M tetrodotoxin (TTX) and 60  $\mu$ M bicuculline. mEPSCs were recorded for 10 min in the absence and presence of HCAR1 agonist and the last 5 min were analyzed. Cells included in the analysis had a membrane potential less than or equal to –55 mV, stable access resistance, and recovery after washout.

We further assessed cell passive properties and firing frequency of WT neurons in control conditions and after HCAR1 activation. The resting membrane potential (RMP) was measured in current-clamp mode after

**Table 2. Summary of behavioral phenotype of WT versus HCAR1 KO**

	WT	n	HCAR1 KO	n
(1) Weight (g)	26.3 $\pm$ 0.4	12	27.4 $\pm$ 0.9 <sup>n.s.</sup>	12
Food consumption (g)	3.5 $\pm$ 0.3	10	3.3 $\pm$ 0.2 <sup>n.s.</sup>	10
Water consumption (ml)	3.1 $\pm$ 0.2	10	3.7 $\pm$ 0.3 <sup>n.s.</sup>	10
Total travel distance (cm)	55,374 $\pm$ 7352	10	52,059 $\pm$ 5197 <sup>n.s.</sup>	10
Dark phase	41,985 $\pm$ 5419		43,263 $\pm$ 4515 <sup>n.s.</sup>	
Light phase	13,389 $\pm$ 2885		8796 $\pm$ 2224 <sup>n.s.</sup>	10
Total time in the nest (min)	46,136 $\pm$ 3363	10	47,686 $\pm$ 3442 <sup>n.s.</sup>	10
Dark phase	21,681 $\pm$ 1781		20,962 $\pm$ 2537 <sup>n.s.</sup>	
Light phase	24,454 $\pm$ 1785		26,724 $\pm$ 1369 <sup>n.s.</sup>	
(2) Rearing (number/min)	8.6 $\pm$ 0.7	12	9.8 $\pm$ 0.5 <sup>n.s.</sup>	12
Number of grooming (number/min)	0.6 $\pm$ 0.1	12	0.6 $\pm$ 0.1 <sup>n.s.</sup>	12
Grooming duration (s)	24 $\pm$ 5.3	12	25 $\pm$ 5.5 <sup>n.s.</sup>	12

Data are shown as the mean  $\pm$  SEM. Experiments were performed on independent animals. (1), PhenoTyper cage observations; (2), free observations; n.s., not significant (Student's unpaired *t* test).

the whole-cell configuration was established. The input resistance ( $R_N$ ) was determined from the linear slope of the current–voltage relationship around the RMP, obtained by a series of 160 ms current steps (starting at –140 pA with 30 pA increments). The rheobase was determined as the minimal current amplitude able to evoke an action potential (AP) and was obtained by applying 3 s steps of positive current (starting at 0 pA, with 50 pA increments). The firing frequency was assessed as the number of AP evoked in response to 1 s current injection steps (0–450 pA, with 50 pA increments). AP frequency was measured as the number of APs in response to 150 pA current injection. The membrane time constant was estimated by fitting an exponential function to a voltage step of –5 mV.

Paired pulse ratio (PPR) experiments were measured using a pipette solutions containing the following (in mM): CsF 121.6, CsCl 8.4, Naphosphocreatine 5, EGTA 1, HEPES 10, Mg-ATP 2, Na<sub>3</sub>-GTP 0.4, and QX-314Cl 1, pH 7.2 (adjusted with CsOH). Neurons were voltage-clamped at –70 mV in the whole-cell configuration. Stimulation was performed using a Pt-Ir concentric bipolar electrodes (tip diameter, 2–3  $\mu$ m; model CEA3, MicroProbes for Life Science) placed near the recorded neuron and connected to an Iso-Flex stimulus isolator (A.M.P.I.). The minimum stimulation intensity able to trigger a single evoked EPSC was determined in the range 0.4–1 mA. Two consecutive 1 ms stimuli were applied with an interval of 50 ms.

**Solutions and drugs.** CO<sub>2</sub>/bicarbonate-buffered experimental solutions contained the following (mM): NaCl 135, KCl 5.4, NaHCO<sub>3</sub> 25, CaCl<sub>2</sub> 1.3, MgSO<sub>4</sub> 0.8, NaH<sub>2</sub>PO<sub>4</sub> 0.78, and glucose 5, bubbled with 5% CO<sub>2</sub>/95% air. Glucose was maintained in a nonlimiting fashion (5 mM) in all solutions. Control extracellular solutions and solutions containing tested drugs were gravity fed at 1 ml/min and at 35°C. The pH of CO<sub>2</sub>-equilibrated solutions was 7.4 and was not altered by the added L-lactate (Bozzo et al., 2013). L-Lactate, 3,5-dihydroxybenzoic acid (3,5-DHBA), 3-chloro-5-hydroxybenzoic acid (3Cl-HBA), 9-(tetrahydro-2-furanyl)-9H-purin-6-amine (SQ 22536), baclofen, guanfacine, gallein, and QX-314Cl were obtained from Sigma-Aldrich. H-89 dihydrochloride (H-89), N<sub>6</sub>-cyclopentyladenosine (CPA), (1-[6-[[[(17 $\beta$ )-3-methoxyestra-1,3,5(10)-trien-17-yl]amino]hexyl]-1H-pyrrole-2,5-dione; U73122), and bi-



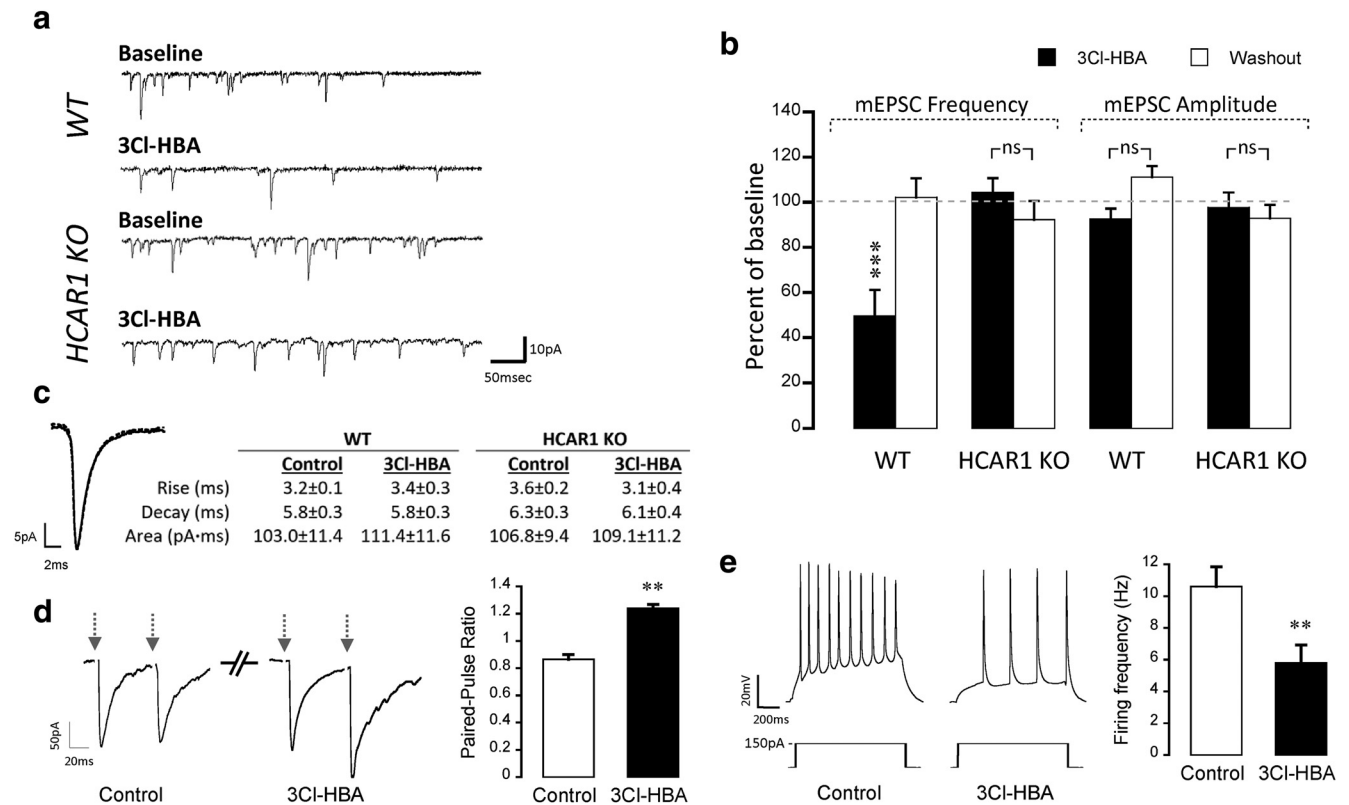


**Figure 2.** HCAR1 activation decreases mEPSC frequency and modulates intrinsic membrane properties of mouse cortical neurons. **a**, Representative mEPSCs traces from a neuron recorded in the presence and in the absence of 3CI-HBA 40  $\mu\text{M}$  for WT and HCAR1 KO. Voltage-clamp recordings of mEPSCs were performed in the presence of TTX (1  $\mu\text{M}$ ) and bicuculline (60  $\mu\text{M}$ ) with neurons clamped at  $-70$  mV. **b**, Summary of mEPSC frequency and amplitude (percentage of baseline) in response to 3CI-HBA application in WT ( $n = 7$ ) and HCAR1 KO neurons ( $n = 6$ ). A depression of mEPSC frequency, but not amplitude, was observed upon HCAR1 activation in neurons prepared from WT mice but not from HCAR1 KO mice. **c**, Representative superimposed averaged traces of 1000 events from the same WT neuron in the absence (full line) and in the presence of 3CI-HBA (dotted line), and a table showing corresponding average kinetic values of all events from WT and KO in the presence and in the absence of 3CI-HBA, demonstrating similar kinetics in WT and KO neurons. Significance is shown compared with baseline and among conditions. **d**, Left, Representative responses to paired pulse protocols using an interstimulus interval of 50 ms in WT neurons before and after HCAR1 activation (left). Arrows represent the stimulation. Right, Summary graph of PPR results ( $n = 7$ ). Significance is shown between the control condition and after 3CI-HBA application. **e**, Representative traces from neurons recorded before and after HCAR1 activation (left), obtained from a series of current injections (0–450 pA, 1 s, 50 pA increments); the response to 150 pA current injection is shown. Summary graph (right) of the effect of HCAR1 activation on neuronal firing frequency following steps of current injection ( $n = 5$ ). The firing frequency (in Hz) was calculated from the number of AP evoked by a 150 pA current injection. Significance is shown between the control and 3CI-HBA conditions.  $^{**}p < 0.01$ ,  $^{***}p < 0.001$ , ns, not significant.

**Table 3. Effect of HCAR1 activation on passive properties of cortical cultured neurons**

	Control	3CI-HBA 40 $\mu\text{M}$
RMP (mV)	$-59.3 \pm 1.1$	$-62.9 \pm 1.3^*$
$R_N$ (M $\Omega$ )	$97.3 \pm 6.4$	$77.5 \pm 6.2^*$
Rheobase (pA)	$78.6 \pm 6.8$	$93.6 \pm 8.7^*$
Time constant (ms)	$16.4 \pm 1.1$	$18.8 \pm 0.5^*$

Data are shown as the mean  $\pm$  SEM. Experiments were performed in five independent WT neurons. All parameters were tested in all cells used for analysis.

$^*p < 0.05$  Student's paired  $t$  test.

cuculline were obtained from Tocris Bioscience. Forskolin was obtained from Biomol and TTX was obtained from BioTrend. All drugs were diluted in  $\text{CO}_2$ /bicarbonate-buffered solution to their final concentration and perfused in the same conditions as the control.

**Experimental design and statistical significance.** Immunohistochemistry data quantification was performed using ImageJ software (RRID: SCR\_003070). We first identified Hoechst-stained nuclei in the field, allowing us to assess the number of cells. We then determined cells that were NeuN-positive and/or mRFP-positive to assess the number of neurons that were expressing mRFP. For each independent experiment, three different fields of view were analyzed. The result of the quantification is shown as the percentage of Hoechst-positive cells.

To assess the HCAR1 functional role in neuronal activity, experiments were performed using a sequential application of drugs. Each individual

experiment represents responses obtained by the application of the tested drugs, one following the other, on the same cells followed by washout with the control solution. Statistical analyses were performed using KaleidaGraph software (Synergy Software; RRID:SCR\_014980). Data are the mean  $\pm$  SEM and are represented as the percentage compared with control;  $n$  represents the number of independent experiments. Data normality was checked using the Shapiro–Wilk test.

When more than one condition was tested on the same experiment, comparisons were made using one-way ANOVA followed by Bonferroni correction for each experimental group to assess statistical significance against respective control, and among the tested conditions. When only one condition was tested, the paired or nonpaired  $t$  test was performed to assess statistical significance ( $^*p < 0.05$ ,  $^{**}p < 0.01$  and  $^{***}p < 0.001$ ). Only experiments where the effect of the tested drugs could be washed out were taken into consideration for analysis.

## Results

### HCAR1 expression in neurons

Localization of HCAR1 protein in neurons has been reported by us and other research groups based on immunohistochemistry (Bozzo et al., 2013; Lauritzen et al., 2014). In this study, qRT-PCR was used to assess HCAR1 mRNA expression in primary neuronal cultures at DIV 14 (Fig. 1a) from WT mice. Figure 1b shows genotyping results of WT and HCAR1 KO mice. In the gene construct of HCAR1 KO mice, the coding sequence of HCAR1

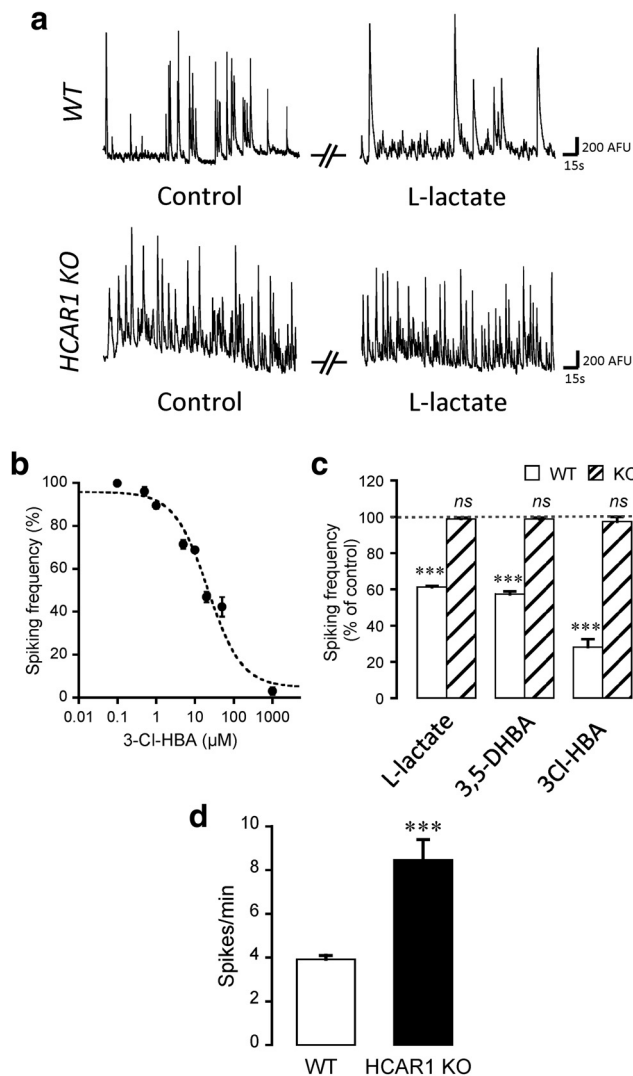


**Figure 3.** Effect of neuronal activation on neuronal calcium spiking activity. *a*, Representative traces of calcium spiking in control or 5 mM L-lactate-containing solutions, for both WT and HCAR1 KO neurons. *b*, The effect of the HCAR1 agonist 3Cl-HBA on spontaneous calcium activity of neurons was concentration dependent, with an IC<sub>50</sub> value of 21.5 ± 6.1 μM ( $n = 177$  neurons from 23 experiments). The IC<sub>50</sub> value was obtained by nonlinear curve fitting using the Levenberg-Marquardt algorithm. *c*, Effect of HCAR1 activation on calcium spiking frequency from WT and HCAR1 KO neurons with 5 mM L-lactate (WT:  $n = 66$  cells, 16 experiments; HCAR1 KO:  $n = 81$  cells, 16 experiments), 1 mM 3,5-DHBA (WT:  $n = 57$ , 16 experiments; HCAR1 KO:  $n = 74$  cells, 12 experiments), or 40 μM 3Cl-HBA (WT:  $n = 31$  cells, 3 experiments; HCAR1 KO:  $n = 32$  cells, 5 experiments). Spiking frequency is shown as a percentage of activity measured in the control condition. The effect of HCAR1 activation was reversible in all experiments (data not shown). Significance is shown compared with control and among conditions. *d*, Comparison of basal spontaneous spiking frequencies of neurons from WT ( $n = 16$ ) and HCAR1 KO ( $n = 16$ ) mice. \*\*\* $p < 0.001$ , ns, not significant.

was replaced by a cassette containing the lacZ and the neomycin resistance genes (Ahmed et al., 2010). Samples from WT shows a PCR HCAR1 band corresponding to a 470 bp product, whereas the ones from HCAR1 KO animals have a neomycin-only, 800 bp product band. In the next phase, we wanted to investigate the HCAR1 protein expression and localization in primary cultured neurons. For this purpose, we took advantage of the HCAR1 KO mice, not available in our first studies, to assess the specificity of commercial antibodies. Table 1 shows that of nine commercial antibodies raised against different epitopes, tested by Western blot and/or immunohistochemistry, none displayed a convincing absence of signal in HCAR1 KO tissue. To circumvent this issue,

we used a transgenic mouse that expresses mRFP under the HCAR1 promoter (Ahmed et al., 2010). This fluorescent reporter protein is not targeted to the plasma membrane but spreads in the cytoplasm, allowing us to identify the cells that endogenously express the HCAR1 transcripts. In primary neurons from mRFP-HCAR1 mice, all Hoechst-positive cells were also mRFP-HCAR1 positive. Among these cells, ~80% were also positive for NeuN (Fig. 1*c,d*). This result indicates that these cultured neurons express mRFP-HCAR1. The 20% of the cells that were mRFP-HCAR1 positive, but NeuN negative, could represent cells that are not mature neurons and that also express HCAR1.

### HCAR1 KO animals show normal general behavior

According to previous studies, HCAR1 KO mice do not show obvious abnormalities when compared with WT mice, which includes no difference in body weight (Ahmed et al., 2010) or locomotion when exposed to high-intensity interval exercises (Morland et al., 2017). We extended the phenotype analysis and performed a basic behavioral neurological screening in these animals. We did not find differences in the quantitative observations obtained with the PhenoTyper cage or during the free observation (Table 2). Neither WT nor HCAR1 KO animals presented traces of compulsive licking, self-destructive biting, retropulsion, or convulsions. No differences were observed in the grip strength test ( $t_{(22)} = 0.49$ ,  $p = 0.63$ , unpaired  $t$  test) and in the hindpaw clasping test (none of the mice failed the test; WT,  $n = 12$  animals; HCAR1 KO,  $n = 12$  animals).

### Activation of HCAR1 decreases mEPSC frequency and excitability

In the next phase, we evaluated the effects of HCAR1 activation on basal neurotransmission using the whole-cell patch-clamp technique. Figure 2*a* shows representative electrophysiological traces of mEPSCs recorded from neurons of WT and HCAR1 KO mice. We observed a significant decrease (~50%) in mEPSC frequency in the WT group during HCAR1 activation by its agonist 3Cl-HBA (40 μM;  $F_{(2,6)} = 12.92$ ,  $p = 0.0013$ , ANOVA). 3Cl-HBA application did not alter the mean amplitude ( $F_{(2,6)} = 5.84$ ;  $p = 0.562$ , ANOVA) or kinetics (rise:  $t_{(6)} = -1.41$ ,  $p = 0.22$ ; decay:  $t_{(6)} = 0.19$ ,  $p = 0.85$ ; area:  $t_{(6)} = -0.77$ ,  $p = 0.48$ , paired  $t$  test) of mEPSCs (Fig. 2*b,c*). Importantly, the frequency ( $F_{(2,5)} = 0.09$ ,  $p = 1$ , ANOVA), amplitude ( $F_{(2,5)} = 0.23$ ,  $p = 1$ , ANOVA), and kinetics (rise:  $t_{(5)} = 1.39$ ,  $p = 0.22$ ; decay:  $t_{(5)} = 0.87$ ,  $p = 0.42$ ; area:  $t_{(5)} = -0.63$ ,  $p = 0.56$ , paired  $t$  test) of mEPSCs were not influenced by HCAR1 activation in neurons from HCAR1 KO mice (Fig. 2*c*). These results are a first indication of a presynaptic mechanism induced by HCAR1. To further test this hypothesis, we performed a PPR experiment before and after HCAR1 activation. These experiments revealed a significant increase in the PPR value ( $t_{(6)} = -5.18$ ,  $p = 0.002$ , paired  $t$  test; Fig. 2*d*), supporting the notion that HCAR1 has a presynaptic component.

However, previous works indicated that HCAR1 activation modulates passive properties and decreases the firing frequency of rat CA1 pyramidal neurons (Herrera-López and Galván, 2018). Thus, we investigated whether HCAR1 activation could modulate intrinsic properties of mouse cortical neurons as well. We observed that the activation of HCAR1 with 3Cl-HBA (40 μM) decreased firing frequency by 45% ( $t_{(4)} = 6.53$ ,  $p = 0.003$ , paired  $t$  test; Fig. 2*e*), as previously observed by Herrera-López and Galván (2018). Table 3 further shows that the activation of HCAR1 causes a significant decrease in  $R_N$  ( $t_{(4)} = 4.35$ ,  $p = 0.01$ , paired  $t$  test) and membrane time constant ( $t_{(4)} = -3.69$ ,  $p = 0.02$ , paired  $t$  test) increases the rheobase current ( $t_{(4)} = -4.09$ ,  $p = 0.01$ , paired  $t$  test), and hyperpolarizes the RMP ( $t_{(4)} = 3.41$ ,

$p = 0.03$ , paired  $t$  test). These experiments indicate that HCAR1 activation induces changes in the intrinsic membrane properties of mouse cortical neurons, eliciting a decrease in excitability in addition to a presynaptic mechanism.

### Activation of HCAR1 decreases neuronal calcium spiking frequency

The spontaneous spiking activity of primary cortical neurons was then measured by calcium imaging. As previously demonstrated (Bozzo et al., 2013), intracellular calcium transients directly correlate with action potentials in single neurons. This approach offers the advantage of recording a number of cells in parallel without altering the intracellular solute composition compared with the whole-cell patch-clamp method.

Activation of HCAR1 was tested in neurons obtained from both WT and HCAR1 KO mice. HCAR1 is endogenously activated by L-lactate in neurons with an apparent  $IC_{50}$  of 4.2 mM (Bozzo et al., 2013). For these experiments, we tested the endogenous ligand L-lactate, as well as two specific nonmetabolized agonists of HCAR1, namely, 3,5-DHBA and the newer, higher affinity agonist 3Cl-HBA. Figure 3*a* shows that application of L-lactate (5 mM) on neurons from WT mice led to a decrease in spontaneous spiking frequency by  $\sim 40\%$ , as observed previously (Bozzo et al., 2013). We then tested the higher-affinity agonist 3Cl-HBA and performed a log-dose analysis of its effect on neuronal activity (Fig. 3*b*). 3Cl-HBA caused a decrease in spiking frequency with an  $IC_{50}$  of  $21.6 \pm 6.1 \mu M$  ( $n = 23$  experiments), virtually identical to the  $22 \mu M$  potency originally found with the mouse HCAR1 isoform (Dvorak et al., 2012). Figure 3*c* summarizes this series of experiments and shows that L-lactate ( $F_{(2,15)} = 555.95$ ,  $p < 0.0001$ , ANOVA), 3,5-DHBA ( $F_{(2,15)} = 429.20$ ,  $p < 0.0001$ , ANOVA), and 3Cl-HBA ( $F_{(2,2)} = 224.57$ ,  $p < 0.0001$ , ANOVA) strongly decreased spiking frequency. In sharp contrast, L-lactate ( $F_{(2,15)} = 45.71$ ,  $p = 0.26$ , ANOVA), 3,5-DHBA ( $F_{(2,11)} = 47.59$ ,  $p = 0.22$ , ANOVA), or 3Cl-HBA ( $F_{(2,4)} = 3.93$ ,  $p = 1$ , ANOVA) did not alter the spontaneous spiking frequency in neurons prepared from HCAR1 KO mice. This result is a strong indication that HCAR1 activation is responsible and required for the modulatory effects of L-lactate on neuronal network spontaneous activity. It should be added that in control conditions, neurons obtained from HCAR1 KO displayed an approximately twofold higher basal activity compared with WT neurons ( $t_{(30)} = -4.83$ ,  $p < 0.0001$ , unpaired  $t$  test; Fig. 3*d*), suggesting that HCAR1 might have a role in the tonic inhibition of neuronal activity.

### Intracellular HCAR1 signaling pathways in neurons

HCA receptors have been reported to be coupled to  $G_i$  proteins in the adipose tissue (Liu et al., 2009). Our group previously demonstrated that the lactate effect on cortical neurons is sensitive to pertussis toxin, which supports the notion that HCAR1 in neurons decreases neuronal activity through the  $G_i$ -protein pathway (Bozzo et al., 2013). Therefore, we investigated whether the downstream effectors of  $G_i$ -protein were involved in the decrease of neuronal activity induced by HCAR1 activation.

Using calcium imaging, we analyzed the effect of HCAR1 activation on neuronal spiking frequency upon pharmacological manipulation of the intracellular pathways known to follow the activation of  $G_i$ -proteins. Activation of AC by forskolin ( $10 \mu M$ ) caused an  $\sim 30\%$  increase in spiking activity in WT neurons, which was reversed by concomitant activation of HCAR1 ( $F_{(3,4)} = 23.16$ ,  $p < 0.0001$ , ANOVA; Fig. 4*a*). In comparison, forskolin was found to have a stronger stimulatory effect on neurons from

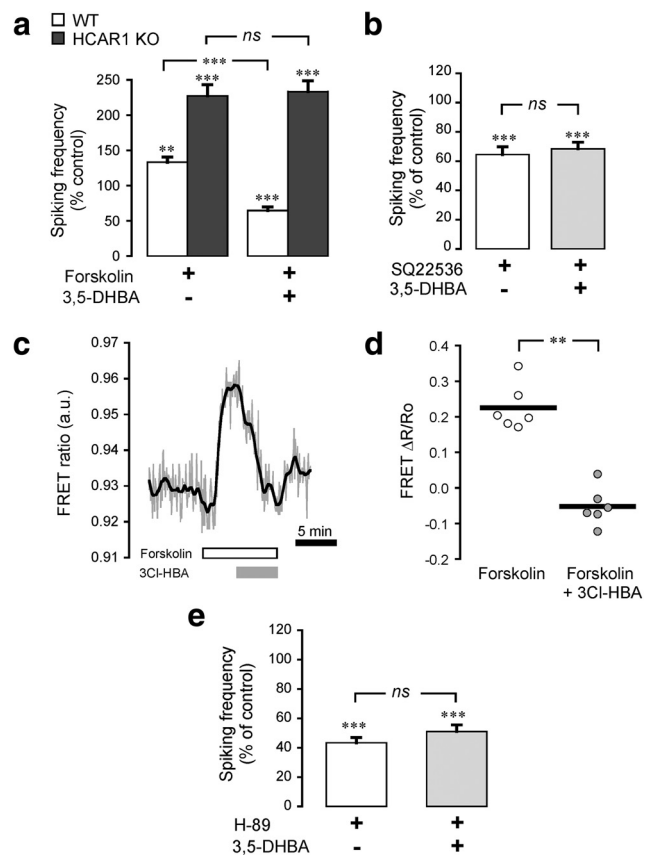


**Figure 4.** Adenylyl cyclase, cAMP, and PKA involvement in neuronal HCAR1 signaling. **a**, Activation of AC with forskolin ( $10 \mu M$ ) increased spiking activity in both WT ( $n = 44$  cells, 5 experiments) and HCAR1 KO ( $n = 29$  cells, 3 experiments) neurons compared with their respective baseline activity. **b**, Application of 3,5-DHBA ( $1 \text{ mM}$ ), in sequence with forskolin, decreased spiking activity in WT, but not in HCAR1 KO neurons. Inhibition of AC with SQ22536 ( $10 \mu M$ ) decreased spiking activity in WT neurons ( $n = 46$  cells, 6 experiments). Application of 3,5-DHBA, in sequence with SQ22536, caused no further decrease in neuronal activity. **c**, Representative trace of the effects of HCAR1 activation on cAMP levels measured using the Epac2-camps FRET sensor. The FRET (CFP/YFP) ratio, proportional to the cAMP levels, is shown for a single neuron along the timeline. Application of the AC activator forskolin ( $10 \mu M$ ) caused a rapid signal rise, and the subsequent HCAR1 activation using 3Cl-HBA ( $40 \mu M$ ) reversed this increase. **d**, Summary of absolute FRET ratio values in the presence of forskolin before and after stimulation of HCAR1 using 3Cl-HBA. The graph shows individual values plotted along with the mean value of all experiments ( $n = 6$  cells, 6 experiments). **e**, Inhibition of PKA with H-89 ( $1 \mu M$ ) decreased spiking activity in WT neurons ( $n = 64$  cells, 6 experiments). Application of 3,5-DHBA, in sequence with H-89, did not further decrease neuronal activity. Significance is shown compared with control and among conditions in **a**, **b**, and **e**.  $**p < 0.01$ ,  $***p < 0.001$ , ns, not significant.

HCAR1 KO animals, suggesting a tonic inhibitory effect operated by HCAR1 on AC. Moreover, the HCAR1 agonist 3,5-DHBA had no effect on the forskolin-induced activity of these neurons ( $F_{(3,2)} = 24.89$ ,  $p = 1$ , ANOVA; Fig. 4*a*). Conversely, the inhibition of AC with SQ22536 ( $10 \mu M$ ) decreased neuronal spiking activity by  $\sim 40\%$ . In this situation, under AC inhibition, HCAR1 activation did not cause further spiking activity decrease ( $F_{(3,6)} = 15.39$ ,  $p = 1$ , ANOVA; Fig. 4*b*). These results indicate that HCAR1 activation impacts AC in neurons. Live-cell imaging of cAMP levels in neurons was then performed using the FRET sensor Epac2-camps. Figure 4*c* shows that forskolin application caused a rapid increase in FRET response, corresponding to cAMP level rise. This cAMP level increase was efficiently reversed by the application of the HCAR1 agonist 3Cl-HBA ( $t_{(5)} = 6.62$ ,  $p = 0.001$ , paired  $t$  test; Fig. 4*c,d*). We then tested PKA as one of the main



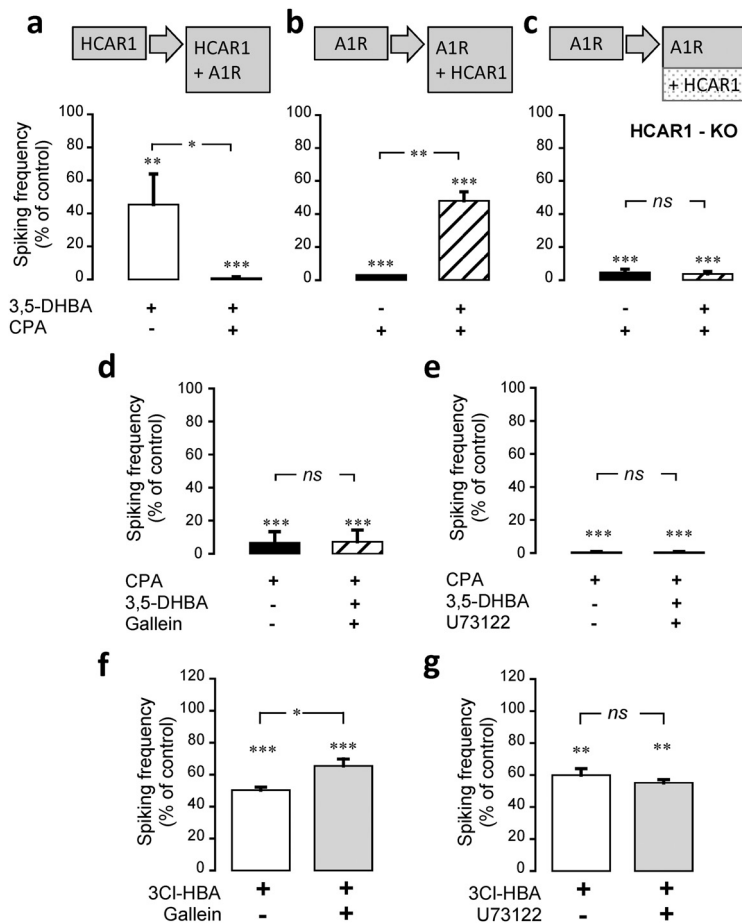


**Figure 5.** HCAR1 interaction with other  $G_i$ -coupled receptors for the modulation of neuronal activity. **a**, HCAR1 was first activated using 3,5-DHBA (1 mM) and in a second phase, the agonist of A1R, CPA (30 nM), was coapplied, which caused a stronger decrease in spiking activity compared with HCAR1 activation alone. The same protocol was performed with a reverse order of receptor activation (i.e., first CPA and then 3,5-DHBA application). **b**, **c**, Although the secondary 3,5-DHBA application caused a partial reversal of inhibition in neurons from WT animals (**b**), it had no effect on neurons from HCAR1 KO animals (**c**). **d**, **e**, The effect of the coactivation of A1R with HCAR1 in the presence of gallein (10  $\mu$ M), a  $\beta\gamma$  subunit signaling inhibitor (**d**), or U73122 (10  $\mu$ M), a PLC blocker (**e**), is shown. Both treatments prevented the partial reversal of inhibition observed in **b**. **f**, **g**, Effect of  $\beta\gamma$  subunit inhibition using gallein (10  $\mu$ M; **f**) and of PLC blockade with U73122 (10  $\mu$ M; **g**) on HCAR1 activation alone using 3CI-HBA-HBA (40  $\mu$ M). Inhibition of  $\beta\gamma$  subunit partially reverted HCAR1 effect on neural activity; however, PLC blockade did not influence the HCAR1 effect. Data are the mean  $\pm$  SEM from 21 cells, 4 experiments (**a**); 20 cells, 4 experiments (**b**); 27 cells, 4 experiments (**c**); 26 cells, 4 experiments (**d**); 14 cells, 3 experiments (**e**); 33 cells, 4 experiments (**f**); and 22 cells, 3 experiments (**g**). Significance is shown compared with control and among conditions. \* $p < 0.05$ , \*\* $p < 0.01$ , \*\*\* $p < 0.001$ , ns, not significant.

downstream targets of AC-cAMP. To this aim, we used H-89 (1  $\mu$ M) to inhibit PKA, which led to a decrease in neuronal network activity. Under PKA blockade, the activation of HCAR1 using 3,5-DHBA did not cause a further decrease in spiking activity ( $F_{(3,6)} = 80.75$ ,  $p = 0.61$ , ANOVA; Fig. 4e). Together, these experiments demonstrate that HCAR1 action on neuronal spiking activity involves the inhibition of AC, causing a decrease in cAMP levels and in turn of PKA activity.

### HCAR1 interacts with $G_i$ -coupled receptors to modulate neuronal activity

A characteristic feature of GPCRs is their ability to cross talk with other GPCRs at the level of their intracellular pathways (Werry et al., 2003). These interactions significantly complexify their effects on cellular or network targets. We therefore asked whether HCAR1 is capable of functionally interacting with other  $G_i$ -coupled receptors, such as the adenosine A1 receptor (A1R), the GABA<sub>B</sub> receptor (GABA<sub>B</sub>R), and the  $\alpha_{2A}$ -adrenoreceptor

( $\alpha_{2A}$ R). To address this question, we used calcium imaging to monitor neuronal activity upon the sequential activation of HCAR1 and one of the  $G_i$ -coupled receptors. We found that the activation of HCAR1 with 3,5-DHBA decreased neuronal spiking frequency, as shown above, and the subsequent coactivation of HCAR1 and A1R using CPA induced a further decrease in neuronal spiking frequency ( $F_{(3,3)} = 20.57$ ,  $p = 0.046$ , ANOVA; Fig. 5a). After washout of the drugs, spiking activity returned to its original frequency (data not shown). The same apparent additive inhibition of spiking was observed when investigating the cooperation of HCAR1 with GABA<sub>B</sub>R or with  $\alpha_{2A}$ R, which were activated using baclofen and guanfacine, respectively (Table 4). It is expected that if the activation of HCAR1 and the other  $G_i$ -coupled receptors are independent, reversing the order of agonist application should result in the same combined inhibition of neuronal spiking. We tested this hypothesis by first stimulating A1R and immediately after coactivating HCAR1. Unexpectedly, when A1R was first activated, the subsequent coactivation of HCAR1 partially reversed the inhibition induced by A1R alone ( $F_{(3,3)} = 32.09$ ,  $p = 0.007$ , ANOVA; Fig. 5b). We repeated the same protocol with GABA<sub>B</sub>R or  $\alpha_{2A}$ R, and the same pattern was observed (Table 4). To ascertain that this effect was specifically brought about by HCAR1, we repeated these experiments with neurons prepared from HCAR1-KO animals. Figure 5c ( $F_{(3,3)} = 193.06$ ,  $p = 1$ , ANOVA) and Table 4 show that in neurons lacking HCAR1, no such interaction was observed, indicating that the observed effects were indeed mediated by the HCAR1. We then asked whether this reversal effect caused by HCAR1 activation was generic to all  $G_i$ -coupled receptors.

We repeated the experiments depicted above for A1R/GABA<sub>B</sub>R, A1R/ $\alpha_{2A}$ R, and  $\alpha_{2A}$ R/GABA<sub>B</sub>R pairs. The results listed in Table 5 indicate that this reversal of inhibition was not observed among these receptor pairs, which did not recapitulate the observations made with HCAR1. This indicates that this reversal of frequency decrease is a distinct property of HCAR1 activation.

Overall, these experiments revealed that, depending on which receptor is activated first in sequence, different levels of inhibition of spiking frequency are obtained upon HCAR1 coactivation with other  $G_i$ -coupled receptors, highlighting the complexity of the modulation of neuronal activity operated by HCAR1.

### The $G_{i\beta\gamma}$ -PLC pathway is involved in the interaction of HCAR1 with $G_i$ -coupled receptors

Although the  $G_i$  pathway is classically known for its ability to inhibit AC, both  $G_{i\alpha}$  and  $G_{i\beta\gamma}$  subunits can transduce signals. One of the key effectors directly regulated by  $G_{\beta\gamma}$  subunits is PLC. PLC catalyzes the hydrolysis of phosphatidylinositol 4,5-

**Table 4. HCAR1 interactions with GABA<sub>B</sub> and  $\alpha_{2A}$  receptors and neuronal activity**

	WT		HCAR1 KO	
	Frequency (%)	$n_{\text{cells}}, n_{\text{exp}}$	Frequency (%)	$n_{\text{cells}}, n_{\text{exp}}$
GABA <sub>B</sub> R/HCAR1				
3,5-DHBA <sup>a</sup>	32.3 ± 6.9	37, 4		
→ + baclofen	2.6 ± 3.3*			
Baclofen	13.9 ± 0.8	12, 3	53.2 ± 3.4	35, 4
→ + 3,5-DHBA	43.6 ± 5.5*		51.7 ± 4.5 <sup>n.s.</sup>	
$\alpha_{2A}$ R/HCAR1				
3,5-DHBA	48.4 ± 8.9	44, 4		
→ + Guanfacine	8.4 ± 3.3*			
Guanfacine	24.2 ± 2.8	36, 4	26.8 ± 8.4	29, 4
→ + 3,5-DHBA	54.2 ± 4.1*		27.2 ± 8.2 <sup>n.s.</sup>	

Data are expressed as the percentage of the frequency observed in baseline conditions and as the mean ± SEM. n.s., not significant. ANOVA, Bonferroni correction, for  $n$  cells from  $n$  experiments. Statistical significance is indicated for comparisons between the two displayed conditions.

<sup>a</sup>Concentrations used: 1 mM 3,5-DHBA, 0.5  $\mu$ M baclofen, and 10  $\mu$ M guanfacine.

\* $p < 0.05$ .

**Table 5. Lack of functional interactions among A1R, GABA<sub>B</sub>, and  $\alpha_{2A}$  receptors**

	Frequency (%)	$n_{\text{cells}}, n_{\text{exp}}$
A1R/GABA <sub>B</sub> R		
CPA <sup>a</sup>	2.4 ± 2.1	20, 3
→ + baclofen	1.8 ± 1.6 <sup>n.s.</sup>	
Baclofen	41.5 ± 7.6	18, 3
→ + CPA	2.7 ± 0.2*	
A1R/ $\alpha_{2A}$ R		
CPA	8.9 ± 8.8	19, 3
→ + Guanfacine	8.4 ± 3.3 <sup>n.s.</sup>	
Guanfacine	39.2 ± 8.3	17, 3
→ + CPA	3.8 ± 1.9*	
$\alpha_{2A}$ R/GABA <sub>B</sub> R		
Guanfacine	51.2 ± 11.6	16, 3
→ + Baclofen	42.4 ± 9.8 <sup>n.s.</sup>	
Baclofen	60.1 ± 5.4	18, 3
→ + Guanfacine	41.6 ± 7.5 <sup>n.s.</sup>	

Data are expressed as a percentage of the frequency observed in baseline conditions or as the mean ± SEM. n.s., not significant. ANOVA, Bonferroni correction, for  $n$  cells from  $n$  experiments. Statistical significance indicated for comparisons between the two displayed conditions.

<sup>a</sup>Concentrations used: 30 nM CPA, 0.5  $\mu$ M baclofen, and 10  $\mu$ M guanfacine.

\* $p < 0.05$ .

biphosphate to generate 1,2-diacylglycerol and inositol 1,4,5-trisphosphate, which binds to its receptor on the endoplasmic reticulum (Rhee, 2001). Thus, we investigated whether PLC activation induced by the G<sub>i $\beta$  $\gamma$</sub>  subunit was involved in the observed effect on the functional interaction between HCAR1 and G<sub>i</sub>-coupled receptors. In experiments repeating the sequence of agonist application presented in Figure 5b, the inhibition of the G<sub>i $\beta$  $\gamma$</sub>  subunit using gallein suppressed the partial reversal of inhibition induced by the coactivation of A1R and HCAR1 ( $F_{(3,3)} = 84.71, p = 1$ , ANOVA; Fig. 5d). The same approach was applied to test the involvement of the G<sub>i $\beta$  $\gamma$</sub>  subunit on the cooperation observed between GABA<sub>B</sub>R or  $\alpha_{2A}$ R and HCAR1. As indicated in Table 6, in both cases, gallein prevented the HCAR1 agonist from reversing the inhibition induced by GABA<sub>B</sub>R or  $\alpha_{2A}$ R stimulation. In all experiments, after washout of gallein and agonists, the spiking frequency returned to its control value (data not shown). These results support the involvement of the G<sub>i $\beta$  $\gamma$</sub>  subunit in the observed effects.

PLC is classically activated by the G<sub>q $\alpha$</sub> - and G<sub>q $\beta$  $\gamma$</sub> -proteins dissociated from G<sub>q</sub>-coupled receptors. However, PLC was also shown to be activated by G<sub>i $\beta$  $\gamma$</sub> -proteins released from G<sub>i</sub>-proteins (Tomura et al., 1997; Mizuta et al., 2011). Thus, we investigated whether PLC was the downstream mechanism activated by the

**Table 6. Mechanism of HCAR1 interaction with GABA<sub>B</sub> and  $\alpha_{2A}$  receptors**

	Frequency (%)	$n_{\text{cells}}, n_{\text{exp}}$
GABA <sub>B</sub> R/HCAR1		
Baclofen <sup>a</sup>	41.5 ± 7.6	13, 3
→ + 3,5-DHBA + gallein	41.3 ± 6.96 <sup>n.s.</sup>	
Baclofen	36.6 ± 16.2	19, 3
→ + 3,5-DHBA + U73122	12.5 ± 2.4 <sup>n.s.</sup>	
$\alpha_{2A}$ R/HCAR1		
Guanfacine	40.5 ± 6.0	22, 4
→ + 3,5-DHBA + gallein	46.0 ± 6.3 <sup>n.s.</sup>	
Guanfacine	51.2 ± 11.7	17, 3
→ + 3,5-DHBA + U73122	47.5 ± 9.5 <sup>n.s.</sup>	

Data are expressed as a percentage of the frequency observed in baseline conditions or as the mean ± SEM. n.s., not significant. ANOVA, Bonferroni correction, for  $n$  cells from  $n$  experiments. Statistical significance indicated for comparisons between the two displayed conditions.

<sup>a</sup>Concentrations used: 1 mM 3,5-DHBA, 0.5  $\mu$ M baclofen, 10  $\mu$ M guanfacine, 10  $\mu$ M gallein, and 10  $\mu$ M U73122.

G<sub>i $\beta$  $\gamma$</sub>  subunit and involved in the interplay between HCAR1 and other G<sub>i</sub>-coupled receptors. The application of U73122, the inhibitor of PLC, prevented HCAR1 agonist from reversing the spiking frequency decrease caused by A1R ( $F_{(3,3)} = 1621.87, p = 1$ , ANOVA; Fig. 5e), GABA<sub>B</sub>R, or  $\alpha_{2A}$ R (Table 6). After washout of U73122 and agonists, the spiking frequency returned to its control value (data not shown). These results indicate that the partial reversal of inhibition caused by HCAR1 activation under these conditions involves G<sub>i $\beta$  $\gamma$</sub>  and PLC. As a control, we assessed the effect of G<sub>i $\beta$  $\gamma$</sub>  and PLC blockade on the HCAR1 signaling itself. Blockade of G<sub>i $\beta$  $\gamma$</sub>  was sufficient to decrease the inhibitory action of HCAR1 ( $F_{(3,3)} = 84.10, p = 0.008$ , ANOVA; Fig. 5f). In contrast, the inhibition of PLC did not influence the effect of HCAR1 activation alone ( $F_{(3,3)} = 59.38, p = 1$ , ANOVA; Fig. 5g). Thus, it appears that the G<sub>i $\beta$  $\gamma$</sub>  subunit is necessary for the modulatory effects of HCAR1, but that PLC is only required upon activation of an additional G<sub>i</sub>-coupled receptor. Together, these results indicate that HCAR1 interacts with G<sub>i</sub>-coupled receptors in a complex but specific manner, through both its G<sub>i $\alpha$</sub>  and G<sub>i $\beta$  $\gamma$</sub>  subunits.

## Discussion

In this study, we demonstrate that HCAR1 in neurons is necessary for the modulation of spontaneous neuronal activity induced by L-lactate. We observed that HCAR1 activation with L-lactate induced a reversible decrease in the neuronal calcium spiking activity by ~40%, in line with first indications reported by our group (Bozzo et al., 2013). Activation of HCAR1 with nonmetabolized agonists 3,5-DHBA and 3Cl-HBA also decreased neuronal calcium spiking, as well as the mEPSCs frequency and AP firing frequency by similar amounts. We observed that HCAR1 activation induced changes in PPR and modulated neuronal intrinsic properties. As decisive arguments for the critical role of HCAR1, the activity of HCAR1 KO neurons was totally insensitive to HCAR1 agonists and the basal activity of these neurons was higher than that of neurons from WT mice. HCAR1 is therefore required for the nonmetabolic effects of L-lactate on spontaneous and tonic neuronal activity.

The HCAR1 pattern of expression in the CNS was first described to localize at the membrane of excitatory synapses of the hippocampus and cerebellar cortex (Lauritzen et al., 2014). However, because of the questionable specificity of HCAR1 antibodies currently available (Table 1; Michel et al., 2009; Wallenius et al., 2017), the precise HCAR1 cellular and regional localization in the brain remains uncertain. At this stage, one can find evidence for HCAR1 brain expression from *in situ* hybridization (the Allen

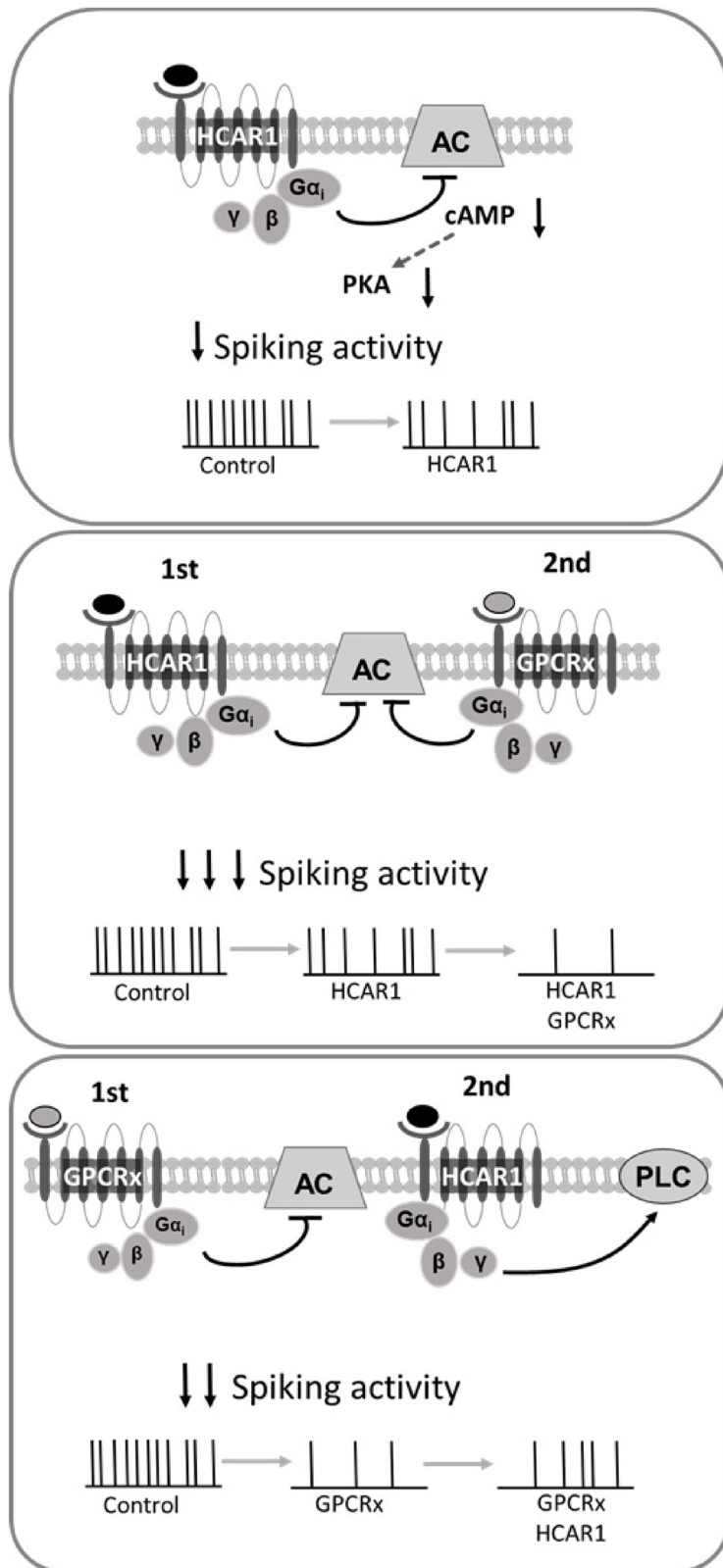


**Figure 6.** HCAR1 modulation of neuronal activity. Scheme depicting the modulatory effect brought about by HCAR1, when activated in isolation (Top) or with concurrent activation of other  $G_i$ -coupled GPCRs (Middle, Bottom).

Brain Atlas, <http://www.brain-map.org>), proteomics (UniProt database, <https://www.uniprot.org>), and transcriptomics (Zhang et al., 2014). HCAR1 expression in the brain was estimated to be one order of magnitude lower than in adipose tissue, where it was initially identified (Lauritzen et al., 2014).

In the CNS, several studies provided evidence for a signaling role of L-lactate. Suzuki et al. (2011) reported that long-term memory formation and maintenance are mechanisms for which L-lactate plays an essential role. Yang et al. (2014) showed that L-lactate stimulates the expression of synaptic plasticity-related genes. *In vivo* administration of L-lactate inhibited firing in the hippocampus (Gilbert et al., 2006), and in the subfornical organ 5 mM L-lactate decreased spiking activity of GABAergic neurons (Shimizu et al., 2007). A recent study showed that 5 mM L-lactate and the HCAR1 agonist 3,5-DHBA, decreased neuronal activity in a nonmetabolic way by modulating neuronal intrinsic excitability, significantly blocking fast-inactivating sodium current and increasing the delay from inactivation to a conducting state of the sodium channel in rat CA1 pyramidal neurons (Herrera-López and Galván, 2018). L-lactate also plays an important protective role in cerebral ischemia. It was observed that intracerebral L-lactate administration, decreases the lesion size and improves the neurological outcome (Berthet et al., 2009). A follow-up study showed that both L-lactate and D-lactate, which is poorly metabolized but also activates HCAR1, equally provides neuroprotection in ischemic conditions, and that 3,5-DHBA reduces cell death, suggesting that L-lactate protective functions involve HCAR1 activation (Castillo et al., 2015). HCAR1 was also shown to be involved in enhanced brain angiogenesis linked with physical activity (Morland et al., 2017).

By using electrophysiological recordings, we observed that HCAR1 activation decreased the frequency of mEPSCs, providing an indication for a presynaptic action of this receptor. This conclusion was supported by PPR experiments. To our knowledge, it is the first evidence of a presynaptic effect of HCAR1. A change in excitability has also been observed by others in rat hippocampal neurons (Herrera-López and Galván, 2018). We investigated whether this was the case in mouse cortical neurons. Activation of HCAR1 reduced  $R_N$  and firing frequency, increased the rheobase current, and caused RMP hyperpolarization. These changes in excitability possibly involve the modulation of potassium conductances and of fast inactivating sodium currents reported by Herrera-López and Galván (2018). These experiments provided evidence supporting a presynaptic as well as a postsynaptic effect of HCAR1.

In adipocytes, HCAR1 signals through a  $G_{i\alpha}$ -protein pathway (Ge et al., 2008) and L-lactate mediates its antilipolytic effect with



an  $IC_{50}$  value of  $\sim 5$  mM (Cai et al., 2008; Liu et al., 2009). In the present study, we investigated whether in cortical neurons the  $G_{i\alpha}$ -protein pathway and its canonical downstream effectors were engaged for the observed inhibition of neuronal activity. Our group was able to reverse the inhibitory effect of L-lactate on neuronal activity by applying pertussis toxin, an inhibitor of  $G_{i\alpha}$ -proteins, which provided a first indication for the involvement of  $G_i$ -coupled receptor-mediated action of lactate in cortical neurons (Bozzo et al., 2013). Here, we found evidence for the involvement of AC, as the enhancement of spiking activity by the AC activator forskolin could be reversed by HCAR1 activation. Importantly, this did not happen in neurons from HCAR1 KO mice. Conversely, inhibiting AC using SQ22536 decreased spontaneous spiking; however, HCAR1 activation had no further effect. By directly measuring cAMP in single living neurons using a cAMP FRET biosensor, we found that the increase of cAMP level induced by AC activation was reversed by the HCAR1 agonist. This result is in agreement with the report made in rat hippocampal slices (Lauritzen et al., 2014). One important downstream target of cAMP is PKA. We found that under PKA inhibition, HCAR1 activation did no longer decrease neuronal spiking activity. Overall, these experiments indicate that the downmodulation of spontaneous neuronal activity by HCAR1 activation requires a functional intracellular AC–cAMP–PKA signaling pathway. Along these lines, cAMP is known to serve as a signal that modulates neuronal vesicular release through PKA-dependent and PKA-independent mechanisms (Seino and Shibasaki, 2005). Moreover, it is known that  $G_i$ -coupled receptors (e.g., A1R, GABA<sub>B</sub>R,  $\alpha_{2A}$ R) regulate neuronal excitability by inducing or modulating ion currents such as various  $K^+$  conductances, including HCN (Wang et al., 2007), two-pore domain  $K^+$  channels (Deng et al., 2009), or GIRK channels (Breton and Stuart, 2017).

In several systems, GPCRs have the properties to interact with each other, enabling them to operate a much more complex modulation than individual transduction pathways acting independently (Werry et al., 2003). It was shown that coactivation of two  $G_{i/o}$ -coupled receptors (e.g., A1 adenosine and cannabinoid CB1 receptors) reduces cAMP formation in rat hippocampus, which causes additive inhibitory effects on neuronal activity (Serpa et al., 2009). Another example of intracellular interaction of combined  $G_i$ -coupled receptor activation was found between adenosine A1 and group II metabotropic glutamate receptors: their sequential activation did not lead to additive presynaptic inhibition, but to a mutual occlusion of effects on retinotectal synapses (Zhang and Schmidt, 1999).

We therefore questioned whether HCAR1 follows such interaction patterns with other classical  $G_i$ -coupled receptors. We selected the adenosine A1, GABA<sub>B</sub>, and  $\alpha_{2A}$ -adrenergic receptors, which are all  $G_i$ -coupled receptors known to be expressed in cortical neurons and to signal through the decrease of AC activity, cAMP levels, and PKA activity. When HCAR1 was stimulated first in sequence followed by the stimulation of the other GPCR, an apparent additive decrease in spiking frequency was observed. However, when the order of receptor activation was permuted, HCAR1 activation rather partly reversed the inhibitory effect of the first receptor. The observation was made with all three receptors (adenosine A1, GABA<sub>B</sub>, and  $\alpha_{2A}$ -adrenergic receptors) and was absent in HCAR1 KO neurons. This type of cooperation was not reproduced when selecting pairs among these three GPCRs. Thus, HCAR1 appears to have distinctive actions on neuronal activity when activated in combination with other receptors sharing similar transduction mechanisms.

The way HCAR1 is interacting with other GPCRs likely involves additional mechanisms than the canonical AC–cAMP–PKA pathway. It was demonstrated that recombinant HCAR1 activation induces ERK1/2 phosphorylation through the activation of its  $G_{\beta\gamma}$ -subunit (Li et al., 2014). HCAR1 may therefore have the ability to signal through both its  $G_{i\alpha}$  and  $G_{i\beta\gamma}$  subunits. We postulated that the partial reversal of inhibition of  $G_i$ -coupled receptors brought about by HCAR1 is mediated by  $G_{i\beta\gamma}$  subunits released from the  $G_i$  complex after receptor stimulation. We found that blocking  $G_{i\beta\gamma}$  subunit not only reduced the inhibitory effect of HCAR1 alone, but also prevented the reversal of spiking inhibition observed when HCAR1 was activated in sequence with another  $G_i$ -coupled receptor. In further support of this hypothesis, the blockade of PLC, a downstream target of  $G_{\beta\gamma}$  (Katz et al., 1992), also prevented the observed partial reversal of inhibition. However, PLC seems to be engaged only when HCAR1 is activated in sequence with another receptor, since PLC blockade did not alter the effect of HCAR1 activation alone.

In this study, we demonstrate that lactate has the ability to modulate neuronal activity through HCAR1, providing further support for the hypothesis that lactate, in addition to being an energy substrate for neurons, can function as a gliotransmitter. HCAR1 mediates its effect through its  $G_{i\alpha}$  subunit and its downstream effectors, resulting in a decrease of neuronal excitability and consequent firing frequency (Fig. 6). The ability of HCAR1 to functionally interact with other GPCRs through both  $G_{i\alpha}$  and  $G_{i\beta\gamma}$  subunits adds a level of complexity to its mechanism of action on neuronal activity and implies that the outcome of its activation *in vivo* will depend on whether other receptors of this class are active at any given time.

## References

- Abi-Saab WM, Maggs DG, Jones T, Jacob R, Srihari V, Thompson J, Kerr D, Leone P, Krystal JH, Spencer DD, Doring MJ, Sherwin RS (2002) Striking differences in glucose and lactate levels between brain extracellular fluid and plasma in conscious human subjects: effects of hyperglycemia and hypoglycemia. *J Cereb Blood Flow Metab* 22:271–279.
- Ahmed K, Tunaru S, Tang C, Müller M, Gille A, Sassmann A, Hanson J, Offermanns S (2010) An autocrine lactate loop mediates insulin-dependent inhibition of lipolysis through GPR81. *Cell Metab* 11:311–319.
- Barros LF (2013) Metabolic signaling by lactate in the brain. *Trends Neurosci* 36:396–404.
- Berthet C, Lei H, Thevenet J, Gruetter R, Magistretti PJ, Hirt L (2009) Neuroprotective role of lactate after cerebral ischemia. *J Cereb Blood Flow Metab* 29:1780–1789.
- Blad CC, Tang C, Offermanns S (2012) G protein-coupled receptors for energy metabolites as new therapeutic targets. *Nat Rev Drug Discov* 11:603–619.
- Bozzo L, Puyal J, Chatton JY (2013) Lactate modulates the activity of primary cortical neurons through a receptor-mediated pathway. *PLoS One* 8:e71721.
- Breton JD, Stuart GJ (2017) GABAB receptors in neocortical and hippocampal pyramidal neurons are coupled to different potassium channels. *Eur J Neurosci* 46:2859–2866.
- Cai TQ, Ren N, Jin L, Cheng K, Kash S, Chen R, Wright SD, Taggart AK, Waters MG (2008) Role of GPR81 in lactate-mediated reduction of adipose lipolysis. *Biochem Biophys Res Commun* 377:987–991.
- Castillo X, Rosafio K, Wyss MT, Drandarov K, Buck A, Pellerin L, Weber B, Hirt L (2015) A probable dual mode of action for both L- and D-lactate neuroprotection in cerebral ischemia. *J Cereb Blood Flow Metab* 35:1561–1569.
- Dalsgaard MK, Quistorff B, Danielsen ER, Selmer C, Vogelsang T, Secher NH (2004) A reduced cerebral metabolic ratio in exercise reflects metabolism and not accumulation of lactate within the human brain. *J Physiol* 554:571–578.
- Deng PY, Xiao Z, Yang C, Rojanathammanee L, Grisanti L, Watt J, Geiger JD, Liu R, Porter JE, Lei S (2009) GABA(B) receptor activation inhibits neu-

- ronal excitability and spatial learning in the entorhinal cortex by activating TREK-2 K<sup>+</sup> channels. *Neuron* 63:230–243.
- Díaz-García CM, Mongeon R, Lahmann C, Koveal D, Zucker H, Yellen G (2017) Neuronal stimulation triggers neuronal glycolysis and not lactate uptake. *Cell Metab* 26:361–374.e4.
- Dienel GA, Ball KK, Cruz NF (2007) A glycogen phosphorylase inhibitor selectively enhances local rates of glucose utilization in brain during sensory stimulation of conscious rats: implications for glycogen turnover. *J Neurochem* 102:466–478.
- Dvorak CA, Liu C, Shelton J, Kuei C, Sutton SW, Lovenberg TW, Carruthers NI (2012) Identification of hydroxybenzoic acids as selective lactate receptor (GPR81) agonists with antilipolytic effects. *ACS Med Chem Lett* 3:637–639.
- Ge H, Weiszmann J, Reagan JD, Gupta J, Baribault H, Gyuris T, Chen JL, Tian H, Li Y (2008) Elucidation of signaling and functional activities of an orphan GPCR, GPR81. *J Lipid Res* 49:797–803.
- Gilbert E, Tang JM, Ludvig N, Bergold PJ (2006) Elevated lactate suppresses neuronal firing in vivo and inhibits glucose metabolism in hippocampal slice cultures. *Brain Res* 1117:213–223.
- Gladden LB (2004) Lactate metabolism: a new paradigm for the third millennium. *J Physiol* 558:5–30.
- Grishchuk Y, Ginet V, Truttman AC, Clarke PG, Puyal J (2011) Beclin 1-independent autophagy contributes to apoptosis in cortical neurons. *Autophagy* 7:1115–1131.
- Herrera-López G, Galván EJ (2018) Modulation of hippocampal excitability via the hydroxycarboxylic acid receptor 1. *Hippocampus* 28:557–567.
- Husted AS, Trauelsen M, Rudenko O, Hjorth SA, Schwartz TW (2017) GPCR-mediated signaling of metabolites. *Cell Metab* 25:777–796.
- Katz A, Wu D, Simon MI (1992) Subunits beta gamma of heterotrimeric G protein activate beta 2 isoform of phospholipase C. *Nature* 360:686–689.
- Lauritzen KH, Morland C, Puchades M, Holm-Hansen S, Hagelin EM, Lauritzen F, Attramadal H, Storm-Mathisen J, Gjedde A, Bergersen LH (2014) Lactate receptor sites link neurotransmission, neurovascular coupling, and brain energy metabolism. *Cereb Cortex* 24:2784–2795.
- Li G, Wang HQ, Wang LH, Chen RP, Liu JP (2014) Distinct pathways of ERK1/2 activation by hydroxy-carboxylic acid receptor-1. *PLoS One* 9:e93041.
- Liu C, Wu J, Zhu J, Kuei C, Yu J, Shelton J, Sutton SW, Li X, Yun SJ, Mirzadegan T, Mazur C, Kamme F, Lovenberg TW (2009) Lactate inhibits lipolysis in fat cells through activation of an orphan G-protein-coupled receptor, GPR81. *J Biol Chem* 284:2811–2822.
- Livak KJ, Schmittgen TD (2001) Analysis of relative gene expression data using real-time quantitative PCR and the 2<sup>-ΔΔC(T)</sup> method. *Methods* 25:402–408.
- Mächler P, Wyss MT, Elsayed M, Stobart J, Gutierrez R, von Faber-Castell A, Kaelin V, Zuend M, San Martin A, Romero-Gómez I, Baeza-Lehnert F, Lengacher S, Schneider BL, Aebischer P, Magistretti PJ, Barros LF, Weber B (2016) In vivo evidence for a lactate gradient from astrocytes to neurons. *Cell Metab* 23:94–102.
- Michel MC, Wieland T, Tsujimoto G (2009) How reliable are G-protein-coupled receptor antibodies? *Naunyn Schmiedeberg Arch Pharmacol* 379:385–388.
- Mizuta K, Mizuta F, Xu D, Masaki E, Panettieri RA Jr, Emala CW (2011) Gi-coupled gamma-aminobutyric acid-B receptors cross-regulate phospholipase C and calcium in airway smooth muscle. *Am J Respir Cell Mol Biol* 45:1232–1238.
- Morland C, Andersson KA, Haugen ØP, Hadzic A, Kleppa L, Gille A, Rinholm JE, Palibrk V, Diget EH, Kennedy LH, Stølen T, Hennestad E, Moldstad O, Cai Y, Puchades M, Offermanns S, Vervaeke K, Bjorås M, Wisløff U, Storm-Mathisen J, et al (2017) Exercise induces cerebral VEGF and angiogenesis via the lactate receptor HCAR1. *Nat Commun* 8:15557.
- Nikolaev VO, Bünemann M, Hein L, Hannawacker A, Lohse MJ (2004) Novel single chain cAMP sensors for receptor-induced signal propagation. *J Biol Chem* 279:37215–37218.
- Offermanns S (2017) Hydroxy-carboxylic acid receptor actions in metabolism. *Trends Endocrinol Metab* 28:227–236.
- Pellerin L, Magistretti PJ (1994) Glutamate uptake into astrocytes stimulates aerobic glycolysis: a mechanism coupling neuronal activity to glucose utilization. *Proc Natl Acad Sci U S A* 91:10625–10629.
- Rhee SG (2001) Regulation of phosphoinositide-specific phospholipase C. *Annu Rev Biochem* 70:281–312.
- Seino S, Shibasaki T (2005) PKA-dependent and PKA-independent pathways for cAMP-regulated exocytosis. *Physiol Rev* 85:1303–1342.
- Serpa A, Ribeiro JA, Sebastião AM (2009) Cannabinoid CB(1) and adenosine A(1) receptors independently inhibit hippocampal synaptic transmission. *Eur J Pharmacol* 623:41–46.
- Shimizu H, Watanabe E, Hiyama TY, Nagakura A, Fujikawa A, Okado H, Yanagawa Y, Obata K, Noda M (2007) Glial nax channels control lactate signaling to neurons for brain [Na<sup>+</sup>] sensing. *Neuron* 54:59–72.
- Sotelo-Hitschfeld T, Niemeyer MI, Mächler P, Ruminot I, Lerchundi R, Wyss MT, Stobart J, Fernández-Moncada I, Valdebenito R, Garrido-Gerter P, Contreras-Baeza Y, Schneider BL, Aebischer P, Lengacher S, San Martín A, Le Douce J, Bonvento G, Magistretti PJ, Sepúlveda FV, Weber B, et al (2015) Channel-mediated lactate release by K(+)-stimulated astrocytes. *J Neurosci* 35:4168–4178.
- Suzuki A, Stern SA, Bozdagi O, Huntley GW, Walker RH, Magistretti PJ, Alberini CM (2011) Astrocyte-neuron lactate transport is required for long-term memory formation. *Cell* 144:810–823.
- Tang F, Lane S, Korsak A, Paton JF, Gourine AV, Kasparov S, Teschemacher AG (2014) Lactate-mediated glia-neuronal signalling in the mammalian brain. *Nat Commun* 5:3284.
- Tomura H, Itoh H, Sho K, Sato K, Nagao M, Ui M, Kondo Y, Okajima F (1997) Betagamma subunits of pertussis toxin-sensitive G proteins mediate A1 adenosine receptor agonist-induced activation of phospholipase C in collaboration with thyrotropin. A novel stimulatory mechanism through the cross talk of two types of receptors. *J Biol Chem* 272:23130–23137.
- Wallenius K, Thalén P, Björkman JA, Johannesson P, Wiseman J, Böttcher G, Fjellström O, Oakes ND (2017) Involvement of the metabolic sensor GPR81 in cardiovascular control. *JCI Insight* 2:92564.
- Wang M, Ramos BP, Paspalas CD, Shu Y, Simen A, Duque A, Vijayraghavan S, Brennan A, Dudley A, Nou E, Mazer JA, McCormick DA, Arnsten AF (2007) Alpha2A-adrenoceptors strengthen working memory networks by inhibiting cAMP-HCN channel signaling in prefrontal cortex. *Cell* 129:397–410.
- Werry TD, Wilkinson GF, Willars GB (2003) Mechanisms of cross-talk between G-protein-coupled receptors resulting in enhanced release of intracellular Ca<sup>2+</sup>. *Biochem J* 374:281–296.
- Yang J, Ruchti E, Petit JM, Jourdain P, Grenningloh G, Allaman I, Magistretti PJ (2014) Lactate promotes plasticity gene expression by potentiating NMDA signaling in neurons. *Proc Natl Acad Sci U S A* 111:12228–12233.
- Zhang C, Schmidt JT (1999) Adenosine A1 and class II metabotropic glutamate receptors mediate shared presynaptic inhibition of retinotectal transmission. *J Neurophysiol* 82:2947–2955.
- Zhang Y, Chen K, Sloan SA, Bennett ML, Scholze AR, O’Keefe S, Phatnani HP, Guarnieri P, Caneda C, Ruderisch N, Deng S, Liddelow SA, Zhang C, Daneman R, Maniatis T, Barres BA, Wu JQ (2014) An RNA-sequencing transcriptome and splicing database of glia, neurons, and vascular cells of the cerebral cortex. *J Neurosci* 34:11929–11947.